Electronic Supplementary Material (ESI) for Green Chemistry.

Development of Magnesium Oxide-Silver Hybrid Nanocatalysts for Synergistic Carbon Dioxide Activation to Afford Esters and Heterocycles at Ambient Pressure

Upasana Gulati,[a,b†] U. Chinna Rajesh,[a†] Diwan S. Rawat[b*] and Jeffrey M. Zaleski[a*]

[a]Department of Chemistry, Indiana University, Bloomington, Indiana 47405, United States. E-mail: zaleski@indiana.edu

[b]Department of Chemistry, University of Delhi, Delhi-110007, India. E-mail: dsrawat@chemistry.du.ac.in

[†]These authors contributed equally to the work.

Table of contents

Contents **Page No.**

EXPERIMENTAL SECTION

Methods

Chemicals Magnesium nitrate hexahydrate ($MgNO_3.6H_2O$, 99%) was purchased from EM Sciences. Sodium oxalate ($Na_2C_2O_4$, >99%) and silver acetate (AgOAc, 99%) were purchased from Strem Chemicals. 4-Tolylacetylene (98%), 3-tolylacetylene, 4-tert-butylphenylacetylene (90%), 4-ethynylanisole (99%), 3-ethynylanisole (96%), 4-fluorophenylacetylene (99%), 3-chloro-1-phenyl-1-propyne (97%), cinnamyl chloride (95%, stab. with sodium carbonate), ethyl-2-chloroacetate (99%) were purchased from Alfa Aesar. Phenylacetylene (99%), sodium borohydride (>98.0) were purchased from Sigma Aldrich. Potassium carbonate (K_2CO_3, 99%) from BDH Chemicals, CO_2 cylinder from Air gases. LR white acrylic resin was purchased from Agar Scientific. **Solvents** N,N-dimethylacetamide **(**DMAC), ethylacetate, hexane, ethanol.

Characterization of nanomaterials. The surface morphologies and SEM-EDX elemental mapping of as synthesized materials were analysed from the FEI Quanta 600 with an electron beam current intensity of 30 eV. The ultramicrotome slices of MgO@Ag-7 were collected using a Leica Ultracut UCT ultramicrotome with a diamond knife. The MgO@Ag-7 sample was mixed with LR white acrylic resin (hydrophilic) in dry EMS embedding capsules and aged for 24 h at 60 °C. The obtained polymer blocks embedded with samples were sectioned at 70 nm thickness. The slices were placed on 300 mesh copper grids for HR-TEM and SEM-EDX mapping analyses. HR-TEM images were attained on a JEOL 3200FS transmission electron microscope at an accelerating voltage of 300 kV. The Powder X-ray diffraction (PXRD) patterns of as synthesized samples were acquired using an Empyrean diffractometer (PANalytical). X-rays were produced from a copper target (Cu Kα = 1.54187 Å). Soller, antiscatter divergence slits and a nickel filter were employed in the beam path to reduce X-Ray beam scatter and background. The spinning sample head with a revolution time of 4s during the measurement in reflection mode. The measurements were carried out with several step-sizes and counting rates. The PXRD pattern of commercially available AgO, Ag_2O and Ag^0 powders were collected under similar parameters and used as standards to compare the phases with corresponding 2θ values of as synthesized materials in the present work. The qualitative and quantitative surface analysis and oxidation states of metal components of samples were characterized by X-ray photoelectron spectroscopy (XPS). XPS experiments were carried out on the PHI VersaProbe II instrument equipped with a monochromatic Al Kα source. The X-ray power of 25 W at 15 kV was utilized for a 200 µm beam size. The calibration of the instrument work function was performed to give an Au $4f_{7/2}$ metallic gold binding energy of 83.9 eV. The spectrometer dispersion is adjusted to give a binding energy of 932.6 eV for metallic Cu $2p_{3/2}$, 284.8 eV, for the C 1s line of adventitious (aliphatic) carbon and 368.3 eV for metallic $Ag3d_{5/2}$. The PHI dual charge compensation system was utilized on all samples. The final Versa Probe II instrumental resolution was found to be better than 0.125 eV using the Fermi edge of the VB for metallic silver. XPS spectra with the energy step of 0.1 eV were recorded with Smart Soft-XPS v2.0 and processed using PHI Multi Pack v9.0 software. Peaks were fitted utilizing a combination of Gaussians and Lorentzians with 10−50% of Lorentzian content. Curve-fitting was carried out using a Shirley background. The powder samples for XPS measurements were fixed onto XPS sample holder by using double-sided adhesive tape. The elemental concentrations of catalyst samples were measured by an Agilent 7700 quadrupole inductively coupled plasma mass spectrometer (ICP-MS). The instrument was equipped with a helium collision/reaction cell to limit spectral interferences. Prior to sample analyses, the instrument was calibrated with a serial dilution of ICP standards of the elements of interest, and the analytical errors on these measurements are estimated at +/- 5% relative, based on repeated measurements of selected samples over multiple analytical sessions.

The CO_2 desorption profile for each catalyst was measured by temperature-programmed desorption (TPD) using an automated gas sorption analyzer, AutoChem II 2920 (Micromeritics Instruments Co., USA). Prior to desorption, a powdered sample was loaded in a U-shape quartz reactor and pre-treated under a helium (He) gas flow at 300 °C for 1 h and allowed to cool to 100 °C. The sample was then saturated with a mixture of 10% CO_2 + 90% He gases for 30 min, followed by stripping with He gas for 30 min to remove the physisorbed CO_2 at 100 °C. Subsequently, the temperature was raised to 800 °C at a ramping rate of 10 °C min^{-1} while maintaining the He gas flow (30 mL min^{-1}) and the desorbed gas was monitored with the Gas Chromatograph with Thermal Conductivity Detector (GC-TCD). Nitrogen adsorption-desorption measurements were carried out using the ASAP 2020 analyzer (Micromeritics) at liquid nitrogen temperature. The powdered samples were degassed at 100 °C in vacuum for overnight. The “t-plot" method was used to determine the surface area from estimates of micropore volume. The total surface area was estimated by the Brunauer Emmet-Teller (BET) method, while the pore size distribution was determined by the Barrett-Joyner-Halenda (BJH) analysis.

Characterization of organic molecules. ^{1}H NMR spectra of all organic molecules were acquired on Varian I400 (400 MHz), Varian VXR400 (400 MHz) or Varian I500 (500 MHz) spectrometers. The chemical shifts (δ) are reported in ppm from tetramethylsilane as the internal standard with the solvent resonance ($CHCl_3$: δ 7.26 ppm). Data are reported as follows: chemical shift, multiplicity (s = singlet, d = doublet, dd = doublet of doublet, dt = doublet of triplet, t = triplet, q = quartet, br = broad, m = multiplet), coupling constants (Hz), and integration. ^{13}C NMR spectra were acquired on Varian I400 (100 MHz) or Varian I500 (125 MHz) spectrometers with complete proton decoupling. Chemical shifts (δ) are reported in ppm from tetramethylsilane with the solvent resonance as the internal standard ($CDCl_3$: δ 77.16 ppm). Infrared (IR) spectra were recorded on Bruker Tensor II FT-IR spectrometer. Bands are characterized as broad (br), strong (s), medium (m), and weak (w). High-resolution mass spectrometry (HRMS) was performed on a Thermo Electron Corporation MAT 95XP-Trap (GC/MS). Melting points were obtained on a Thomas Hoover capillary melting point apparatus without correction. Unless otherwise noted, all reactions have been carried out with distilled and degassed solvents with standard vacuum-line techniques and under an atmosphere of dry N_2.

Synthesis of porous MgO. The porous MgO was prepared by the reported method.[S1] In a typical procedure, the aqueous solution of $MgNO_3.6H_2O$ (59.9 mmol, 100 mL deionized water) was dissolved in 500 mL round bottom flask and heated at 50 °C. The preheated aqueous solution of $Na_2C_2O_4$ (60 mmol, 200 mL deionized water at 50 °C) was added to the $MgNO_3.6H_2O$ solution under vigorous stirring followed by aging for 1 h at 50 °C. The obtained $MgC_2O_4.2H_2O$ was filtered, washed with deionized water (3x) and dried at 70 °C for 5 h. The porous MgO was obtained by calcination of $MgC_2O_4.2H_2O$ at 800 °C for 3 h in a muffle furnace.

Synthesis of MgO@Ag hybrid cubes. The ethanolic solution of porous MgO (2.5 mmol, 25 mL ethanol) was added to an ethanolic solution of AgOAc (n mmol, 25 mL ethanol; where n = 0.07, 0.14, 0.20, 0.30) and the mixture stirred at room temperature for 16 h. The resulting yellowish-brown precipitate was filtered and washed with ethanol to obtain AgOAc stabilised porous MgO (MgO@AgOAc) nanocomposites. The obtained MgO@AgOAc nanocomposites were dispersed in 30 mL of ethanol and the solution of $NaBH_4$ (n mmol, 10 mL ethanol; where n = 0.5, 1.0, 1.4, 2.1) was added and stirred at room temperature for 2 h. The obtained MgO@Ag hybrid cubes were filtered, washed with ethanol, and dried at 80 °C overnight. The notations for hybrid cubes are based on the percentages of Ag3d and Mg1s from peak areas in high resolution XPS. MgO@Ag-2 (Ag3d-2%: Mg1s-98%); MgO@Ag-5 (Ag3d-5%: Mg1s-95%); MgO@Ag-7 (Ag3d-7%: Mg1s-93%); MgO@Ag-8 (Ag3d-8%: Mg1s-92%).

The bulk concentration of Ag in these hybrid samples are analysed by ICP-MS and compared with their surface XPS values (**Table S1**).

Table S1. Comparison of Ag loadings in hybrid samples by XPS and ICP-MS measurements.

Samples	**XPS (Ag)**		**ICP-MS (Ag)**	
	at %	wt %	at %	wt %
MgO@Ag-8	8	28	5	19
MgO@Ag-7	7	25	4	15
MgO@Ag-5	5	19	3	12
MgO@Ag-2	2	8	1	5

Synthesis of oleylamine capped ultra-small Ag^0 NPs. The Ag^0 NPs were synthesized by modified reported method.[S2] The mixture of silver acetate (10 mmol, 1.7 g), oleylamine (0.5 mL) and oleic acid (4.5 mL) was degassed and refilled with nitrogen gas (3x) at 70 ^oC for 90 min. The mixture was heated to 180 ^oC with the heating rate of 1 ^oC/min and left for 30 min at that temperature. After cooling down to room temperature naturally, the mixture of ethanol 80 mL and toluene 20 mL was added, and the silver nanoparticles were collected by centrifugation at 6500 rpm.

MgO@Ag hybrid nanocatalysed synthesis of esters and lactones by CO_2 insertion into alkyne feedstocks. The mixture of alkynes **1** (1 mmol), allylic chloride **2** (1 mmol), catalyst (6 mg), dry K_2CO_3 (1.2 mmol) and anhydrous DMAc solvent (0.5 mL) in a Pyrex glass Schlenk tube was degassed and purged with CO_2 (3x). The mixture was then equipped with a CO_2 balloon and heated at 55 °C (for esters) or 90 °C (for lactones) for 24 h. The reaction was quenched by addition of water and the organic compounds were extracted with ethylacetate (3 × 6 mL). The catalyst was recovered from the aqueous layer by centrifugation. The combined organic layers were dried over sodium sulphate, filtered, and concentrated in vacuum. The crude organic mixture was purified by silica gel column chromatography to obtain pure ester products and characterized by ^1H NMR, ^{13}C NMR, FT-IR and HR-MS spectroscopic techniques.

Characterization of MgO@Ag hybrid nanocatalysts

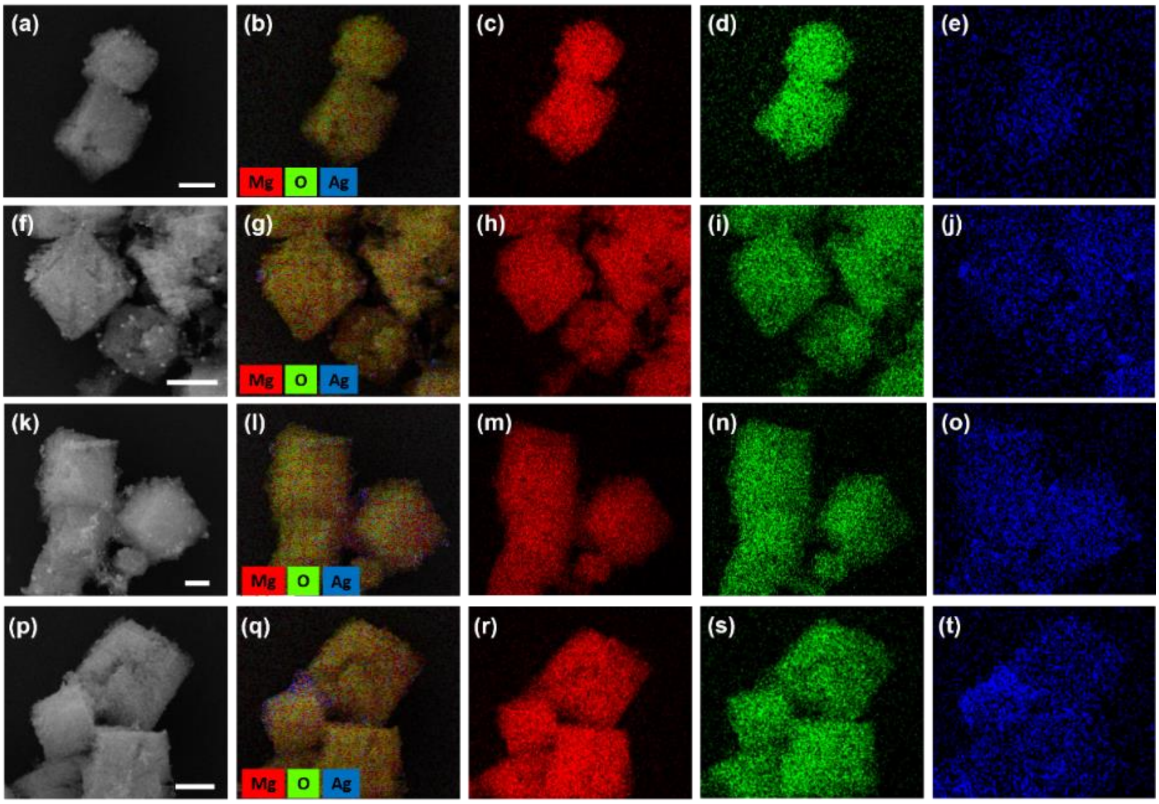

Figure S1. SEM-EDX mapping images of MgO@Ag-2 (**a-e**), MgO@Ag-5 (**f-j**), MgO@Ag-7 (**k-o**) and MgO@Ag-8 (**p-t**). All scale bars are 1 μm.

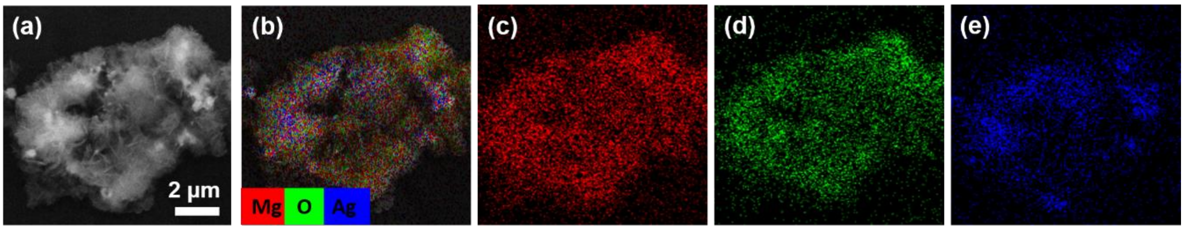

Figure S2. SEM-EDX mapping images of MgO@Ag-7 synthesised in water (**a-e**).

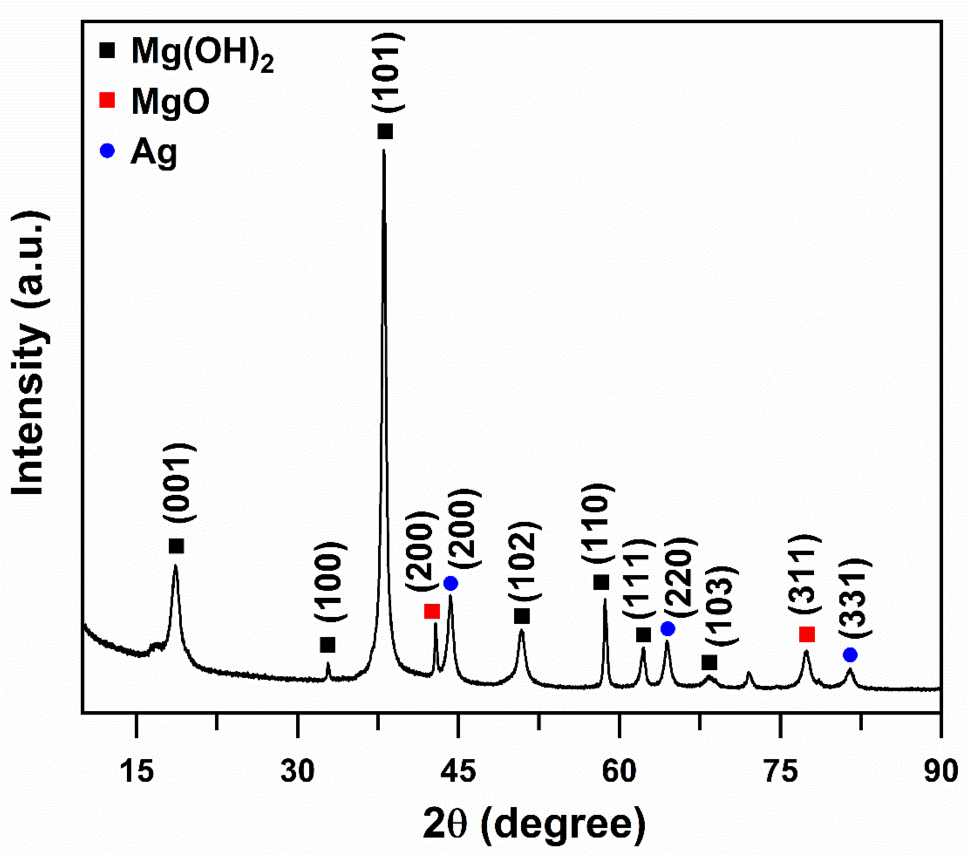

Figure S3. PXRD of MgO@Ag-7 synthesised in water.

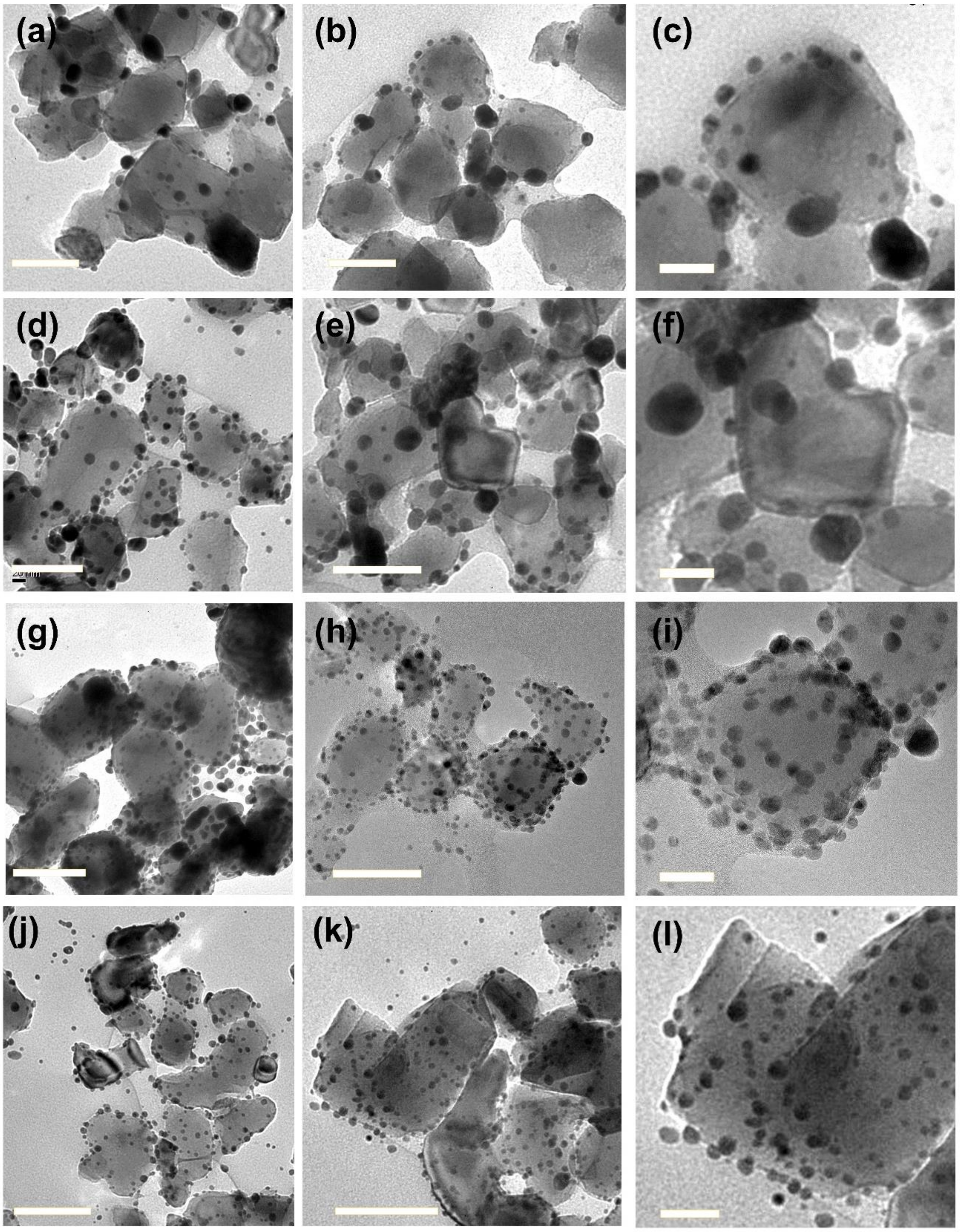

Figure S4. **TEM images of microtome sliced hybrid cubes** MgO@Ag-2 (**a-c**); MgO@Ag-5 (**d-f**); MgO@Ag-7 (**g-i**); MgO@Ag-8 (**j-l**) at different spots and magnifications. Scale bars 100 nm (left, middle) and 20 nm (right)

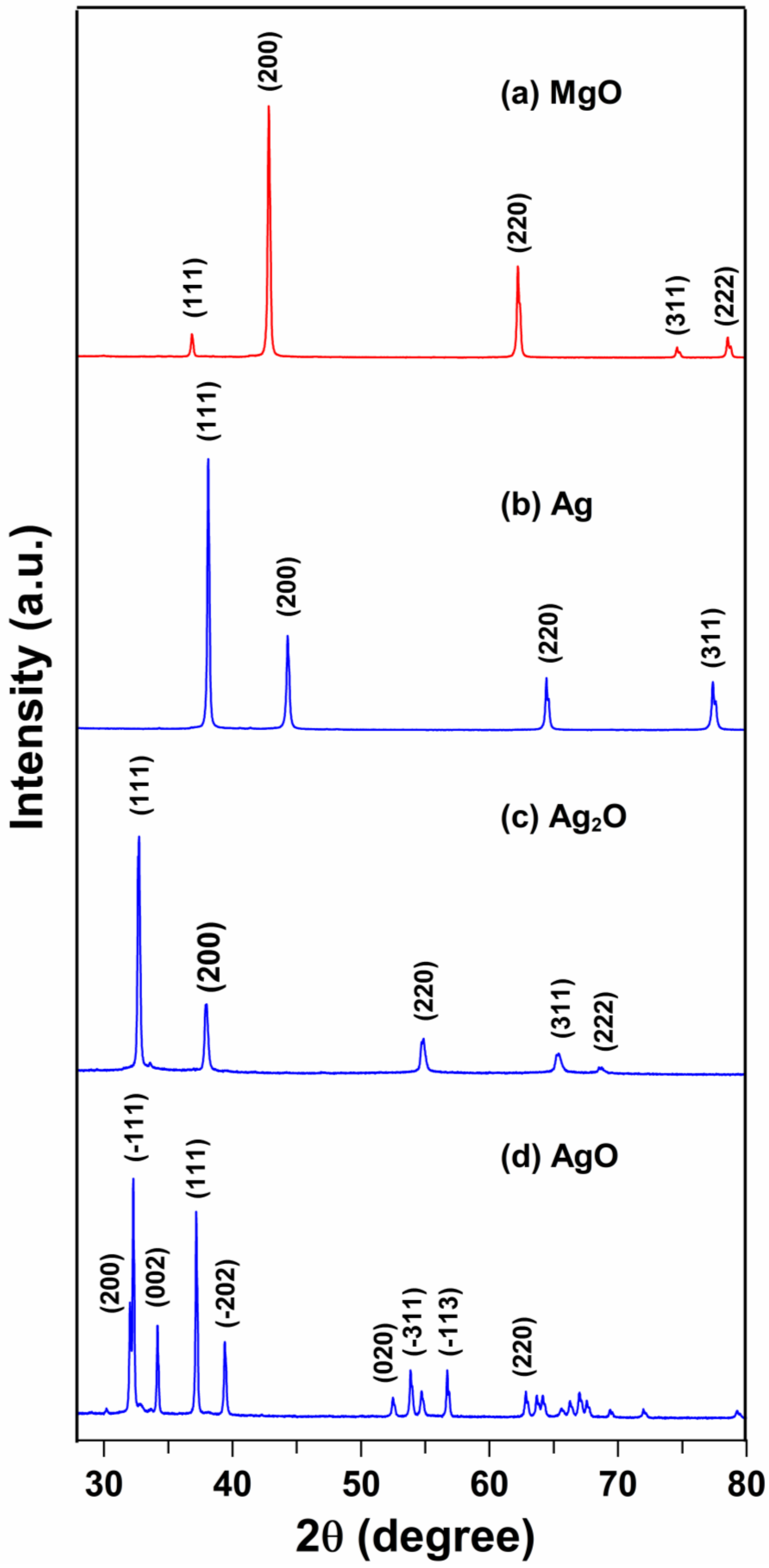

Figure S5. PXRD spectra of pure MgO (**a**), Ag metal (**b**), Ag_2O (**c**) and AgO (**d**) as standards.

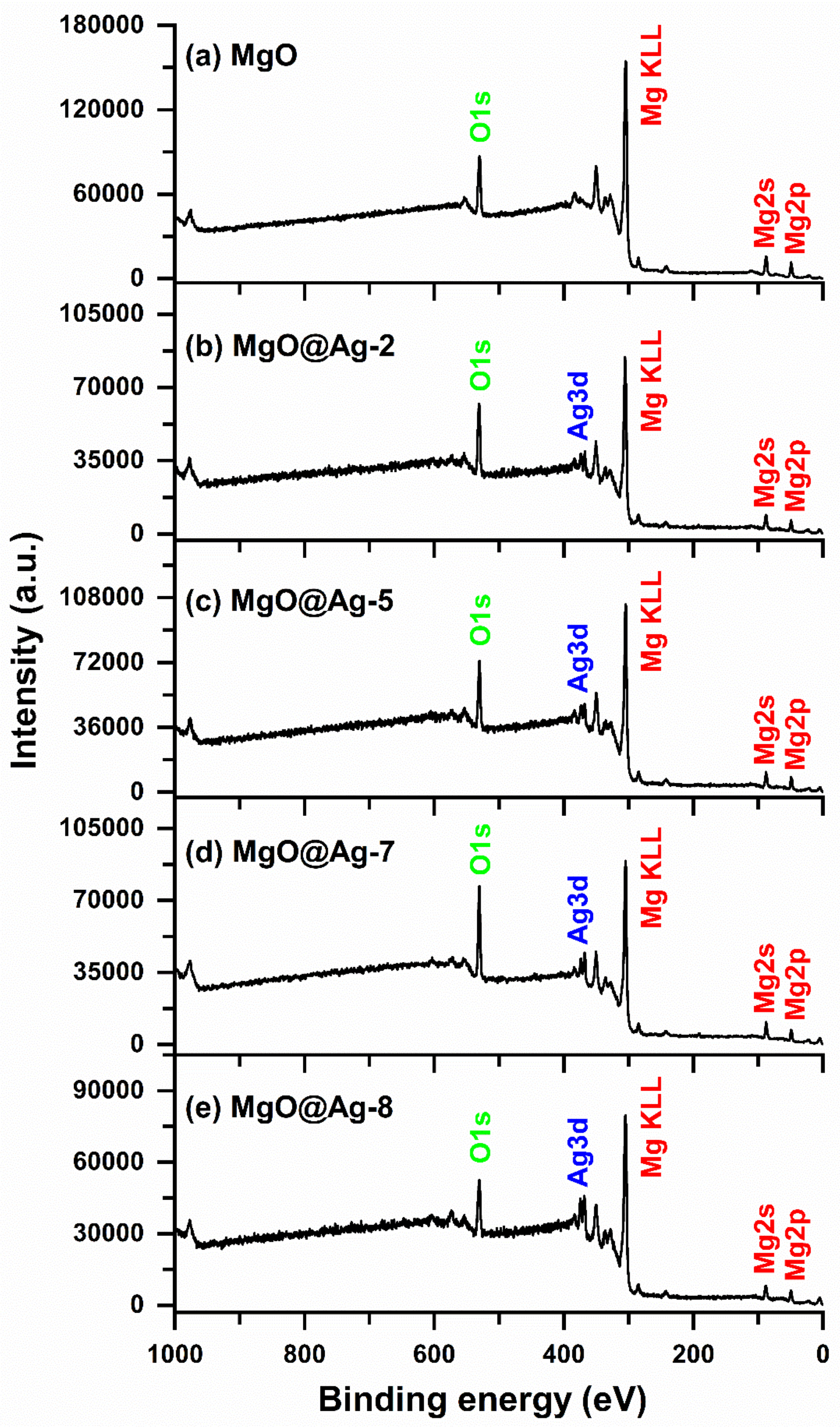

Figure S6. Survey scan XPS of MgO (**a**), MgO@Ag-2 (**b**), MgO@Ag-5 (**c**), MgO@Ag-7 (**d**), and MgO@Ag-8 (**e**).

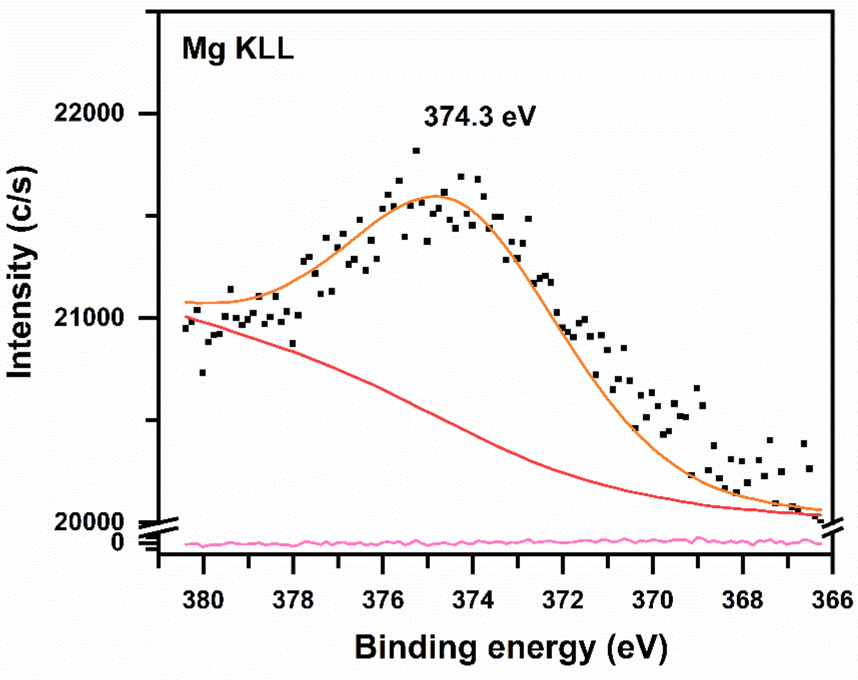

Figure S7. Mg KLL peak in Ag 3d region.

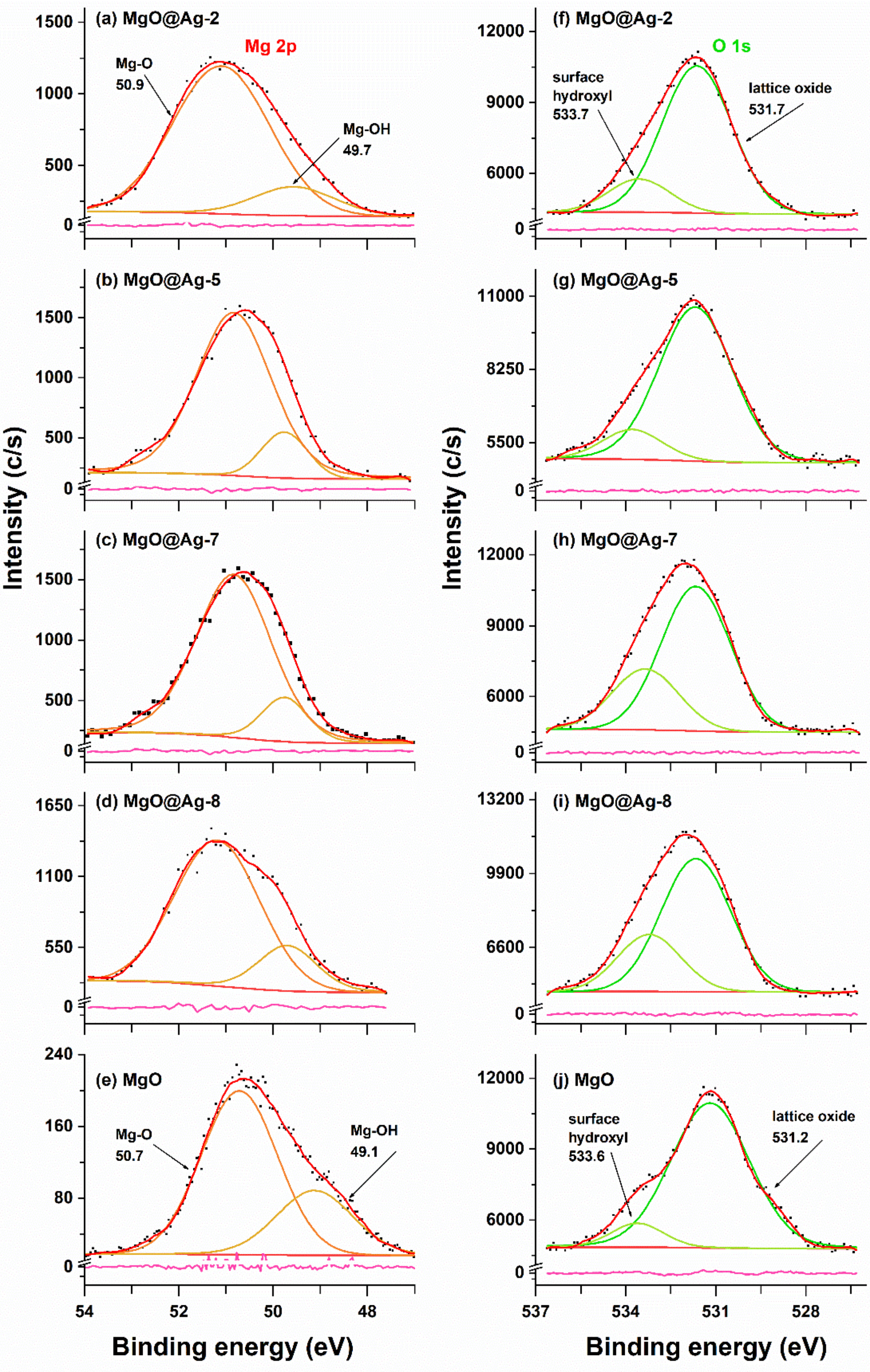

Figure S8. High resolution core level XPS of Mg2p and O1s regions for MgO@Ag-2 (**a**, **f**), MgO@Ag-5 (**b**, **g**), MgO@Ag-7 (**c**, **h**), MgO@Ag-8 (**d**, **i**), and MgO (**e**, **j**), respectively.

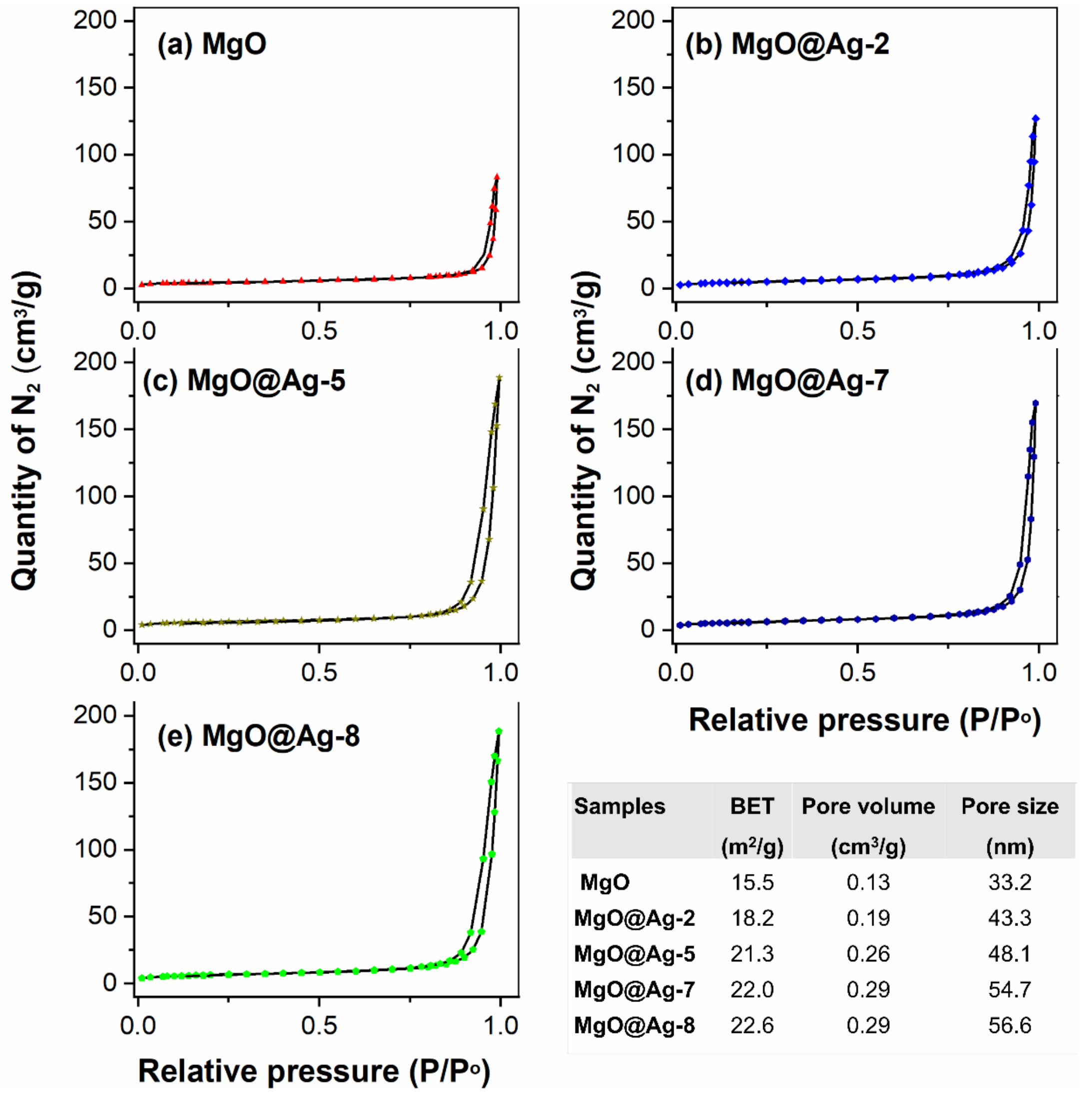

Samples	BET (m²/g)	Pore volume (cm³/g)	Pore size (nm)
MgO	15.5	0.13	33.2
MgO@Ag-2	18.2	0.19	43.3
MgO@Ag-5	21.3	0.26	48.1
MgO@Ag-7	22.0	0.29	54.7
MgO@Ag-8	22.6	0.29	56.6

Figure S9. Nitrogen adsorption–desorption isotherms of MgO (**a**), MgO@Ag-2 (**b**); MgO@Ag-5 (**c**); MgO@Ag-7 (**d**); MgO@Ag-8 (**e**) and their BET surface area, pore volume and pore size values (inset table).

Temperature Programmed Desorption (TPD)-CO_2. The strength of basic sites on the MgO surface can be divided into three categories based on the TPD-CO_2 desorption curves at different temperatures.[S3, S4] The weakly basic surface hydroxyl groups of MgO bind CO_2 as a bicarbonate species HCO_3^- on the surface which desorbs at 20-160 °C. The medium basicity lattice oxygen in the form of Mg^{2+} and O^{2-} pairs generates a bidentate carbonate species b-CO_3^{2-} on the surface that exhibits desorption features from 160–400 °C. Finally, the strongly basic O^{2-} species on MgO surface forms a monodentate (m-CO_3^{2-}) species and desorbs above

400 °C.[S4] The strength of basic sites on MgO can be improved by decreasing the number of surface hydroxyl groups at high calcination (dehydration) temperature (800 °C).[S5]

Table S2. TPD-CO_2 analysis results of MgO and MgO@Ag hybrid samples

Samples	Temp (° C)	CO_2 chemisorption (mmol/g)
MgO@Ag-8	430 + 770	2.4 + 0.3 = **2.7**
MgO@Ag-7	410 + 525 + 770	1.42 + 0.82 + 0.4 = **2.64**
MgO@Ag-5	400 + 770	1.12 + 0.15 = **1.27**
MgO@Ag-2	390 + 750	0.53 + 0.12 = **0.65**
MgO	380 + 750	0.32 + 0.10 = **0.42**

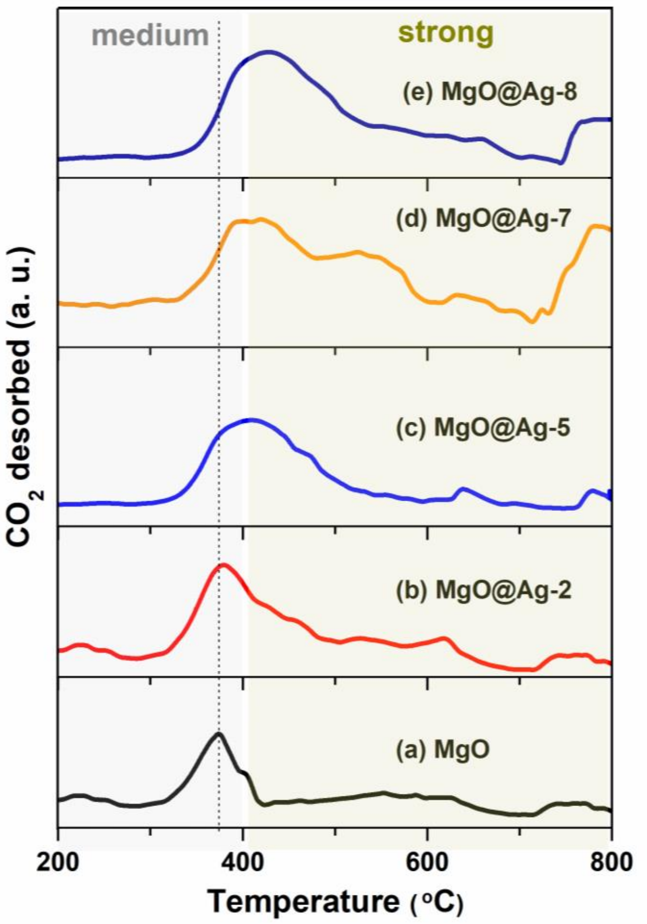

Figure S10. TPD-CO_2 curves of MgO and MgO@Ag hybrid samples.

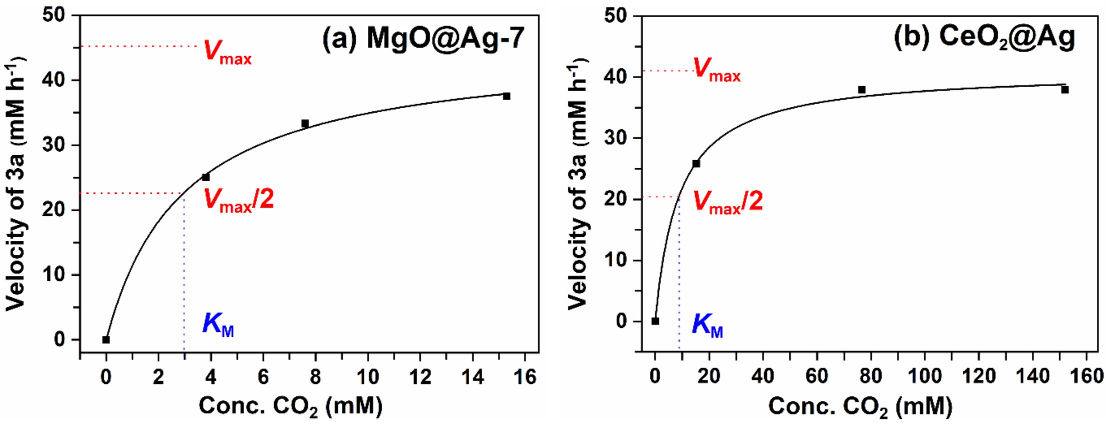

Figure S11. Nonlinear fitting of Michaelis-Menten plot of velocity of ester **3a** product formation vs. CO_2 concentration over the MgO@Ag-7 catalyst at 1 mmol scale (1 mL DMAc solvent) under optimized reaction conditions.

Table S3. Comparison of Michaelis-Menten constant (K_M) values of MgO@Ag-7 with CeO_2@Ag catalyst to afford ester **3a** under variation of CO_2 pressure.[a]

S. No.	Catalysts	K_M (mM)	V_{max} (mM h^{-1})	Velocity (mM h^{-1}) 1 atm CO_2	References
1	CeO_2@Ag[b]	8.80	41.03	25	Ref. S7
2	MgO@Ag-7[c]	2.95	45.19	37.5	Present work

[a] Henry constant (K_H) for CO_2 in DMF 65.3 atm M^{-1} (Ref. S6) and the concentrations of CO_2 are calculated from Henry's Law. The ester product **3a** concentrations are calculated from the mmol of isolated product **3a** (yields) in 1 mL solvent. [b] The pressures of CO_2 are 1, 5 and 10 atm. [c] The pressures CO_2 are 1 atm and 50%, 25% mixture of CO_2 with N_2 (1 atm).

Table S4. Comparison of MgO@Ag-7 with reported catalysts for CO_2 insertion in phenylacetylene and cinnamyl chloride to afford ester **3a**.[a]

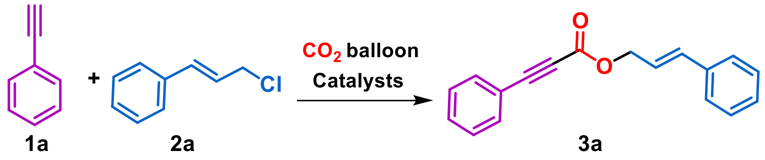

S. No.	Catalyst (mg)	Active species Ag (mmol)	Product Yield (%)	TON	TOF (h^{-1})	References
1	CeO_2@Ag (120 mg)[b]	0.03	62	20.6	0.9	Ref. S7
2	**MgO@Ag-7 (6 mg)**	**0.008**	**90**	**112**	**4.7**	**Present work**

[a] Reaction conditions: phenylacetylene (1.0 mmol, **1a**), cinnamyl chloride (1.0 mmol, **2a**), catalyst (mg), K_2CO_3 (1.2 mmol), CO_2 (1 atm), 60 °C, solvent (mL), 24 h. [b] Cinnamyl chloride (1.5 mmol, **2a**) and Cs_2CO_3 (2.0 mmol).

Table S5. Comparison of MgO@Ag-7 with reported catalysts for CO_2 insertion in phenylacetylene to afford phenylpropiolic acid.[a]

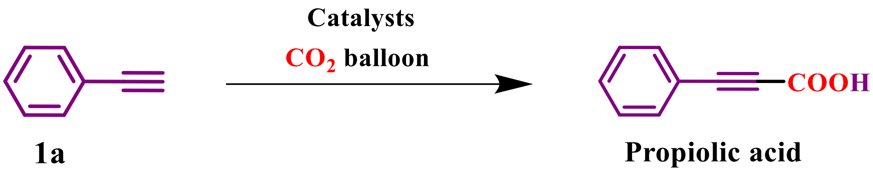

S. No.	Catalyst (mg)	Active site Ag (mmol)	Product Yield (%)	TON	TOF (h^{-1})	References
1	MIL-101-Cr@Ag (70 mg)	0.027	96.5	36	2.4	Ref. S8
2	MIL-100-Fe@Ag (70 mg)	0.022	94.6	43	2.9	Ref. S9
3	UIO-66-Zr@Ag (70 mg)	0.046	97.7	21	1.4	Ref. S9
3	ZIF-8-Zn@Ag (50 mg)[c]	0.045	97	87	5.3	Ref. S10
4	Flower MgO@Ag (50 mg)	0.021	98	47	3.9	Ref. S11
5	**MgO@Ag-7 (6 mg)[b]**	**0.008**	**97**	**121**	**10**	**Present work**

[a]Reaction conditions: phenylacetylene (1.0 mmol), catalyst, Cs_2CO_3 (1.5 mmol), CO_2 (1.0 atm), 50 °C, solvent (5 mL), 15 h. [b]K_2CO_3 (1.2 mmol). [c]Phenylacetylene (4.0 mmol), K_2CO_3 (7.2 mmol), 12 h.

Table S6: E-factor comparison of present work with reported catalysts to afford ester **3a**.

E-factor	Phenylacetylene (eq)	Allylic chloride (eq)	Base (eq)	Solvent (mL)	Catalyst	References
40.9	1	1.5	2	20.0	(IPr)CuCl.	Ref. S12
40.7	1	1.5	1.5	20.0	AgI	Ref S13
21.2	1	1.5	2	5.0	CeO_2@Ag	Ref. S7
2.8	**1**	**1**	**1.2**	**0.5**	**MgO@Ag[a]**	**Our work**

[a]The calculated E-factor = 22.2 for reported flower MgO@Ag catalyst (Ref. S10) to afford phenylpropiolic acid is 10-fold higher than the present MgO@Ag catalyst.

Characterization data of CO_2 inserted products

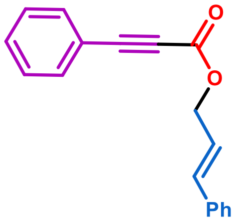

Cinnamyl 3-phenylpropiolate (**3a**)

TLC *Rf* = 0.16 (5% ethyl acetate/hexanes) [silica gel, UV]

Physical state: colourless liquid

^{1}H NMR (400 MHz, $CDCl_3$): 7.59-7.61 (m, 2H), 7.28-7.48 (m, 8H), 6.74 (d, 1H, *J* = 15.63 Hz), 6.34 (dt, 1H, *J* = 6.64, 16.02 Hz), 4.90 (dd, 2H, *J* = 1.17, 6.25 Hz) ppm; **^{13}C NMR (100 MHz, $CDCl_3$)**: 153.84, 135.98, 135.37, 133.03, 130.69, 128.64, 128.58, 128.27, 122.06, 119.56, 86.63, 80.47, 66.55 ppm; **IR (thin film):** 2219, 1708, 1280, 1168, 963, 745, 689 cm^{-1}; **HRMS**: [M-H] calcd for $C_{18}H_{13}O_2$: 261.0910, found 261.0911.

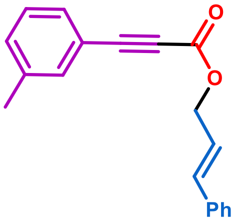

Cinnamyl 3-(p-tolyl)propiolate (**3b**)

TLC *Rf* = 0.16 (5% ethyl acetate/hexanes) [silica gel, UV]

Physical state: Yellow liquid

^{1}H NMR (400 MHz, $CDCl_3$): 7.49 (d, 2H, *J* = 8.20 Hz), 7.34-7.43 (m, 2H), 7.28-7.36 (m, 3H), 7.18 (d, 2H, *J* = 8.20 Hz), 6.73 (d, 1H, *J* = 15.63 Hz), 6.34 (dt, 1H, *J* = 6.64, 16.02 Hz), 4.89 (dd, 2H, *J* = 1.17, 6.64 Hz), 2.38 (s, 3H) ppm; **^{13}C NMR (100 MHz, $CDCl_3$)**: 153.99, 141.39, 136.04, 135.29, 133.05, 129.38, 129.30, 128.64, 128.49, 128.25, 126.74, 126.51, 126.03, 122.18, 116.45, 87.22, 80.16, 66.47, 21.73 ppm; **IR (thin film):** 2217, 1709, 1286, 1189, 1167, 965, 746 cm^{-1}; **HRMS**: [M-H] calcd for $C_{19}H_{17}O_2$: 275.1067, found 275.1068.

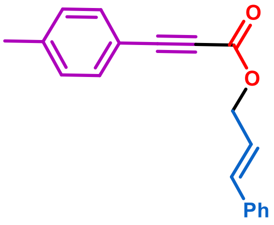

Cinnamyl 3-(m-tolyl)propiolate (**3c**)

TLC *Rf* = 0.16 (5% ethyl acetate/hexanes) [silica gel, UV]

Physical state: colourless liquid

^{1}H NMR (400 MHz, $CDCl_3$): 7.38-7.40 (m, 4H), 7.31-7.34 (m, 3H), 7.24-7.25 (m, 2H), 6.71 (d, 1H, *J* = 16.11 Hz), 6.32 (dt, 1H, *J* = 6.83, 15.62 Hz), 4.87 (d, 2H, *J* = 6.83 Hz), 2.33 (s, 3H) ppm; **^{13}C NMR (100 MHz, $CDCl_3$)**: 153.86, 138.39, 136.00, 135.26, 133.51, 131.61, 130.13, 128.62, 128.46, 128.24, 126.71, 122.12, 119.34, 86.96, 80.20, 66.47, 21.13 ppm; **IR (thin film):** 2218, 1709, 1213, 1154, 744, 667 cm^{-1}; **HRMS**: [M-H] calcd for $C_{19}H_{17}O_2$: 275.1067, found 275.1068.

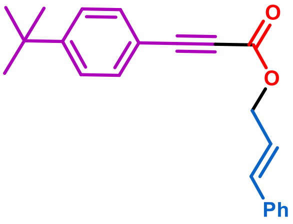

Cinnamyl 3-(4-(tert-butyl)phenyl)propiolate (**3d**)

TLC *Rf* = 0.38 (5% ethyl acetate/hexanes) [silica gel, UV]

Physical state: colourless liquid

^{1}H NMR (400 MHz, $CDCl_3$): 7.54 (d, 2H, *J* = 8.60 Hz), 7.28-7.53 (m, 7H), 6.74 (d, 1H, *J* = 16.02 Hz), 6.35 (dt, 1H, *J* = 6.64, 16.02 Hz), 4.89 (dd, 2H, *J* = 1.17, 6.64 Hz), 1.32 (s, 9H) ppm; **^{13}C NMR (100 MHz, $CDCl_3$)**: 154.42, 154.01, 136.03, 135.29, 132.95, 128.64, 128.49, 128.25, 127.69, 126.74, 126.51, 126.03, 125.66, 122.18, 116.44, 87.21, 80.12, 66.48, 35.07, 31.05 ppm; **IR (thin film):** 2222, 1708, 1214, 743, 667 cm^{-1}; **HRMS**: [M-H] calcd for $C_{22}H_{21}O_2$: 317.1536, found 317.1538.

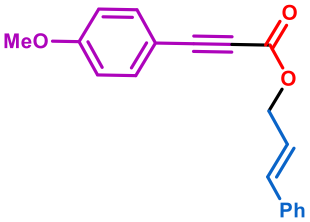

Cinnamyl 3-(4-methoxyphenyl)propiolate (**3e**)

TLC *Rf* = 0.14 (5% ethyl acetate/hexanes) [silica gel, UV]

Physical state: colourless solid, MP 51–54 °C

^{1}H NMR (400 MHz, CDCl$_3$): 7.53 (d, 2H, *J* = 8.59 Hz), 7.28-7.41 (m, 5H), 6.87 (d, 2H, *J* = 8.98 Hz), 6.71 (d, 1H, *J* = 16.01 Hz), 6.32 (dt, 1H, *J* = 6.64, 15.62 Hz), 4.87 (dd, 2H, *J* = 1.17, 6.44 Hz), 3.81 (s, 3H) ppm; **^{13}C NMR (100 MHz, CDCl$_3$)**: 161.53, 154.05, 135.99, 135.16, 134.95, 128.59, 128.19, 126.68, 122.19, 114.27, 111.25, 87.49, 79.93, 66.35, 55.34 ppm; **IR (thin film):** 2211, 1702, 1603, 1159, 964, 745, 666 cm^{-1}; **HRMS**: [M+H] calcd for $C_{19}H_{17}O_3$: 293.1172, found 293.1174.

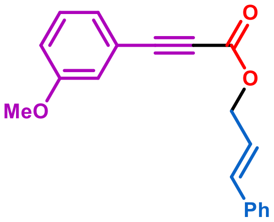

Cinnamyl 3-(3-methoxyphenyl)propiolate (**3f**)

TLC *Rf* = 0.27 (5% ethyl acetate/hexanes) [silica gel, UV]

Physical state: Pale yellow liquid

^{1}H NMR (400 MHz, CDCl$_3$): 7.39-7.42 (m, 2H), 7.34 (t, 2H, *J* = 7.32 Hz), 7.26-7.29 (m, 2H), 7.19-7.20 (m, 1H), 7.10-7.11 (m, 1H), 6.99-7.02 (m, 1H), 6.73 (d, 1H, *J* = 16.11 Hz), 6.34 (dt, 1H, *J* = 6.83, 15.62 Hz), 4.89 (d, 2H, *J* = 6.83 Hz), 3.81 (s, 3H) ppm; **^{13}C NMR (100 MHz, CDCl$_3$)**: 159.38, 153.81, 135.99, 135.41, 129.71, 128.65, 128.30, 126.74, 125.58, 122.06, 120.48, 117.64, 117.45, 86.58, 80.17, 66.58, 55.39 ppm; **IR (thin film):** 2221, 1710, 1598, 1215, 751 cm^{-1}; **HRMS**: [M-H] calcd for $C_{19}H_{15}O_3$: 291.1016, found 291.1014.

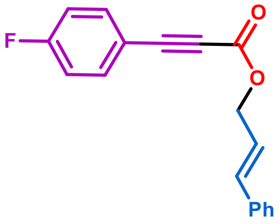

Cinnamyl 3-(4-fluorophenyl)propiolate (**3g**)

TLC *Rf* = 0.13 (5% ethyl acetate/hexanes) [silica gel, UV]

Physical state: colourless liquid

^{1}H NMR (400 MHz, CDCl$_3$): 7.58-7.61 (m, 2H), 7.39-7.42 (m, 2H), 7.28-7.35 (m, 3H), 7.08 (t, 2H, *J* = 8.60 Hz), 6.73 (d, 1H, *J* = 16.02 Hz), 6.33 (dt, 1H, *J* = 6.64, 16.02 Hz), 4.89 (dd, 2H, *J* = 0.78, 6.64 Hz) ppm; **^{13}C NMR (100 MHz, CDCl$_3$)**: 163.96 (d, $^1J_{C\text{-}F}$ = 254.11 Hz), 153.73, 135.97, 135.46, 135.30 (d, $^3J_{C\text{-}F}$ = 8.63 Hz), 128.65, 128.56, 128.32, 126.73, 126.51, 121.99, 116.15 (d, $^2J_{C\text{-}F}$ = 22.05 Hz), 85.57, 80.40, 66.59 ppm; **IR (thin film):** 2243, 1725, 1214, 743, 667 cm^{-1}; **HRMS**: [M-H] calcd for $C_{18}H_{12}FO_2$: 279.0816, found 279.0816.

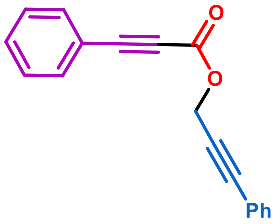

3-Phenylprop-2-yn-1-yl 3-phenylpropiolate (**3h**)

TLC *Rf* = 0.16 (5% ethyl acetate/hexanes) [silica gel, UV]

Physical state: white solid, MP 50–52 °C

^{1}H NMR (400 MHz, CDCl$_3$): 7.59-7.62 (m, 2H), 7.45-7.49 (m, 3H), 7.32-7.40 (m, 5H), 5.07 (s, 2H) ppm; **^{13}C NMR (100 MHz, CDCl$_3$)**: 153.31, 133.12, 131.97, 130.88, 128.94, 128.63, 128.34, 121.95, 119.39, 87.50, 87.35, 81.98, 80.04, 54.21 ppm; **IR (thin film):** 2220, 1710, 1598, 1282, 1166, 756 cm^{-1}; **HRMS**: [M+H] calcd for $C_{18}H_{13}O_2$: 261.0910, found 261.0911.

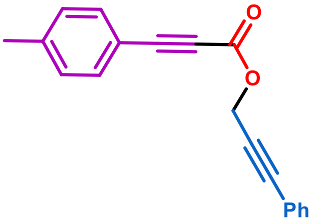

3-Phenylprop-2-yn-1-yl 3-(p-tolyl)propiolate (**3i**)

TLC *Rf* = 0.2 (5% ethyl acetate/hexanes) [silica gel, UV]

Physical state: Yellow liquid

^{1}H NMR (400 MHz, CDCl$_3$): 7.50 (d, 2H, *J* = 8.30 Hz), 7.47-7.49 (m, 3H), 7.32-7.34 (m, 2H), 7.19 (d, 2H, *J* = 7.81 Hz), 5.06 (s, 2H), 2.39 (s, 3H) ppm; **^{13}C NMR (100 MHz, CDCl$_3$)**: 153.43, 141.58, 133.25, 133.11, 131.95, 129.85, 129.41, 128.89, 128.77, 128.43, 128.32, 121.98, 116.27, 88.09, 87.27, 82.05, 79.73, 54.12, 21.75 ppm; **IR (thin film):** 2218, 1709, 1586, 1214, 743 cm^{-1}; **HRMS**: [M+H] calcd for $C_{19}H_{15}O_2$: 275.1067, found 275.1067.

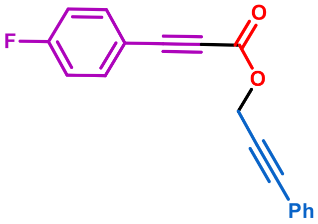

3-Phenylprop-2-yn-1-yl 3-(4-fluorophenyl)propiolate (**3j**)

TLC *Rf* = 0.13 (5% ethyl acetate/hexanes) [silica gel, UV]

Physical state: Yellow liquid

^{1}H NMR (400 MHz, CDCl$_3$): 7.60 (dd, 2H, *J* = 5.37, 8.79 Hz), 7.47-7.48 (m, 2H), 7.30-7.35 (m, 3H), 7.08 (t, 2H, *J* = 8.79 Hz), 5.06 (s, 2H) ppm; **^{13}C NMR (100 MHz, CDCl$_3$)**: 164.06 (d, $^{1}J_{C\text{-}F}$ = 254.11 Hz), 153.19, 135.40 (d, $^{3}J_{C\text{-}F}$ = 8.63 Hz), 131.95, 128.95, 128.43, 121.92, 116.20 (d, $^{2}J_{C\text{-}F}$ = 22.05 Hz), 115.50, 87.39, 86.42, 81.91, 79.97, 54.24 ppm; **IR (thin film):** 2221, 1600, 1288, 1154, 756 cm^{-1}; **HRMS**: [M+H] calcd for $C_{18}H_{12}FO_2$: 279.0816, found 279.0818.

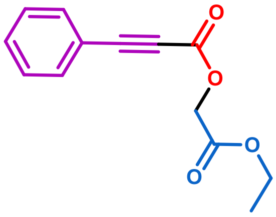

2-Ethoxy-2-oxoethyl 3-phenylpropiolate (**3k**)

TLC *Rf* = 0.1 (5% ethyl acetate/hexanes) [silica gel, UV]

Physical state: Colourless liquid

^{1}H NMR (400 MHz, CDCl$_3$): 7.60 (d, 2H, *J* = 6.83 Hz), 7.45-7.48 (m, 1H), 7.38 (t, 2H, *J* = 7.56 Hz), 4.74 (s, 2H), 4.26 (q, 2H, *J* = 7.32 Hz), 1.30 (t, 3H, *J* = 7.32 Hz) ppm; **^{13}C NMR (100 MHz, CDCl$_3$)**: 166.93, 153.15, 133.11, 130.90, 128.59, 119.28, 88.05, 79.78, 61.69, 61.63, 14.08 ppm; **IR (thin film):** 2227, 1758, 1717, 1293, 1164, 755, 689 cm^{-1}; **HRMS**: [M+H] calcd for $C_{13}H_{13}O_4$: 233.0808, found 233.0808.

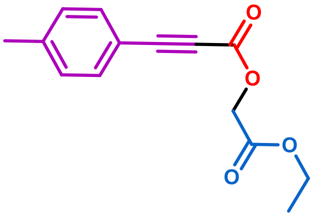

2-Ethoxy-2-oxoethyl 3-(p-tolyl)propiolate (**3l**)

TLC *Rf* = 0.07 (5% ethyl acetate/hexanes) [silica gel, UV]

Physical state: White solid, MP 60-63 °C

^{1}H NMR (400 MHz, CDCl$_3$): 7.49 (d, 2H, *J* = 8.20 Hz), 7.18 (d, 2H, *J* = 8.20 Hz), 4.73 (s, 2H), 4.26 (q, 2H, *J* = 7.03 Hz), 2.38 (s, 3H), 1.29 (t, 3H, *J* = 7.42 Hz) ppm; **^{13}C NMR (100 MHz, CDCl$_3$)**: 166.98, 153.26, 141.63, 133.11, 133.05, 129.38, 116.14, 88.64, 79.47, 61.66, 61.56, 21.69, 14.10 ppm; **IR (thin film):** 2225, 1724, 1718, 1214, 1162, 743, 667 cm^{-1}; **HRMS**: [M+H] calcd for $C_{14}H_{15}O_4$: 247.0965, found 247.0964.

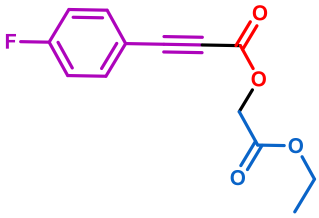

2-Ethoxy-2-oxoethyl 3-(4-fluorophenyl)propiolate (**3m**)

TLC *Rf* = 0.07 (5% ethyl acetate/hexanes) [silica gel, UV]

Physical state: Pale yellow liquid

^{1}H NMR (400 MHz, CDCl$_3$): 7.61 (dd, 2H, *J* = 5.37, 8.79 Hz), 7.07-7.11 (m, 2H), 4.74 (s, 2H), 4.26 (q, 2H, *J* = 7.32, 6.83 Hz), 1.31 (t, 3H, *J* = 7.32, 6.83 Hz) ppm; **^{13}C NMR (100 MHz, CDCl$_3$)**: 166.91, 164.09 (d, $^1J_{C\text{-}F}$ = 254.11 Hz), 153.07, 135.45 (d, $^3J_{C\text{-}F}$ = 9.59 Hz), 116.21 (d, $^2J_{C\text{-}F}$ = 23.01 Hz), 115.43, 87.03, 79.75, 61.76, 61.67, 14.11 ppm; **IR (thin film):** 2229, 1758, 1712, 1600, 1298, 1154, 840, 753 cm^{-1}; **HRMS**: [M+H] calcd for $C_{13}H_{12}FO_4$: 251.0714, found 251.0713.

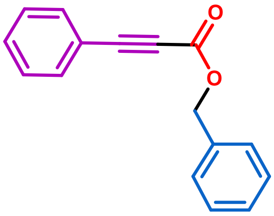

Benzyl 3-phenylpropiolate (**3n**)

TLC *Rf* = 0.16 (5% ethyl acetate/hexanes) [silica gel, UV]

Physical state: Colourless liquid

^{1}H NMR (400 MHz, CDCl$_3$): 7.58 (d, 2H, *J* = 8.59 Hz), 7.35-7.47 (m, 8H), 5.27 (s, 2H) ppm; **^{13}C NMR (100 MHz, CDCl$_3$)**: 153.88, 134.92, 132.99, 130.67, 128.92, 128.65, 128.59, 128.55, 128.29, 119.53, 86.71, 80.49, 67.68 ppm; **IR (thin film):** 2225, 1712, 1288, 1162, 758, 689 cm^{-1}; **HRMS**: [M+H] calcd for $C_{16}H_{13}O_2$: 237.0910, found 237.0911.

Benzyl 3-(p-tolyl)propiolate (**3o**)

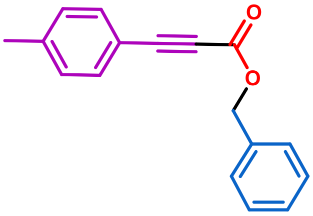

TLC *Rf* = 0.16 (5% ethyl acetate/hexanes) [silica gel, UV]

Physical state: White solid, MP 62–65 °C

^{1}H NMR (400 MHz, CDCl$_3$): 7.48 (d, 2H, *J* = 8.20 Hz), 7.36-7.44 (m, 5H), 7.18 (d, 2H, *J* = 8.20 Hz), 5.27 (s, 2H), 2.38 (s, 3H) ppm; **^{13}C NMR (100 MHz, CDCl$_3$)**: 154.02, 141.35, 134.99, 133.00, 129.35, 128.64, 128.59, 116.39, 87.28, 80.17, 67.60, 21.69 ppm; **IR (thin film):** 2214, 1703, 1605, 1285, 1158, 815, 745 cm^{-1}; **HRMS**: [M+H] calcd for $C_{17}H_{15}O_2$: 251.1067, found 251.1068.

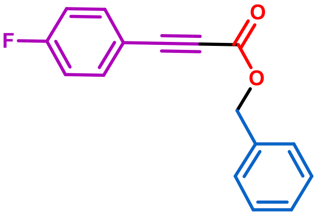

Benzyl 3-(4-fluorophenyl)propiolate (**3p**)

TLC *Rf* = 0.23 (5% ethyl acetate/hexanes) [silica gel, UV]

Physical state: Colourless liquid

^{1}H NMR (400 MHz, CDCl$_3$): 7.58 (dd, 2H, *J* = 5.37, 8.79 Hz), 7.35-7.44 (m, 5H), 7.07 (t, 2H, *J* = 8.79 Hz), 5.27 (s, 2H) ppm; **^{13}C NMR (100 MHz, CDCl$_3$)**: 164.09 (d, $^1J_{C\text{-}F}$ = 254.11 Hz), 153.92, 135.44 (d, $^3J_{C\text{-}F}$ = 8.63 Hz), 128.84, 128.81, 128.79, 116.29 (d, $^2J_{C\text{-}F}$ = 23.01 Hz), 115.82, 85.81, 80.60, 67.91 ppm; **IR (thin film):** 2219, 1704, 1599, 1504, 1287, 1170, 744 cm^{-1}; **HRMS**: [M+H] calcd for $C_{16}H_{12}FO_2$: 255.0816, found 255.0817.

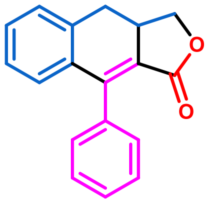

9-Phenyl-3a,4-dihydronaphtho[2,3-c]furan-1(3*H*)-one (**4a**)

TLC *Rf* = 0.10 (15% ethyl acetate/hexanes) [silica gel, UV]

Physical state: Yellow solid, MP 160-164 °C

^{1}H NMR (400 MHz, CDCl$_3$): 7.33-7.39 (m, 3H), 7.19-7.25 (m, 4H), 7.12 (t, 1H, *J* = 7.32, 6.83 Hz), 6.91 (d, 1H, *J* = 7.81 Hz), 4.67 (t, 1H, *J* = 8.79 Hz), 3.99 (t, 1H, *J* = 8.79 Hz), 3.36-3.44 (m, 1H), 3.01 (dd, 1H, *J* = 6.83, 14.89 Hz), 2.83 (t, 1H, *J* = 15.13, 15.62 Hz) ppm; **^{13}C NMR (100 MHz, CDCl$_3$)**: 168.24, 147.34, 135.92, 135.44, 134.29, 129.86, 129.15, 128.61, 128.55, 128.09, 127.87, 127.29, 126.48, 122.14, 71.21, 33.59, 33.03 ppm; **IR (thin film):** 3019, 1725, 1214, 743 cm^{-1}; **HRMS**: [M+H] calcd for $C_{18}H_{15}O_2$: 263.1067, found 263.1069.

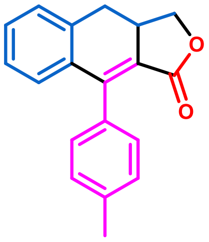

9-(p-Tolyl)-3a,4-dihydronaphtho[2,3-c]furan-1(3*H*)-one (**4b**)

TLC *Rf* = 0.10 (15% ethyl acetate/hexanes) [silica gel, UV]

Physical state: Yellow solid, MP 170-173 °C

^{1}H NMR (400 MHz, CDCl$_3$): 7.13-7.25 (m, 7H), 6.96 (t, 1H, *J* = 7.81 Hz), 4.69 (t, 1H, *J* = 8.79 Hz), 4.00 (t, 1H, *J* = 8.79 Hz), 3.37-3.45 (m, 1H), 3.01 (dd, 1H, *J* = 6.34, 15.13 Hz), 2.84 (t, 1H, *J* = 15.13, 15.62 Hz), 2.38 (s, 3H) ppm; **^{13}C NMR (100 MHz, CDCl$_3$)**: 168.31, 147.56, 138.39, 136.08, 135.49, 131.22, 129.97, 129.77, 129.23, 128.80, 128.59, 128.03, 127.21, 121.79, 71.15, 35.62, 33.08, 21.46 ppm; **IR (thin film):** 3021, 1745, 1221, 1062, 1015, 763 cm^{-1}; **HRMS**: [M+H] calcd for $C_{19}H_{17}O_2$: 277.1223, found 277.1225.

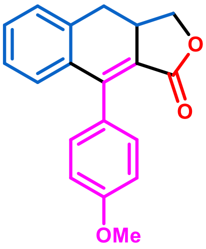

9-(4-Methoxyphenyl)-3a,4-dihydronaphtho[2,3-c]furan-1(3*H*)-one (**4c**)

TLC *Rf* = 0.07 (15% ethyl acetate/hexanes) [silica gel, UV]

Physical state: Yellow solid, MP 168-172 °C

^{1}H NMR (400 MHz, CDCl$_3$): 7.27-7.34 (m, 4H), 7.17-7.21 (m, 1H), 7.02 (d, 1H, *J* = 7.81 Hz), 6.97 (d, 2H, *J* = 8.98 Hz), 4.72 (t, 1H, *J* = 8.59, 8.98 Hz), 4.04 (t, 1H, *J* = 8.59 Hz), 3.87 (s, 3H), 3.39-3.49 (m, 1H), 3.04 (dd, 1H, *J* = 6.25, 14.84 Hz), 2.89 (t, 1H, *J* = 15.23 Hz) ppm; **^{13}C NMR (100 MHz, CDCl$_3$)**: 168.41, 159.84, 147.34, 136.16, 135.62, 131.46, 129.74, 129.26, 127.99, 127.16, 126.16, 121.44, 113.19, 71.10, 55.19, 35.64, 33.11 ppm; **IR (thin film):** 2898, 1744, 1607, 1493, 1246, 740 cm^{-1}; **HRMS**: [M+H] calcd for $C_{19}H_{16}O_3$: 293.1172, found 293.1174.

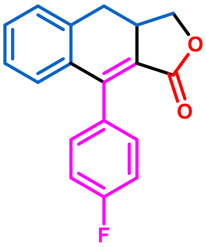

9-(4-Fluorophenyl)-3a,4-dihydronaphtho[2,3-c]furan-1(3*H*)-one (**4d**)

TLC *Rf* = 0.10 (15% ethyl acetate/hexanes) [silica gel, UV]

Physical state: Yellow solid, MP 188-191 °C

^{1}H NMR (400 MHz, CDCl$_3$): 7.28-7.40 (m, 4H), 7.18-7.23 (m, 1H), 7.11-7.15 (m, 2H), 6.95 (d, 1H, *J* = 7.81 Hz), 4.74 (t, 1H, *J* = 8.59, 8.98 Hz), 4.05 (t, 1H, *J* = 8.59, 8.98 Hz), 3.41-3.51 (m, 1H), 3.07 (dd, 1H, *J* = 6.64, 14.84 Hz), 2.88 (t, 1H, *J* = 15.62 Hz) ppm; **^{13}C NMR (100 MHz, CDCl$_3$)**: 168.44, 163.17 (d, $^1J_{C\text{-}F}$ = 236.16 Hz), 146.54, 135.80 (d, $^2J_{C\text{-}F}$ = 29.92 Hz), 130.19, 129.19, 128.79, 128.35, 127.53, 126.66, 122.61, 120.74, 115.17 (d, $^3J_{C\text{-}F}$ = 21.48 Hz), 71.42, 35.78, 33.16 ppm; **IR (thin film):** 3019, 1742, 1598, 1214, 743 cm^{-1}; **HRMS**: [M+H] calcd for $C_{18}H_{14}FO_2$: 281.0972, found 281.0975.

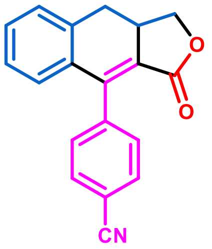

4-(3-oxo-1,3,9,9a-tetrahydronaphtho[2,3-c]furan-4-yl)benzonitrile (**4e**)

TLC *Rf* = 0.10 (15% ethyl acetate/hexanes) [silica gel, UV]

Physical state: Yellow solid, MP 189-193 °C

^{1}H NMR (400 MHz, CDCl$_3$): 7.73 (d, 2H, *J* = 8.30 Hz), 7.31-7.43 (m, 4H), 7.21 (d, 1H, *J* = 7.32 Hz), 6.83 (d, 1H, *J* = 7.81 Hz), 4.77 (t, 1H, *J* = 8.79 Hz), 4.08 (t, 1H, *J* = 8.79 Hz), 3.45-3.53 (m, 1H), 3.11 (dd, 1H, *J* = 6.83, 15.13 Hz), 2.90 (t, 1H, *J* = 15.13 Hz) ppm; **^{13}C NMR (100 MHz, CDCl$_3$)**: 167.94, 145.07, 139.27, 135.29, 134.81, 131.86, 131.72, 131.02, 130.39, 128.62, 128.43, 127.55, 127.44, 123.56, 121.39, 118.69, 112.44, 71.39, 35.52, 32.75 ppm; **IR (thin film):** 3019, 2230, 1741, 1596, 1211, 742 cm^{-1}; **HRMS**: [M+H] calcd for $C_{19}H_{14}NO_2$: 288.1025, found 288.1035.

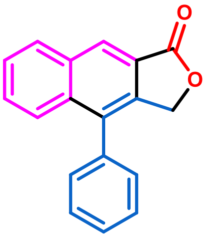

4-Phenylnaphtho[2,3-c]furan-1(3*H*)-one (**5a**)

TLC *Rf* = 0.4 (15% ethyl acetate/hexanes) [silica gel, UV]

Physical state: Yellow solid, MP 158–160 °C

^{1}H NMR (400 MHz, CDCl$_3$): 8.53 (s, 1H), 8.09 (d, 1H, *J* = 7.03 Hz), 7.82 (d, 1H, *J* = 7.03 Hz), 7.49-7.62 (m, 5H), 7.39 (d, 2H, *J* = 6.64 Hz), 5.27 (s, 2H) ppm; **^{13}C NMR (100 MHz, CDCl$_3$)**: 171.19, 138.46, 135.83, 134.84, 133.71, 130.17, 129.37, 129.06, 128.46, 126.77, 126.46, 125.90, 122.99, 69.58 ppm; **IR (thin film):** 2918, 2849, 1755, 1632, 1512, 1493, 1233 cm^{-1}; **HRMS**: [M+Na] calcd for $C_{18}H_{12}O_2Na$: 283.0730, found 283.0731.

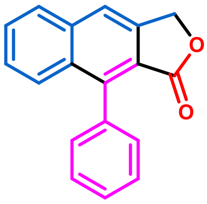

9-Phenylnaphtho[2,3-c]furan-1(3*H*)-one (5a')

TLC Rf = 0.2 (15% ethyl acetate/hexanes) [silica gel, UV]

Physical state: Yellow solid, MP 174–176 °C

^{1}H NMR (400 MHz, CDCl$_3$): 7.97 (d, 1H, *J* = 8.30 Hz), 7.91 (s, 1H), 7.82 (d, 1H, *J* = 8.79 Hz), 7.63-7.66 (m, 1H), 7.47-7.56 (m, 4H), 7.38-7.40 (m, 2H), 5.46 (s, 2H) ppm; **^{13}C NMR (100 MHz, CDCl$_3$)**: 169.57, 142.23, 140.12, 136.25, 134.44, 132.80, 130.04, 128.65, 128.30, 128.09, 128.01, 126.76, 120.29, 119.94, 68.17 ppm; **IR (thin film):** 2921, 2851, 1761, 1641, 1583, 1443, 1349, 1202 cm^{-1}; **HRMS**: [M+Na] calcd for $C_{18}H_{12}O_2Na$: 283.0730, found 283.0732.

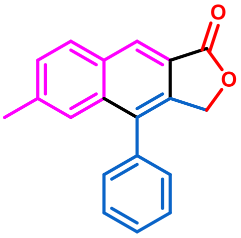

6-Methyl-4-phenylnaphtho[2,3-c]furan-1(3*H*)-one (5**b**)

TLC Rf = 0.4 (15% ethyl acetate/hexanes) [silica gel, UV]

Physical state: Yellow solid, MP 120–122 °C

^{1}H NMR (400 MHz, CDCl$_3$): 8.45 (s, 1H), 7.97 (d, 1H, *J* = 8.20 Hz), 7.49-7.58 (m, 4H), 7.43 (d, 1H, *J* = 8.60 Hz), 7.38 (d, 2H, *J* = 7.81 Hz), 5.22 (s, 2H), 2.46 (s, 3H) ppm; **^{13}C NMR (100 MHz, CDCl$_3$)**: 171.38, 139.49, 138.72, 136.04, 135.11, 133.29, 132.02, 129.95, 129.37, 129.14, 129.05, 128.35, 126.20, 124.71, 122.12, 69.57, 22.21 ppm; **IR (thin film):** 3046, 2921, 2858, 1765, 1659, 1529, 1444, 1345, 1235 cm^{-1}; **HRMS**: [M+Na] calcd for $C_{19}H_{14}O_2Na$: 297.0886, found 297.0889.

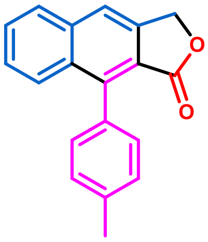

9-(p-Tolyl)naphtho[2,3-c]furan-1(3*H*)-one (5b')

TLC Rf = 0.2 (15% ethyl acetate/hexanes) [silica gel, UV]

Physical state: Yellow solid, MP 180–182 °C

^{1}H NMR (400 MHz, CDCl$_3$): 7.95 (d, 1H, *J* = 8.20 Hz), 7.89 (s, 1H), 7.85 (d, 1H, *J* = 8.60 Hz), 7.63 (t, 1H, *J* = 7.42 Hz), 7.47 (t, 1H, *J* = 7.42, 7.81 Hz), 7.35 (d, 2H, *J* = 7.81 Hz), 7.28 (d, 2H, *J* = 8.20 Hz), 5.44 (s, 2H), 2.48 (s, 3H) ppm; **^{13}C NMR (100 MHz,**

$CDCl_3$): 169.69, 142.48, 140.17, 138.02, 136.27, 132.94, 131.35, 129.97, 128.79, 128.61, 128.19, 128.09, 126.66, 120.09, 68.14, 21.49 ppm; **IR (thin film):** 2921, 2349, 1753, 1659, 1629, 1452, 1347, 1324, 1205, 1109 cm^{-1}; **HRMS**: [M+Na] calcd for $C_{19}H_{14}O_2Na$: 297.0886, found 297.0882.

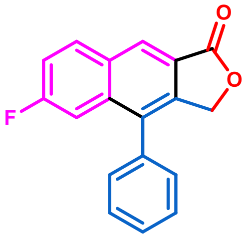

6-Fluoro-4-phenylnaphtho[2,3-c]furan-1(3*H*)-one (**5c**)

TLC Rf = 0.3 (15% ethyl acetate/hexanes) [silica gel, UV]

Physical state: Yellow crystals, MP 183–185 °C

^{1}H NMR (400 MHz, $CDCl_3$): 8.51 (s, 1H), 8.11 (dd, 1H, *J* = 5.86, 8.99 Hz), 7.51-7.59 (m, 3H), 7.37-7.43 (m, 4H), 5.27 (s, 2H) ppm; **^{13}C NMR (100 MHz, $CDCl_3$)**: 170.94, 162.62 (d, $^1J_{C\text{-}F}$ = 237.15 Hz), 139.59, 135.34, 132.76 (d, $^4J_{C\text{-}F}$ = 9.98 Hz), 130.80, 129.24 (d, $^5J_{C\text{-}F}$ = 7.67 Hz), 128.75, 126.43, 117.61 (d, $^2J_{C\text{-}F}$ = 26.09 Hz), 117.61 (d, $^3J_{C\text{-}F}$ = 23.02 Hz), 69.49 ppm; **IR (thin film):** 2918, 2849, 1766, 1659, 1630, 1513, 1450, 1345, 1288, 1138 cm^{-1}; **HRMS**: [M+Na] calcd for $C_{18}H_{11}O_2FNa$: 301.0635, found 301.0637.

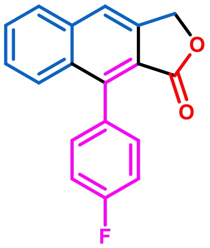

9-(4-Fluorophenyl)naphtho[2,3-c]furan-1(3*H*)-one (**5c'**)

TLC Rf = 0.2 (15% ethyl acetate/hexanes) [silica gel, UV];

Physical state: Yellow crystals, MP 194–196 °C.

^{1}H NMR (400 MHz, $CDCl_3$): 8.04 (d, 1H, *J* = 8.59 Hz), 7.99 (s, 1H), 7.86 (d, 1H, *J* = 8.59 Hz), 7.72 (t, 1H, *J* = 7.03, 7.81 Hz), 7.57 (t, 1H, *J* = 7.42, 7.81 Hz), 7.41-7.44 (m, 2H), 7.29-7.32 (m, 2H), 5.52 (s, 2H) ppm; **^{13}C NMR (100 MHz, $CDCl_3$)**: 169.63, 141.06, 140.11, 136.29, 132.82, 131.86 (d, $^2J_{C\text{-}F}$ = 8.44 Hz), 130.16 (d, $^3J_{C\text{-}F}$ = 3.84 Hz), 128.76, 128.24, 127.80, 126.96, 120.55, 120.11, 115.20 (d, $^1J_{C\text{-}F}$ = 21.48 Hz), 68.22 ppm; **IR (thin film):** 2917, 2849, 1763, 1691, 1630, 1548, 1502, 1324, 1200, 1156 cm^{-1}; **HRMS**: [M+Na] calcd for $C_{18}H_{11}O_2FNa$: 301.0635, found 301.0637.

NMR Characterization spectra of CO_2 inserted products

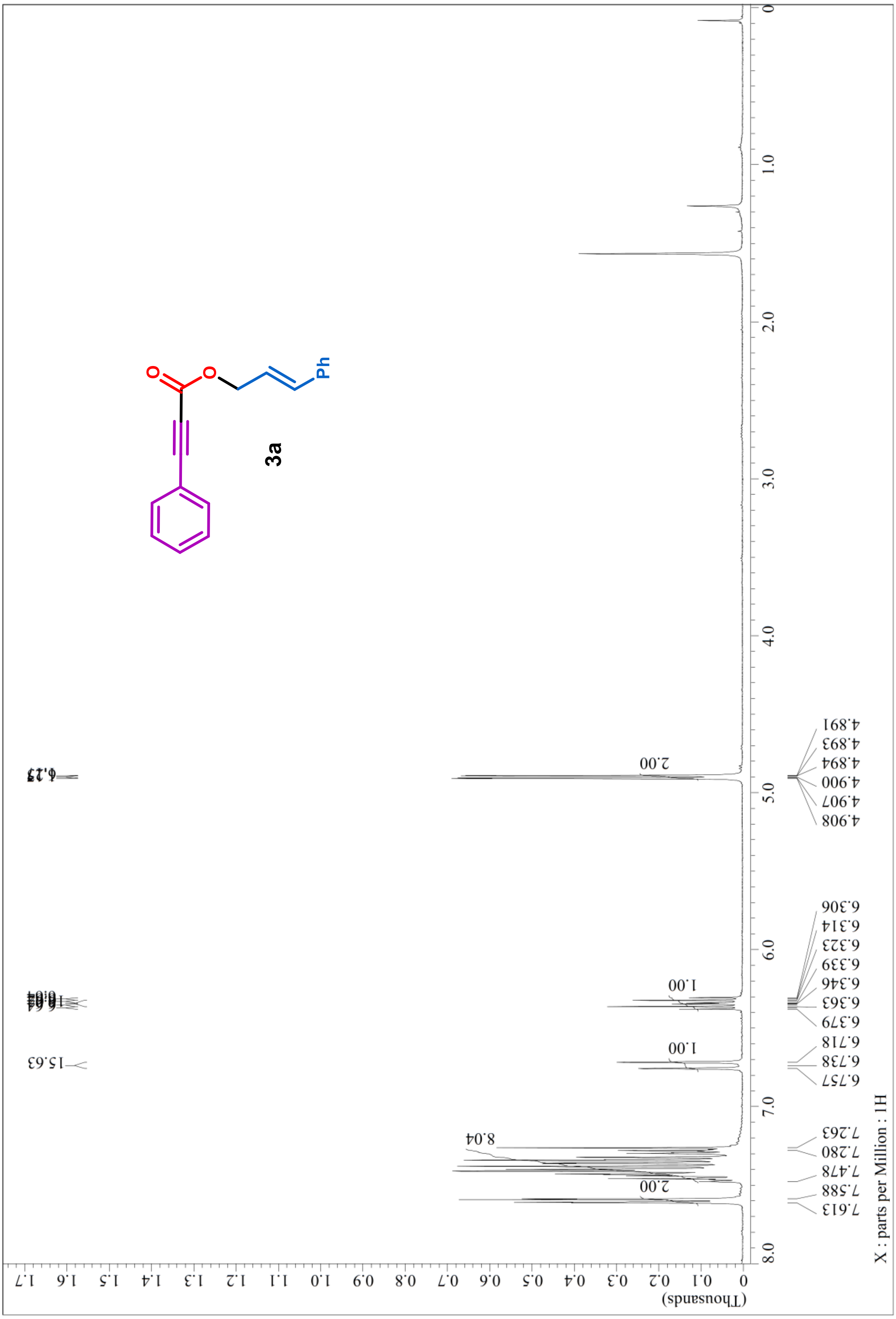

Figure S12. ^{1}H NMR spectrum of Cinnamyl 3-phenylpropiolate (**3a**).

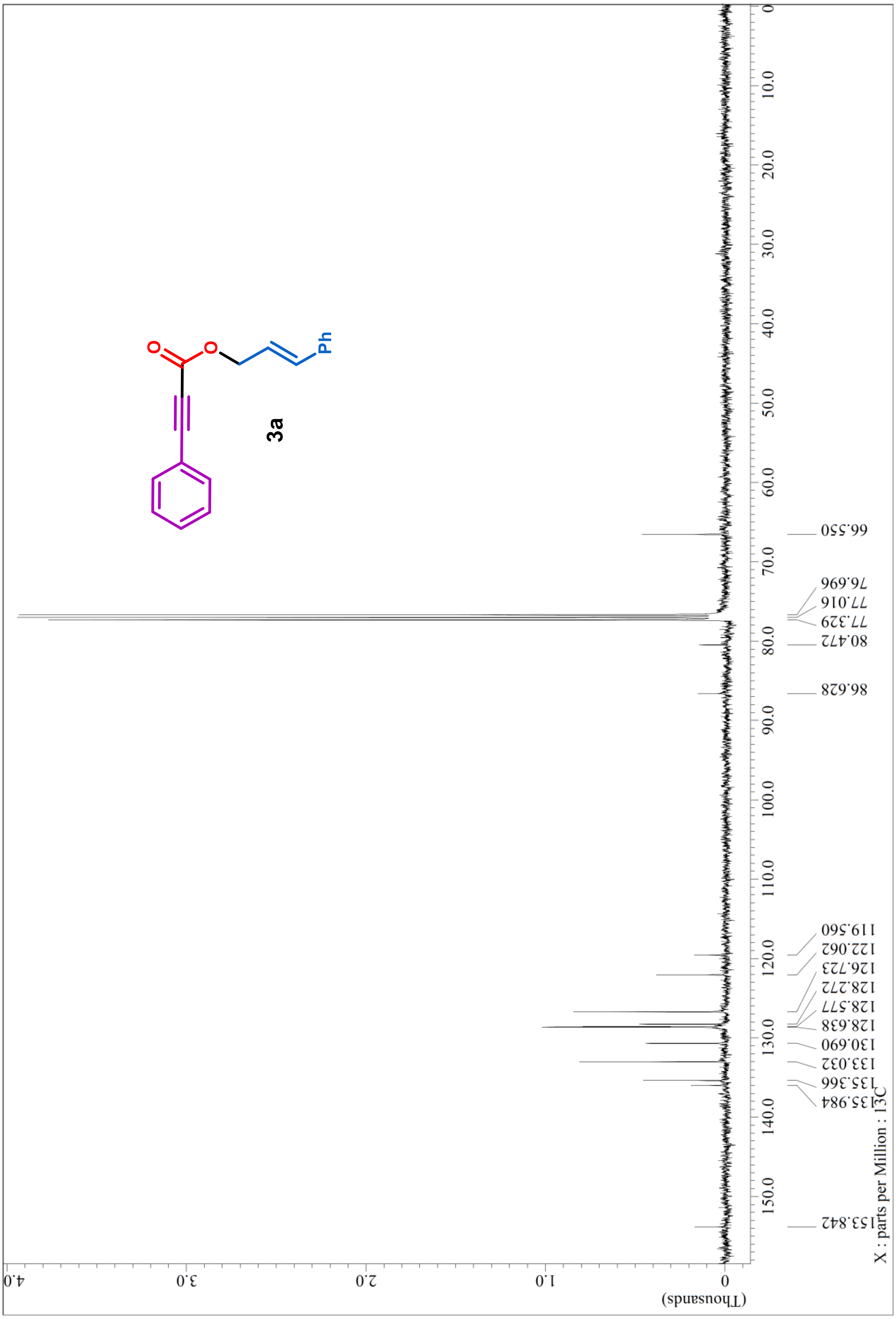

Figure S13. ^{13}C NMR spectrum of Cinnamyl 3-phenylpropiolate (**3a**).

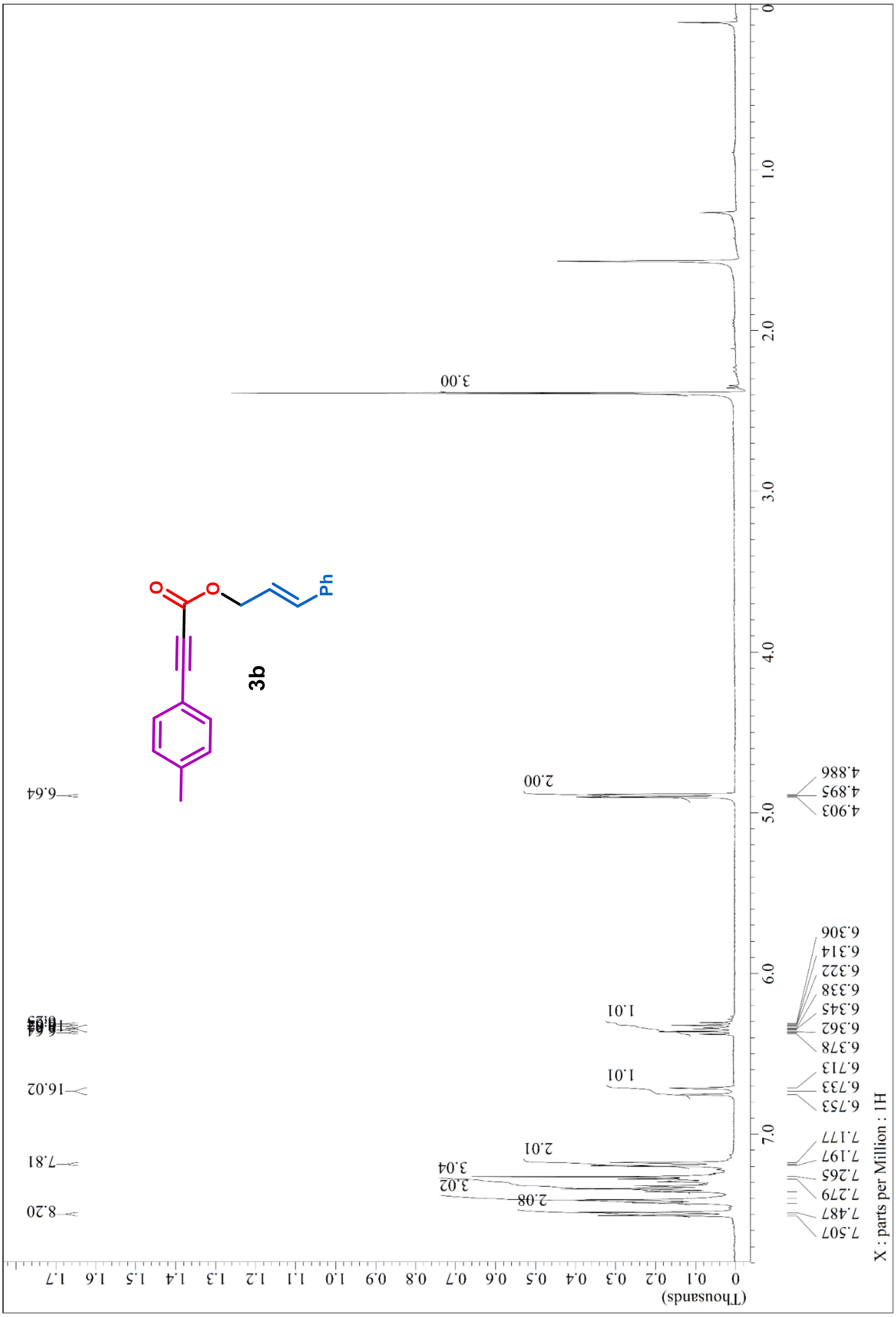

Figure S14. ^{1}H NMR spectrum of Cinnamyl 3-(p-tolyl)propiolate (**3b**).

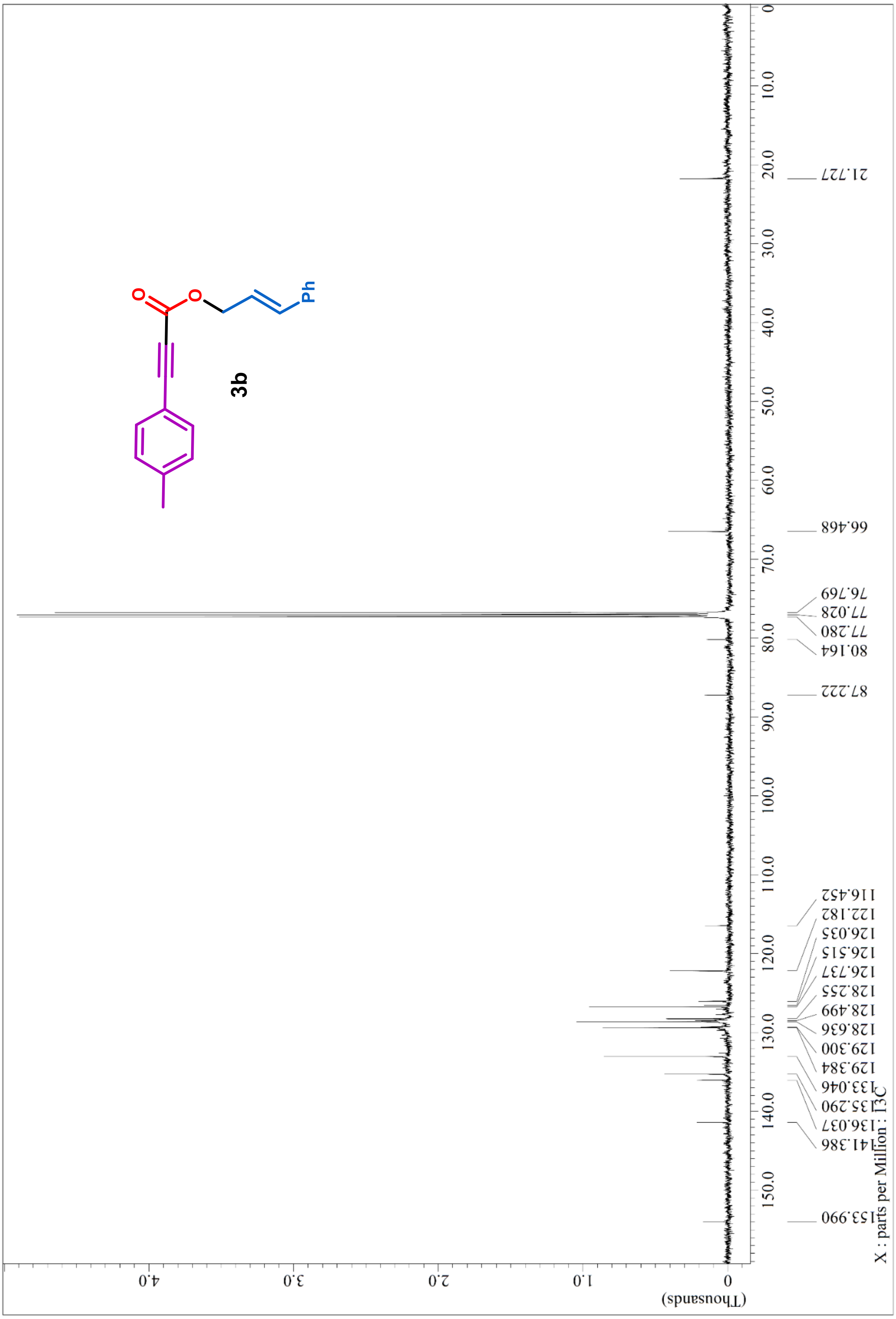

Figure S15. ^{13}C NMR spectrum of Cinnamyl 3-(p-tolyl)propiolate (**3b**).

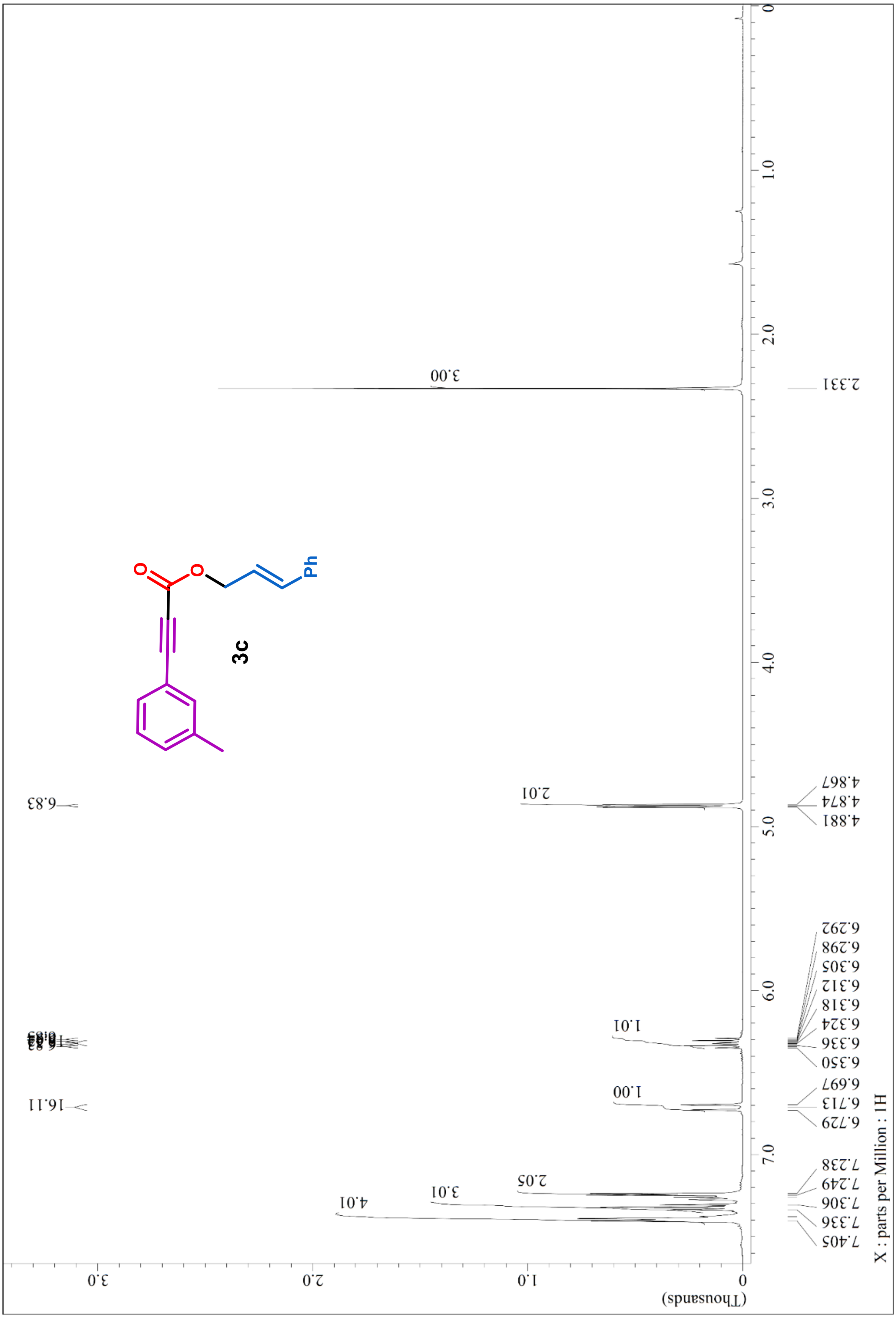

Figure S16. ^{1}H NMR spectrum of Cinnamyl 3-(m-tolyl)propiolate (**3c**).

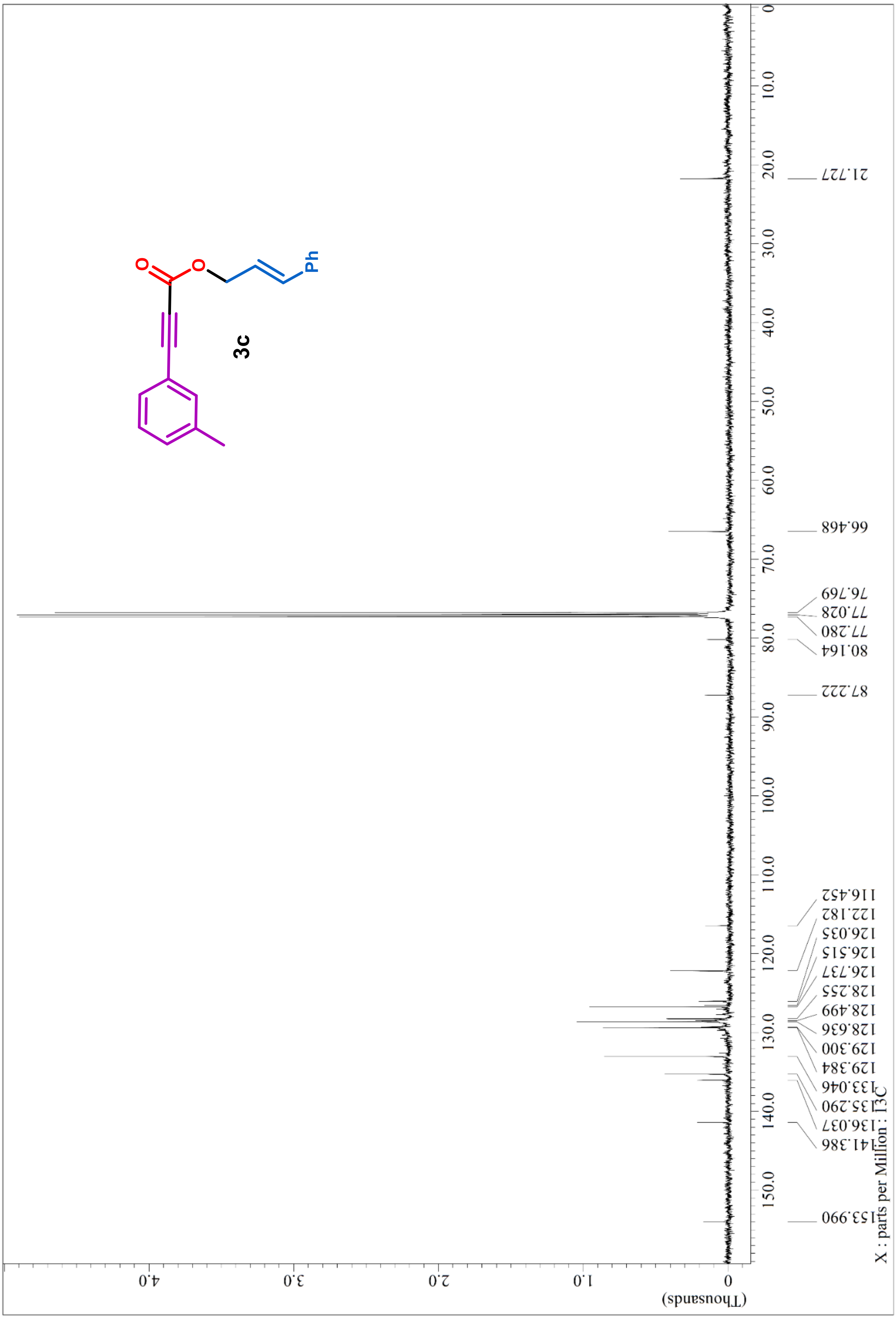

Figure S17. ^{13}C NMR spectrum of Cinnamyl 3-(m-tolyl)propiolate (**3c**).

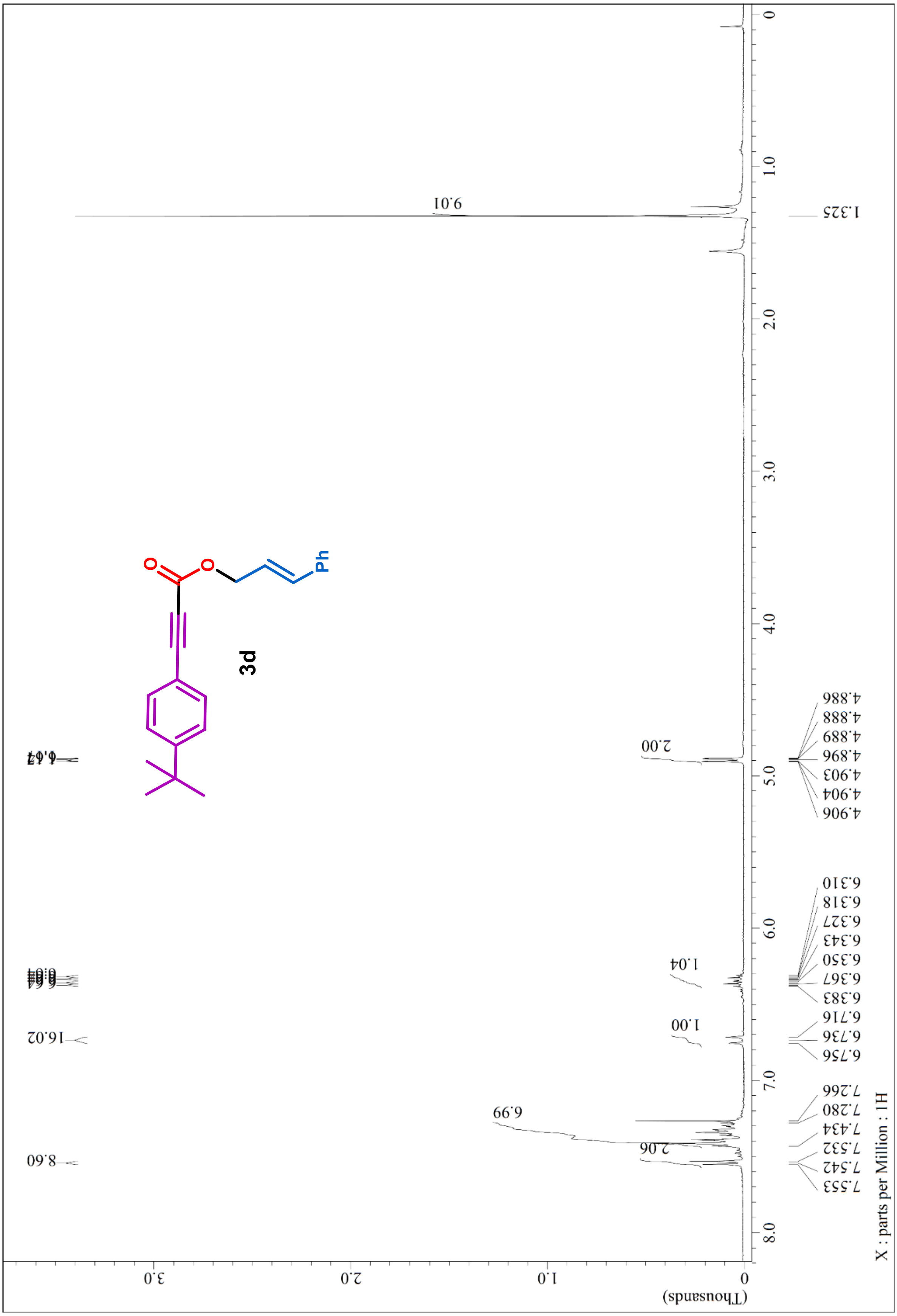

Figure S18. ^{1}H NMR spectrum of Cinnamyl 3-(4-(tert-butyl)phenyl)propiolate (**3d**).

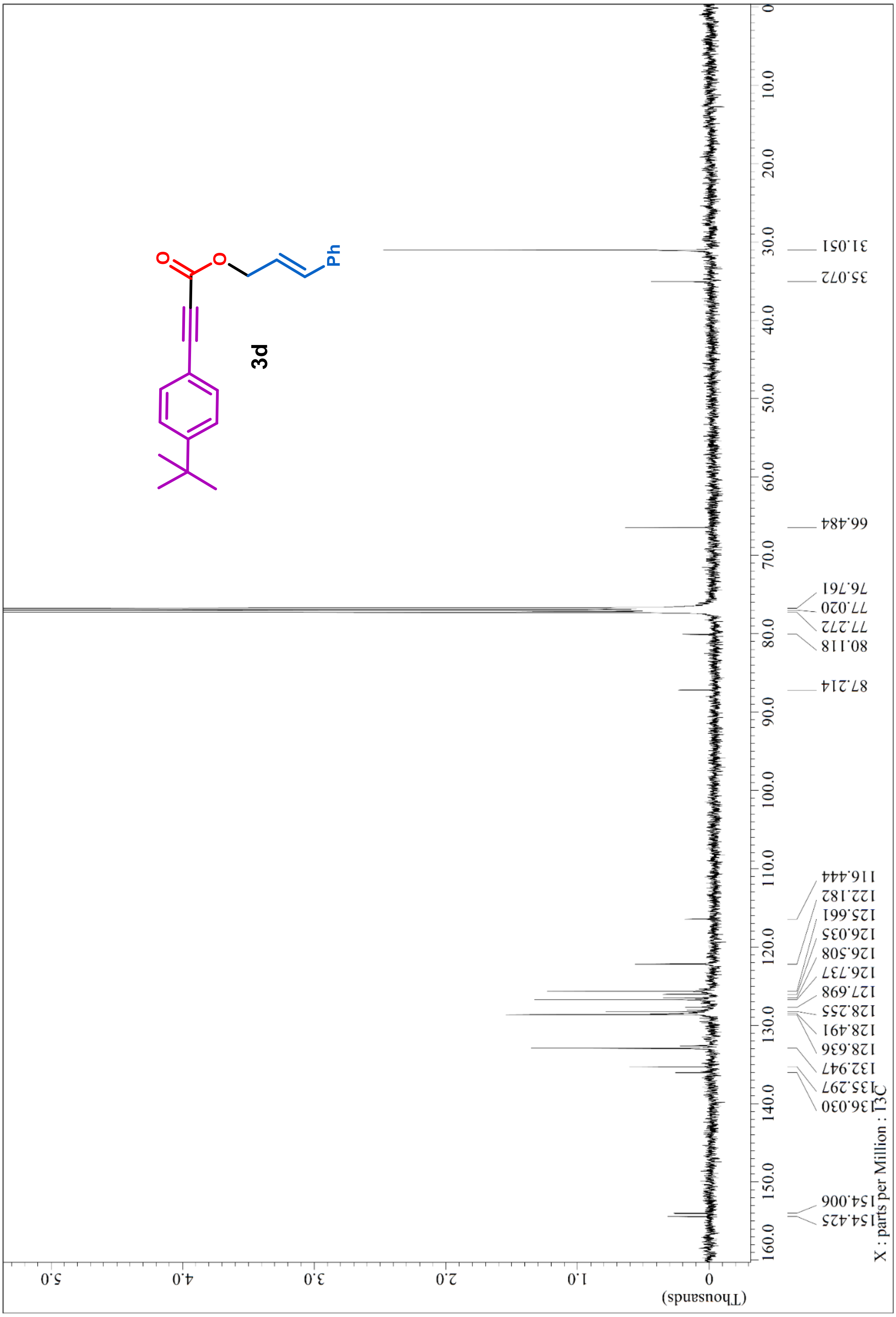

Figure S19. ^{13}C NMR spectrum of Cinnamyl 3-(4-(tert-butyl)phenyl)propiolate (**3d**).

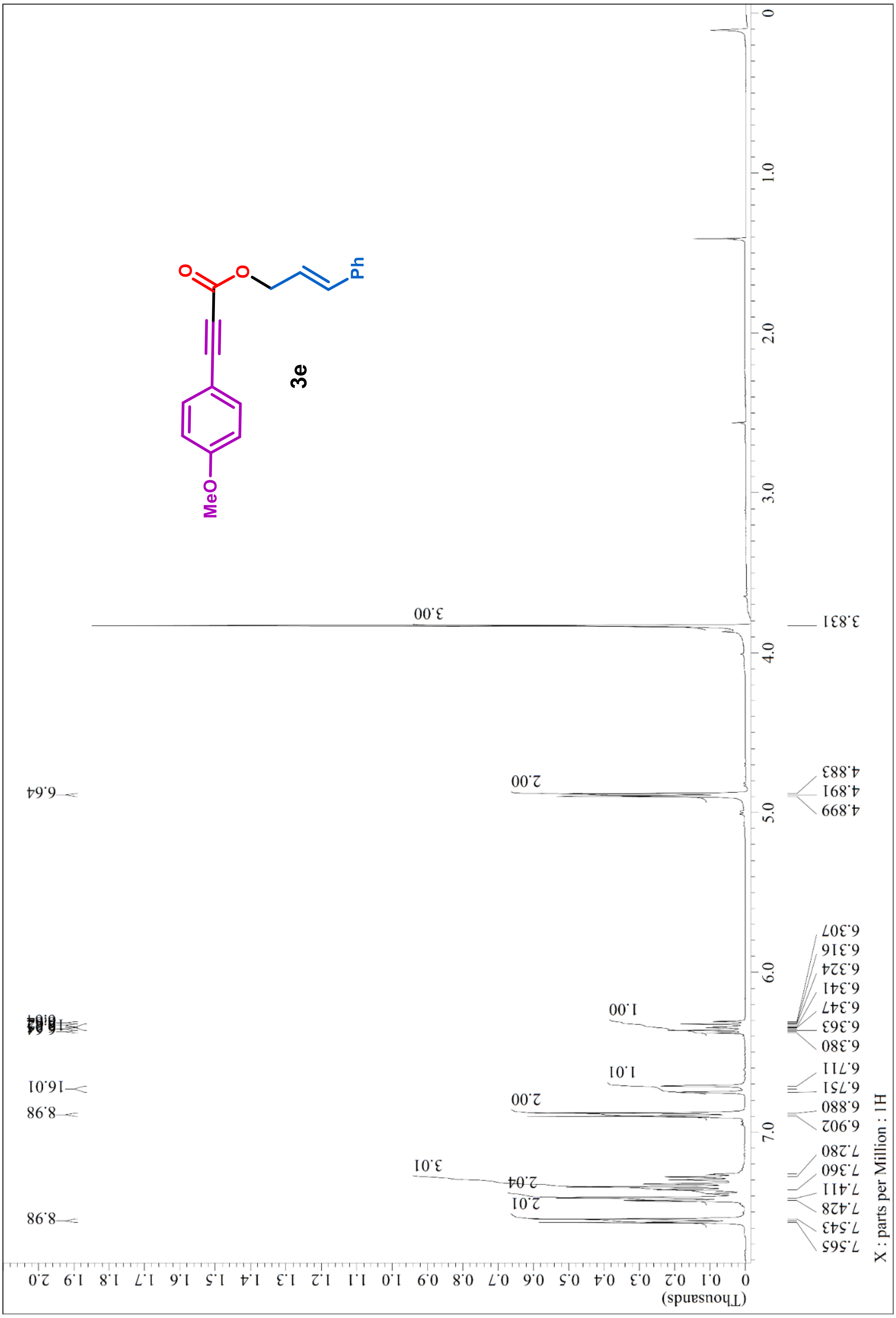

Figure S20. ^{1}H NMR spectrum of Cinnamyl 3-(4-methoxyphenyl)propiolate (**3e**).

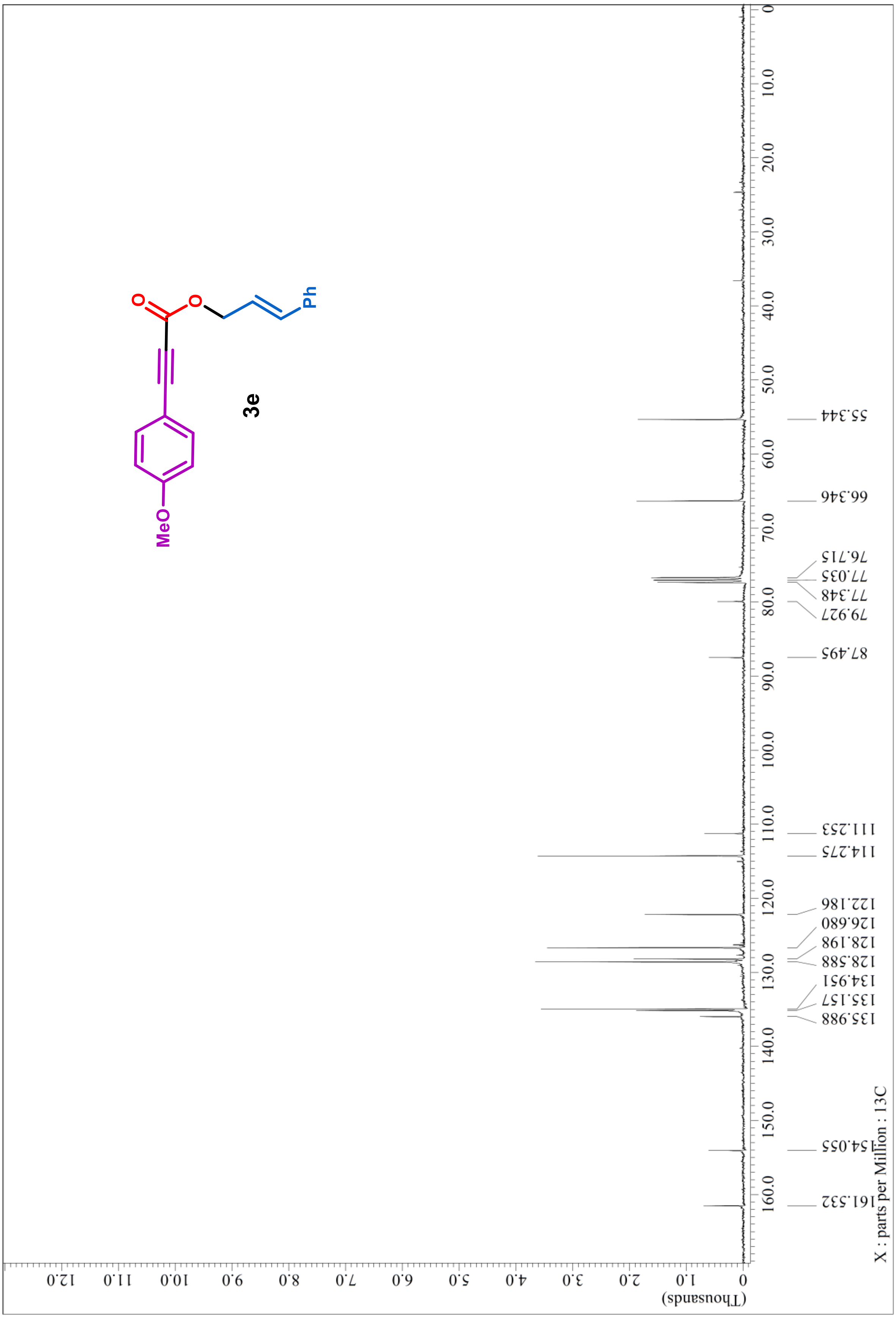

Figure S21. ^{13}C NMR spectrum of Cinnamyl 3-(4-methoxyphenyl)propiolate (**3e**).

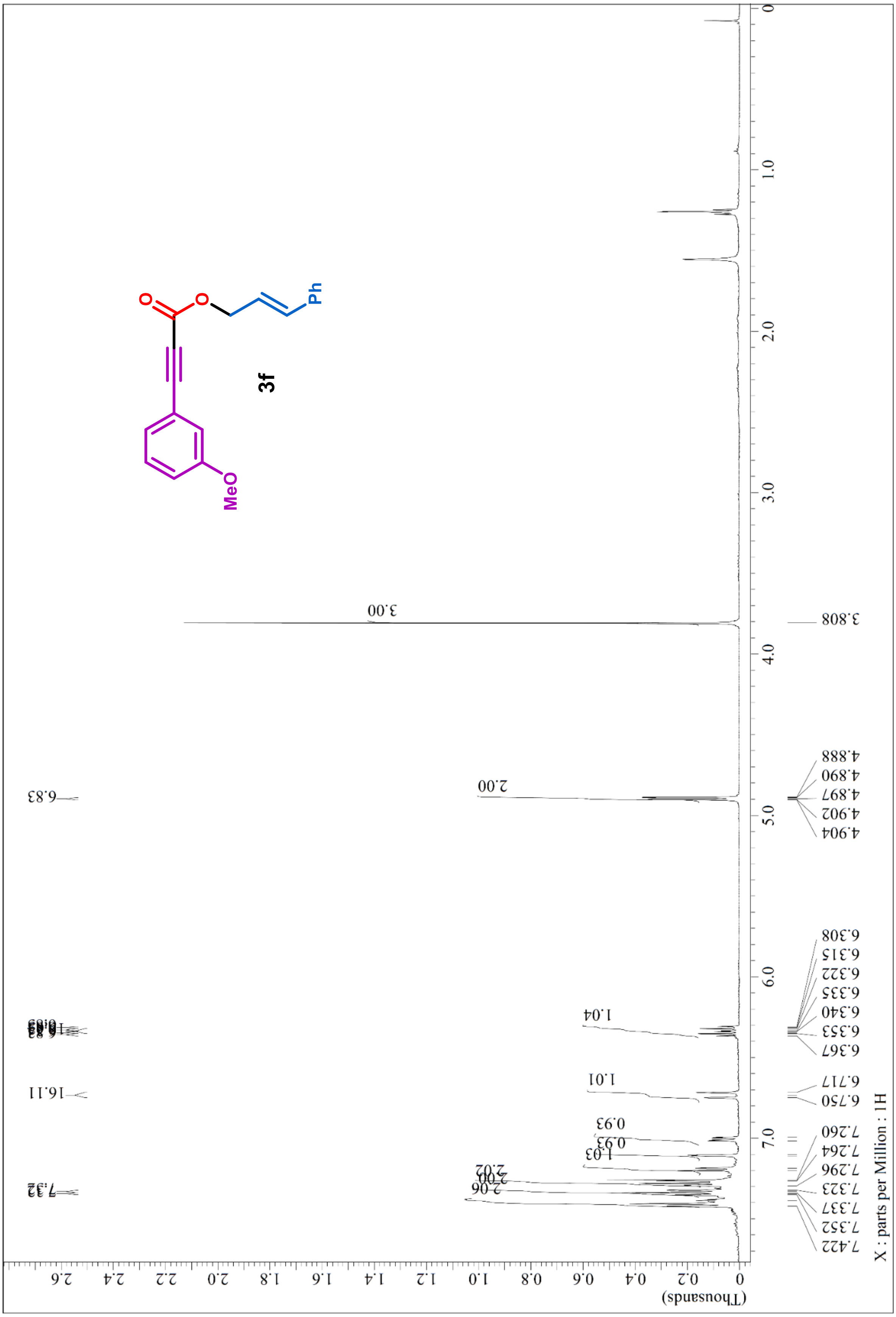

Figure S22. ^{1}H NMR spectrum of Cinnamyl 3-(3-methoxyphenyl)propiolate (**3f**).

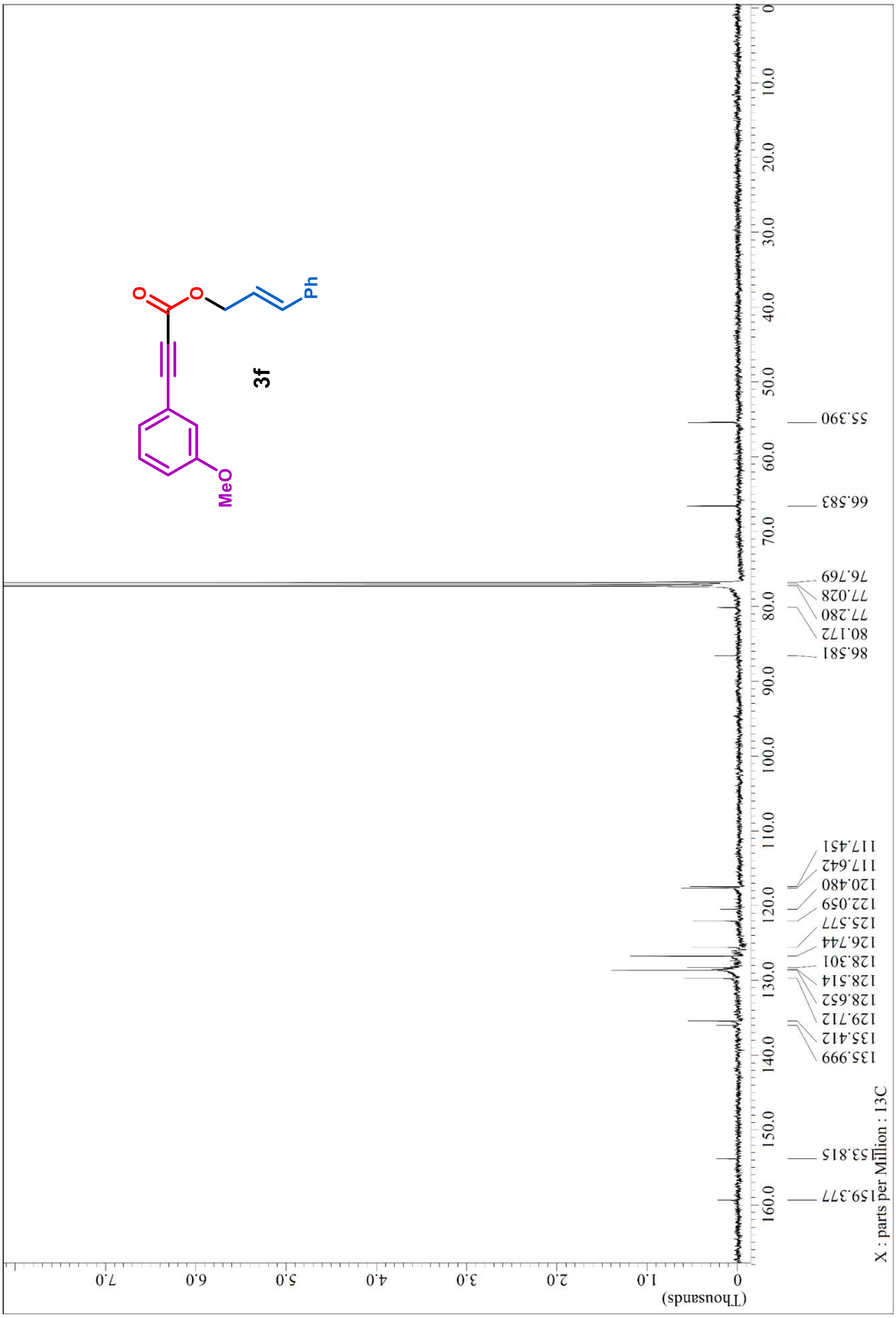

Figure S23. ^{13}C NMR spectrum of Cinnamyl 3-(3-methoxyphenyl)propiolate (**3f**).

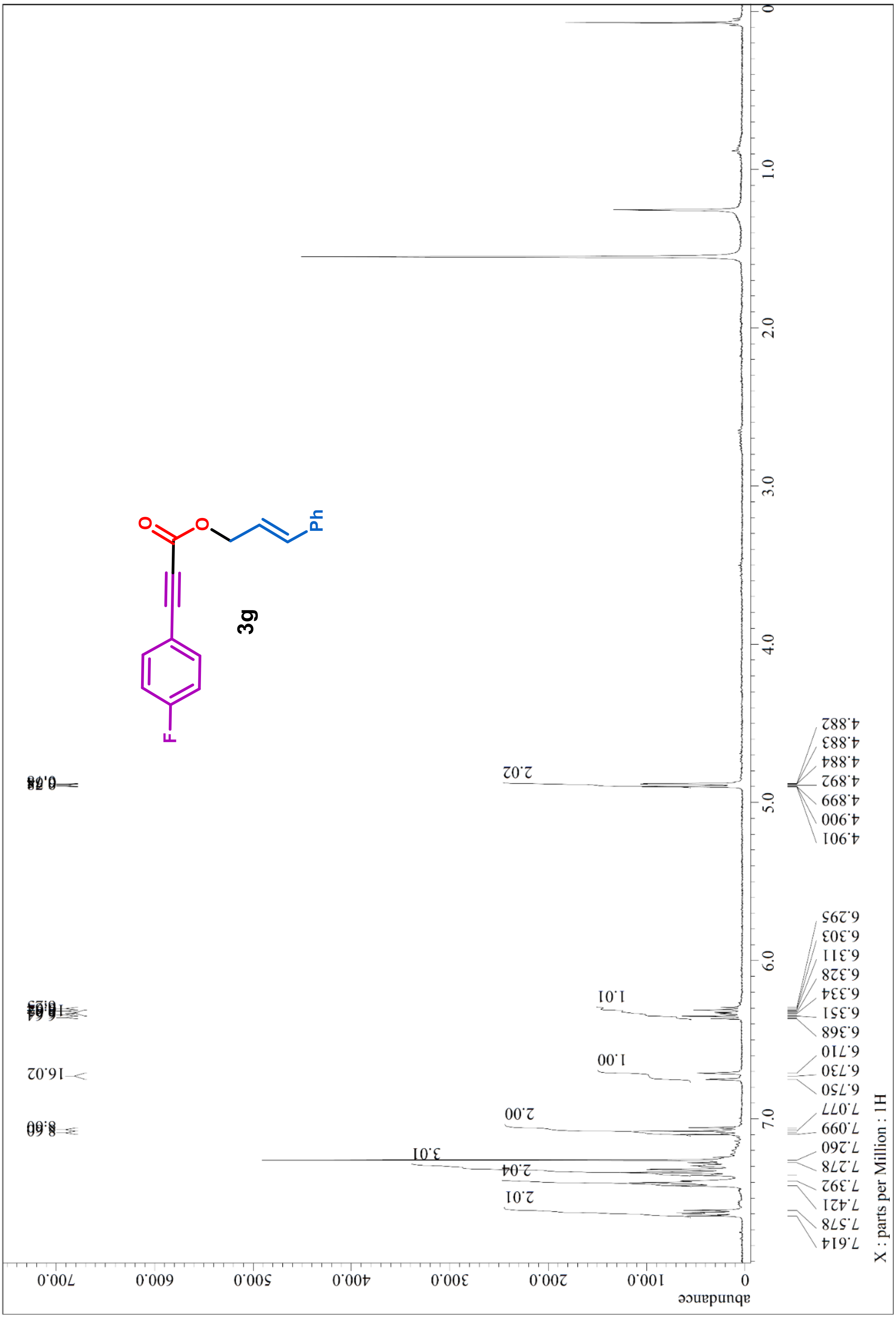

Figure S24. ^{1}H NMR spectrum of Cinnamyl 3-(4-fluorophenyl)propiolate (**3g**).

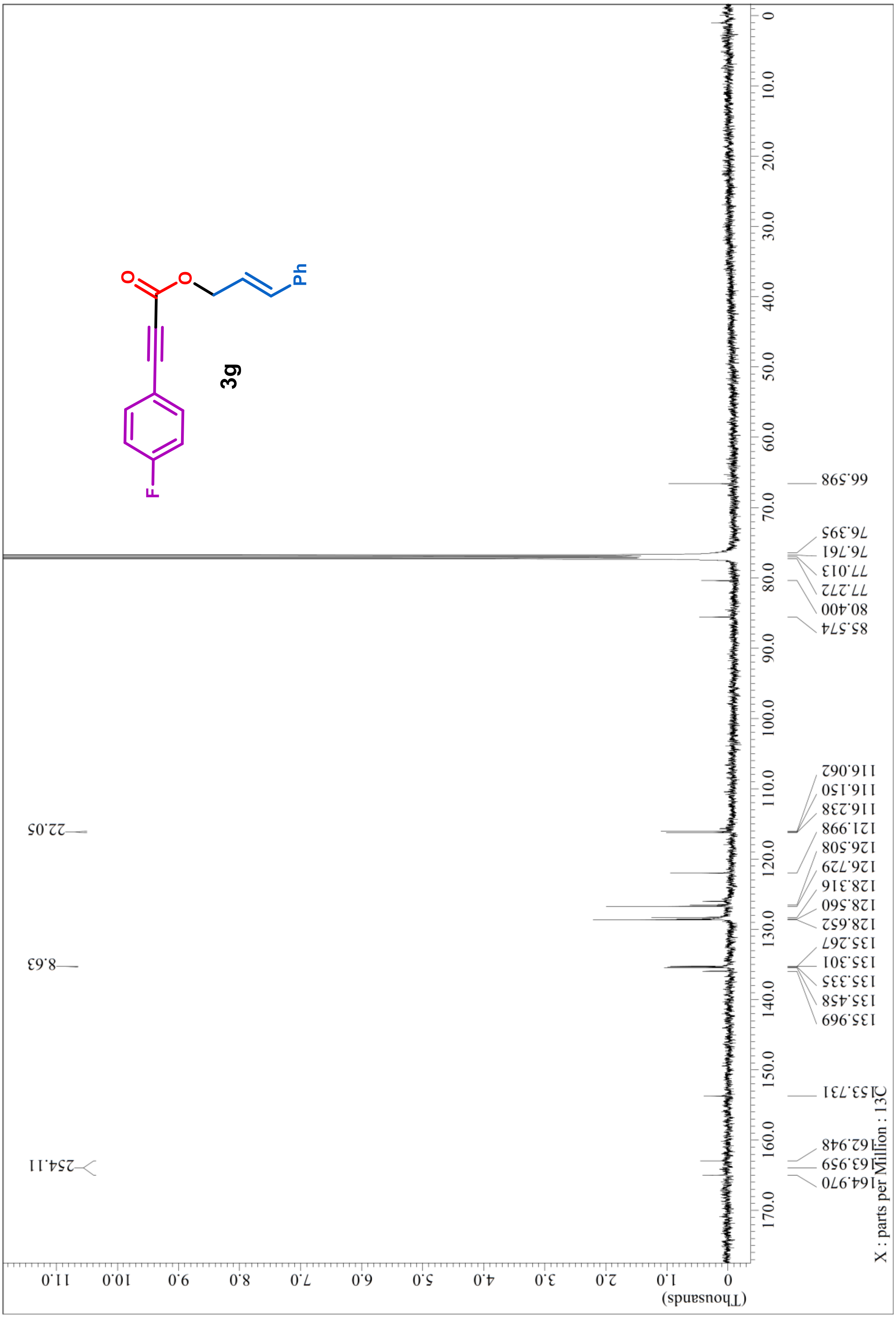

Figure S25. ^{13}C NMR spectrum of Cinnamyl 3-(4-fluorophenyl)propiolate (**3g**).

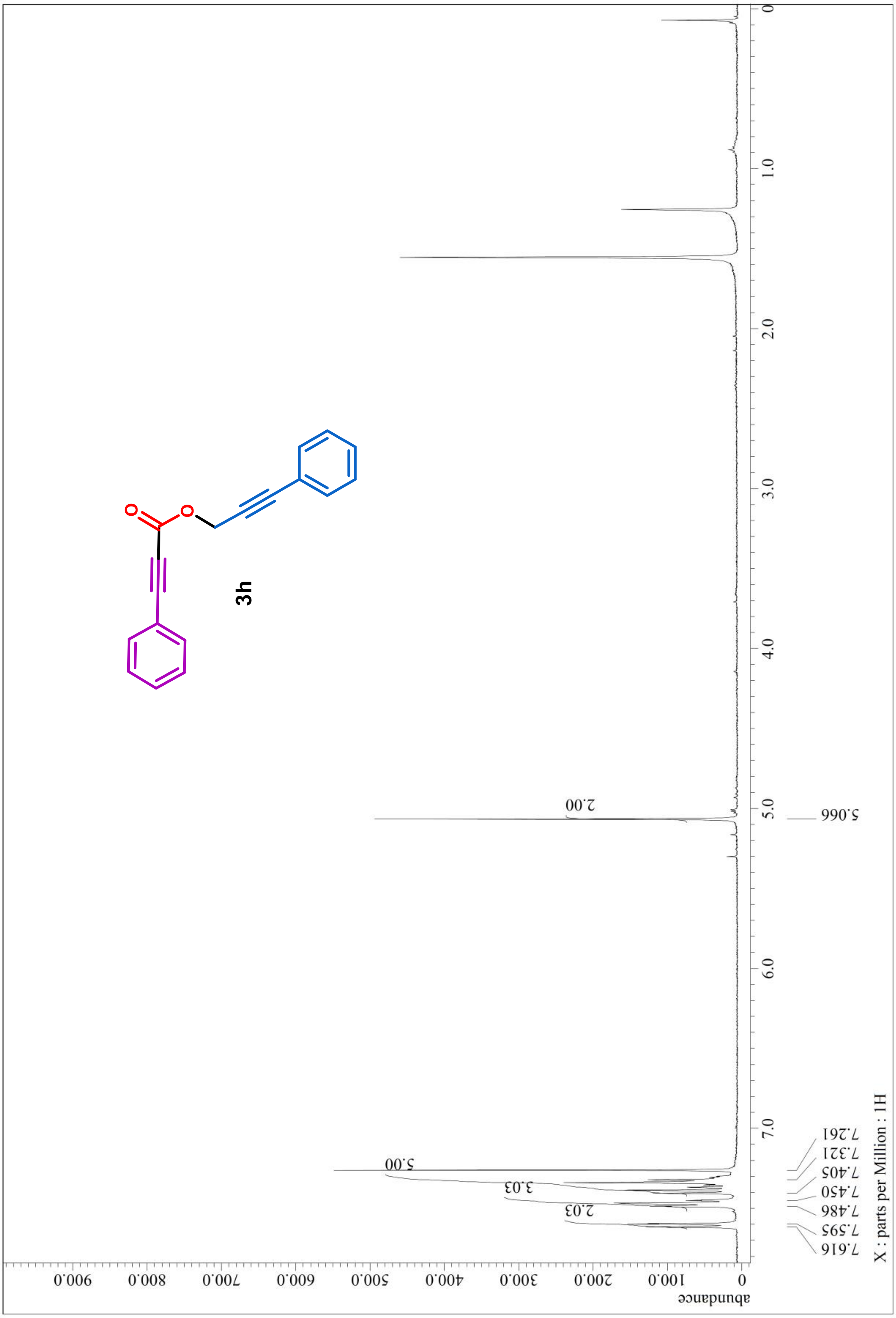

Figure S26. ^{1}H NMR spectrum of 3-Phenylprop-2-yn-1-yl 3-phenylpropiolate (**3h**).

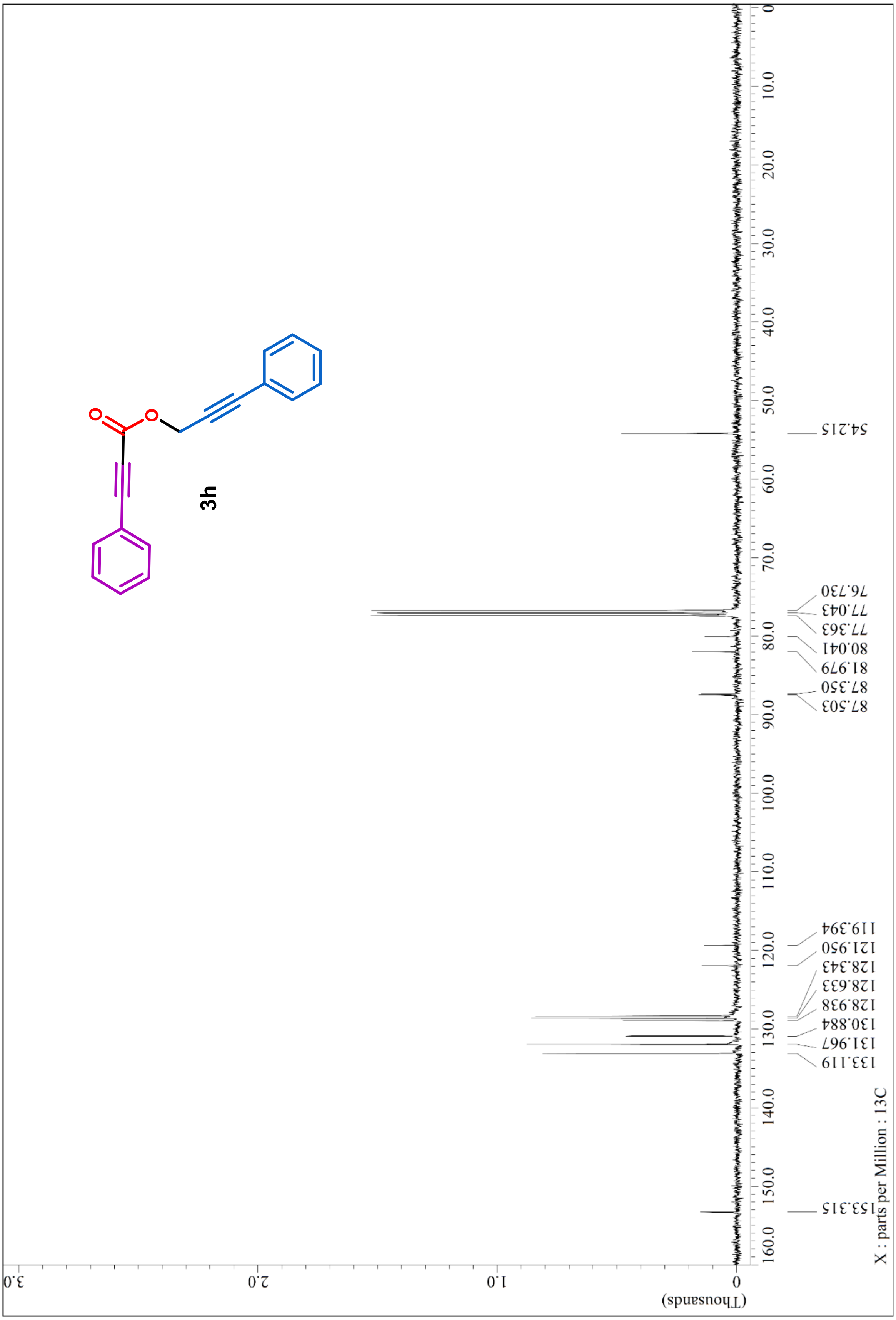

Figure S27. ^{13}C NMR spectrum of 3-Phenylprop-2-yn-1-yl 3-phenylpropiolate (**3h**).

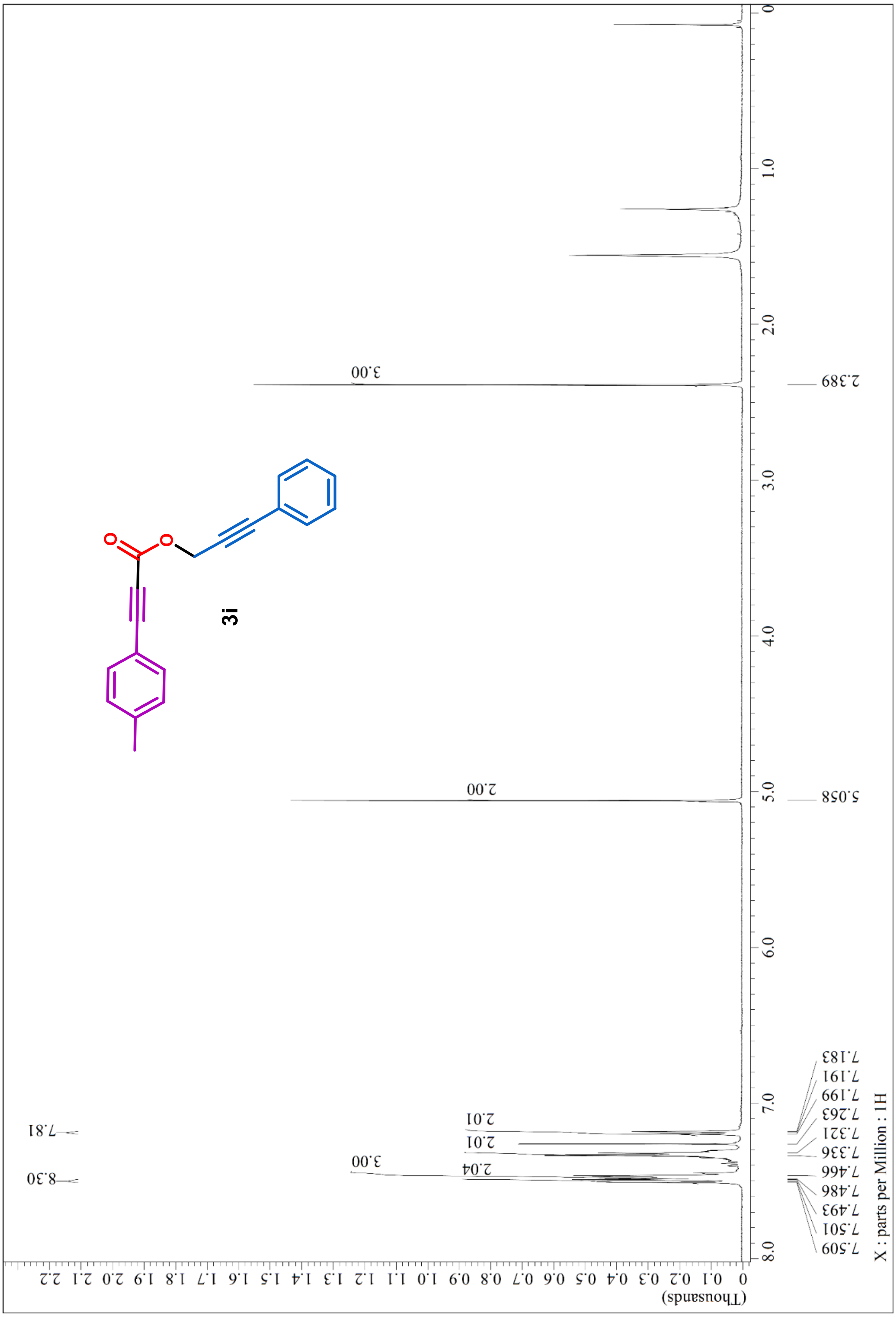

Figure S28. ^{1}H NMR spectrum of 3-Phenylprop-2-yn-1-yl 3-(p-tolyl)propiolate (**3i**).

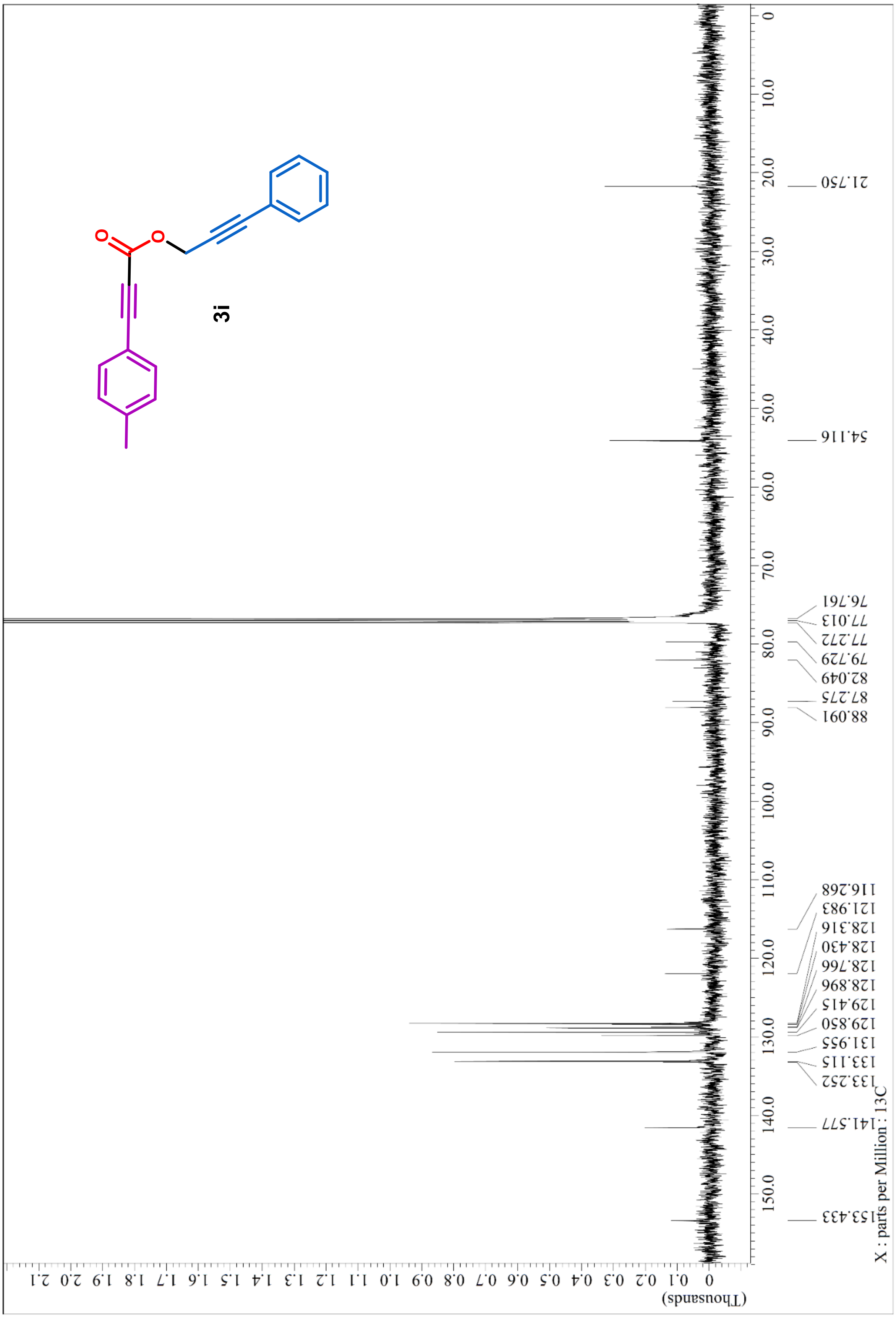

Figure S29. ^{13}C NMR spectrum of 3-Phenylprop-2-yn-1-yl 3-(p-tolyl)propiolate (**3i**).

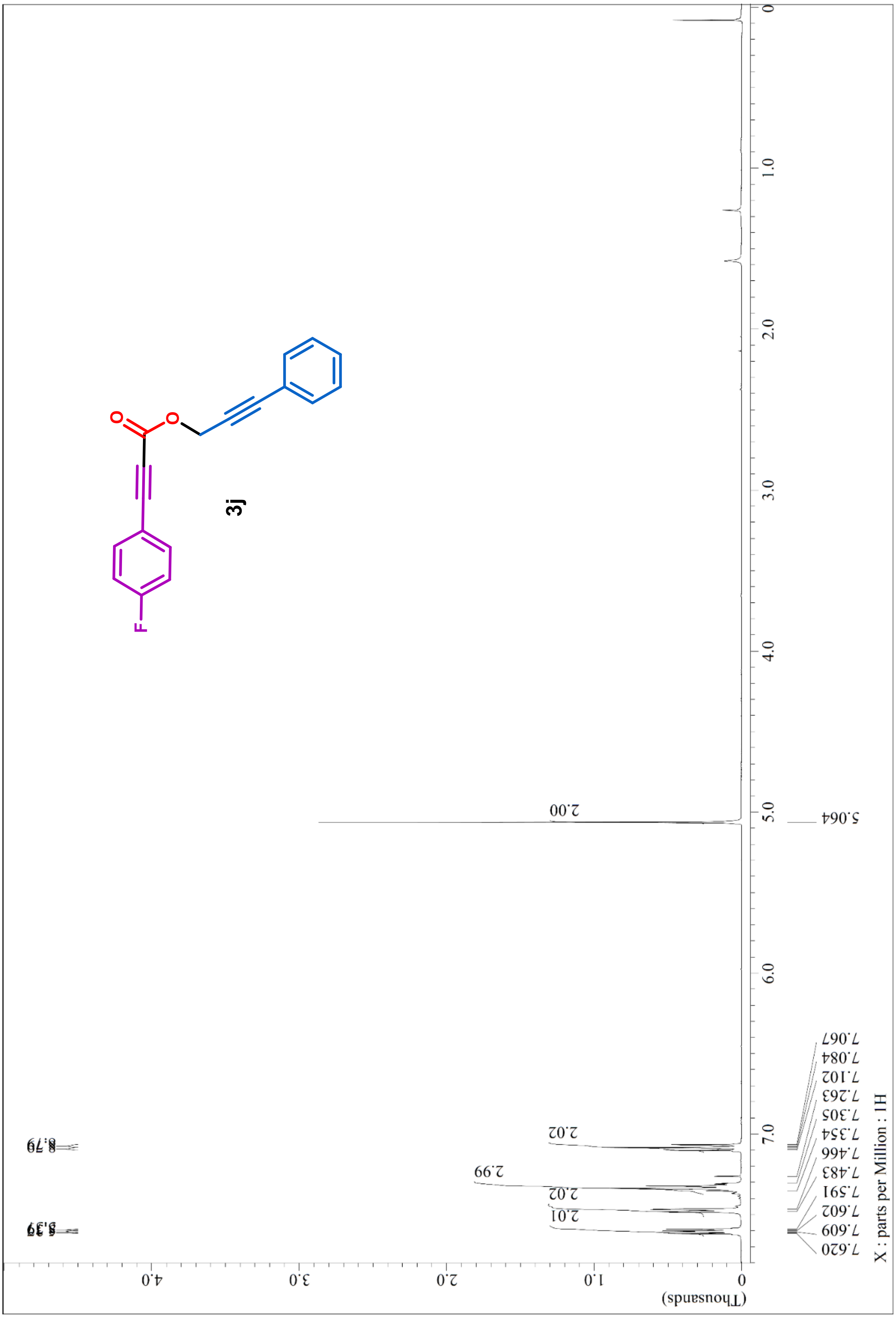

Figure S30. ^{1}H NMR spectrum of 3-Phenylprop-2-yn-1-yl 3-(4-fluorophenyl)propiolate (**3j**).

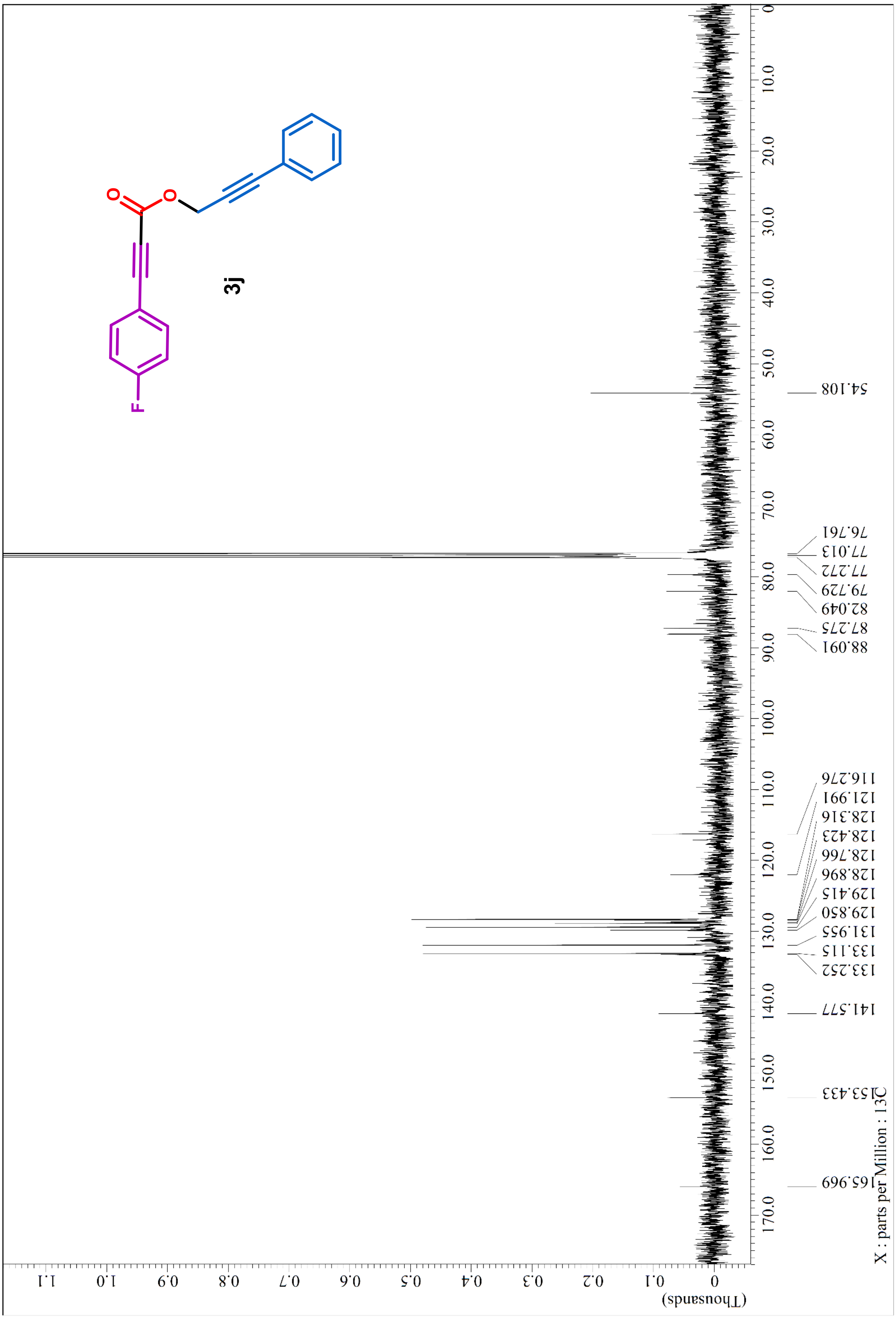

Figure S31. ^{13}C NMR spectrum of 3-Phenylprop-2-yn-1-yl 3-(4-fluorophenyl)propiolate (**3j**).

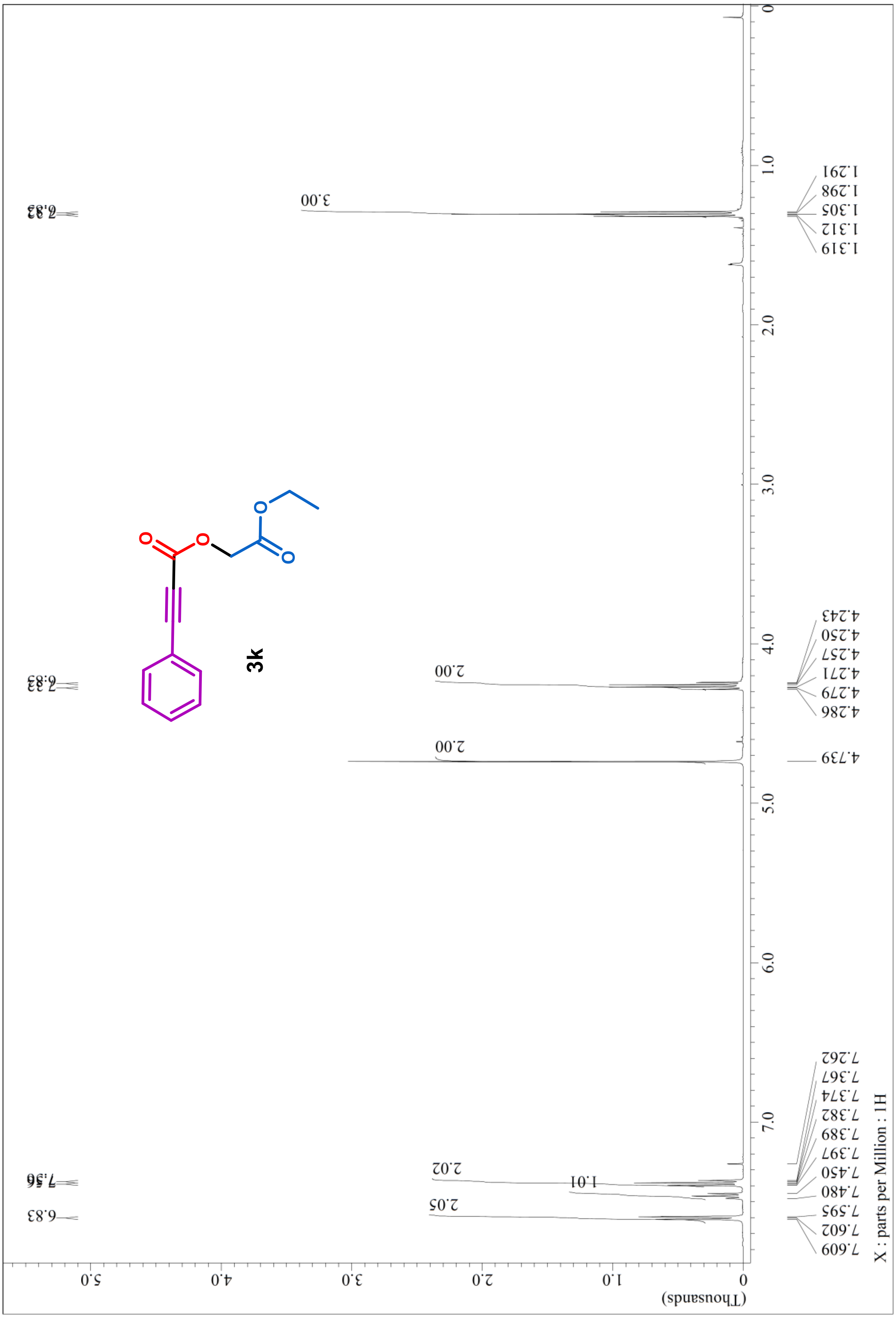

Figure S32. ^{1}H NMR spectrum of 2-Ethoxy-2-oxoethyl 3-phenylpropiolate (**3k**).

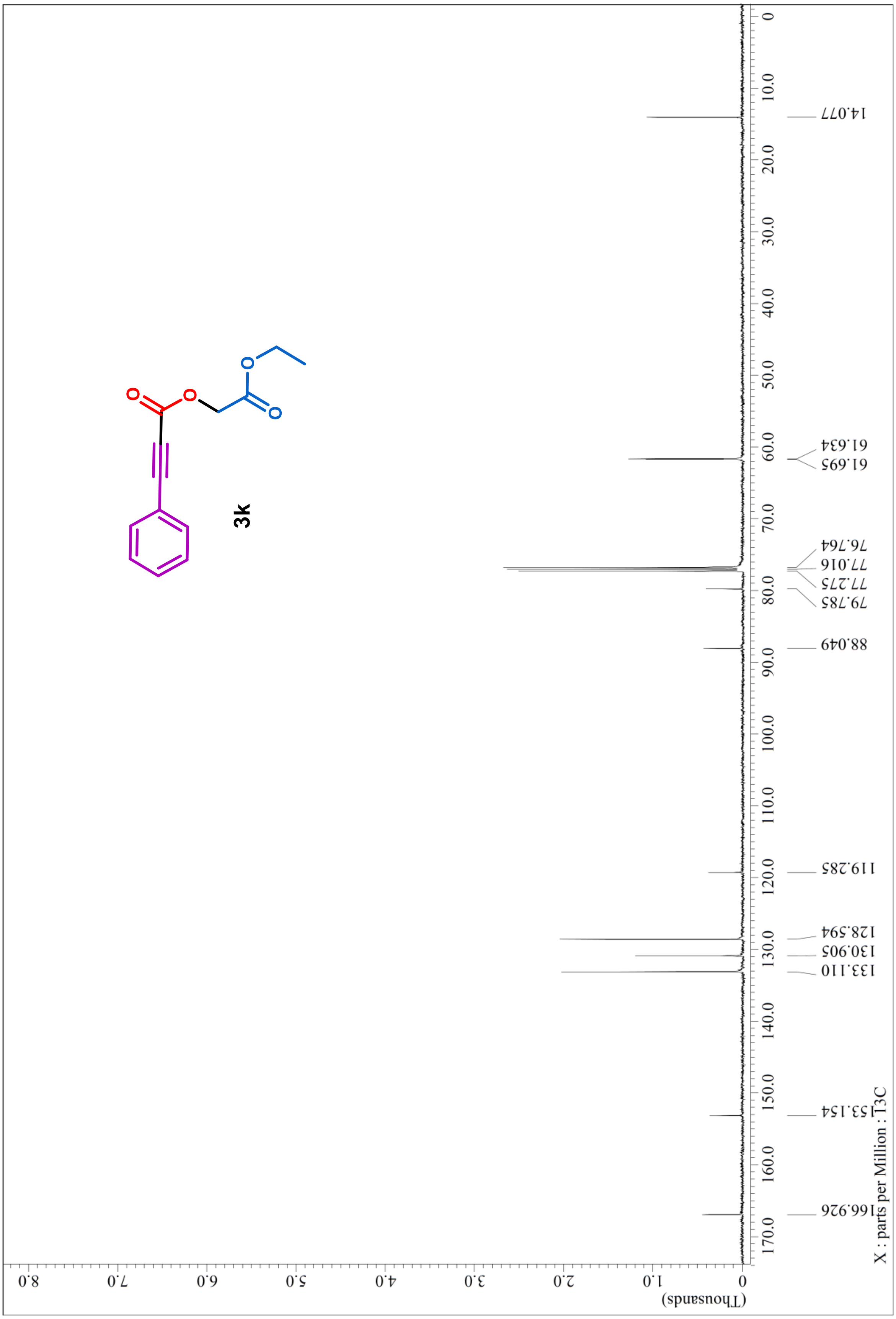

Figure S33. ^{13}C NMR spectrum of 2-Ethoxy-2-oxoethyl 3-phenylpropiolate (**3k**).

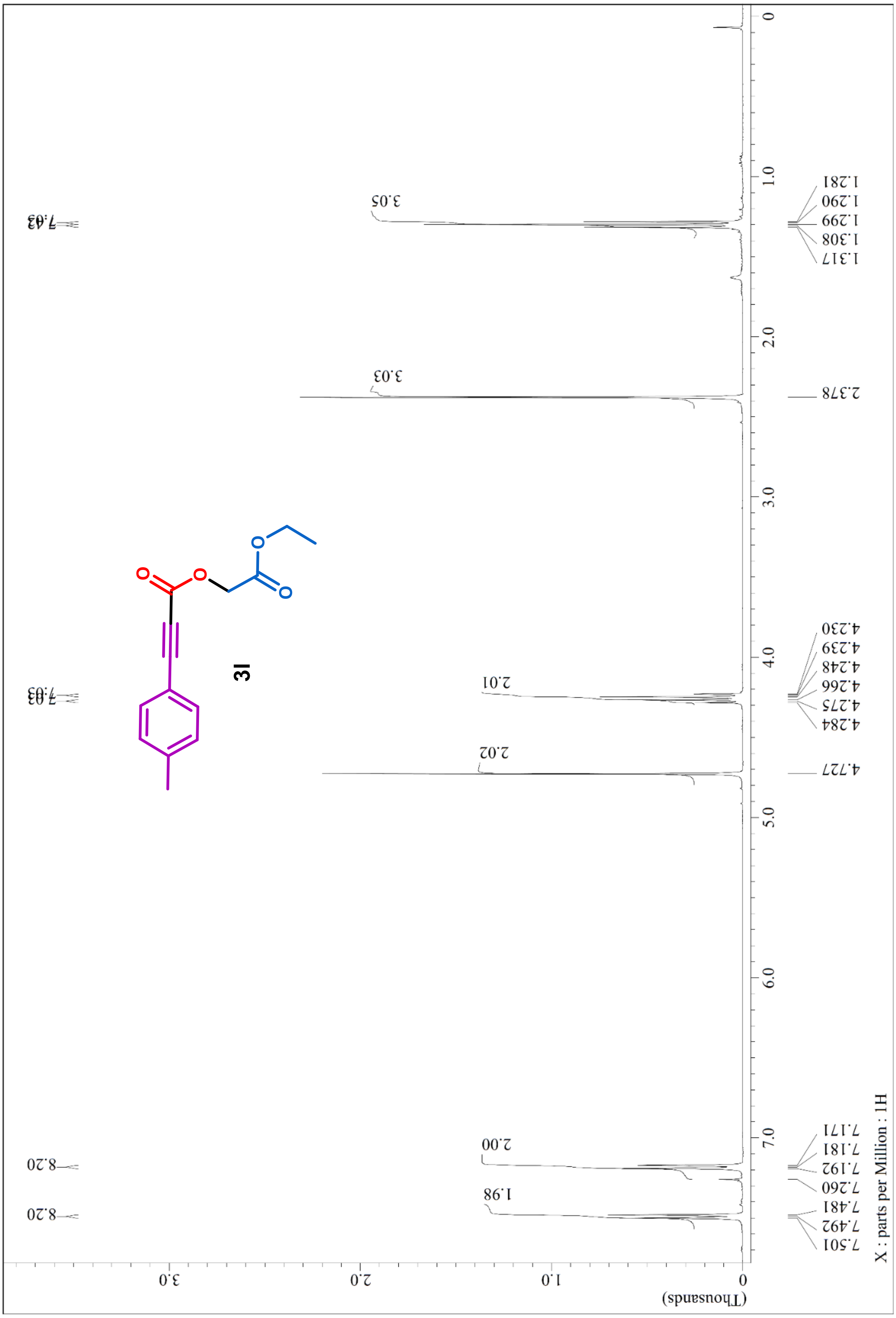

Figure S34. ^{1}H NMR spectrum of 2-Ethoxy-2-oxoethyl 3-(p-tolyl)propiolate (**3l**).

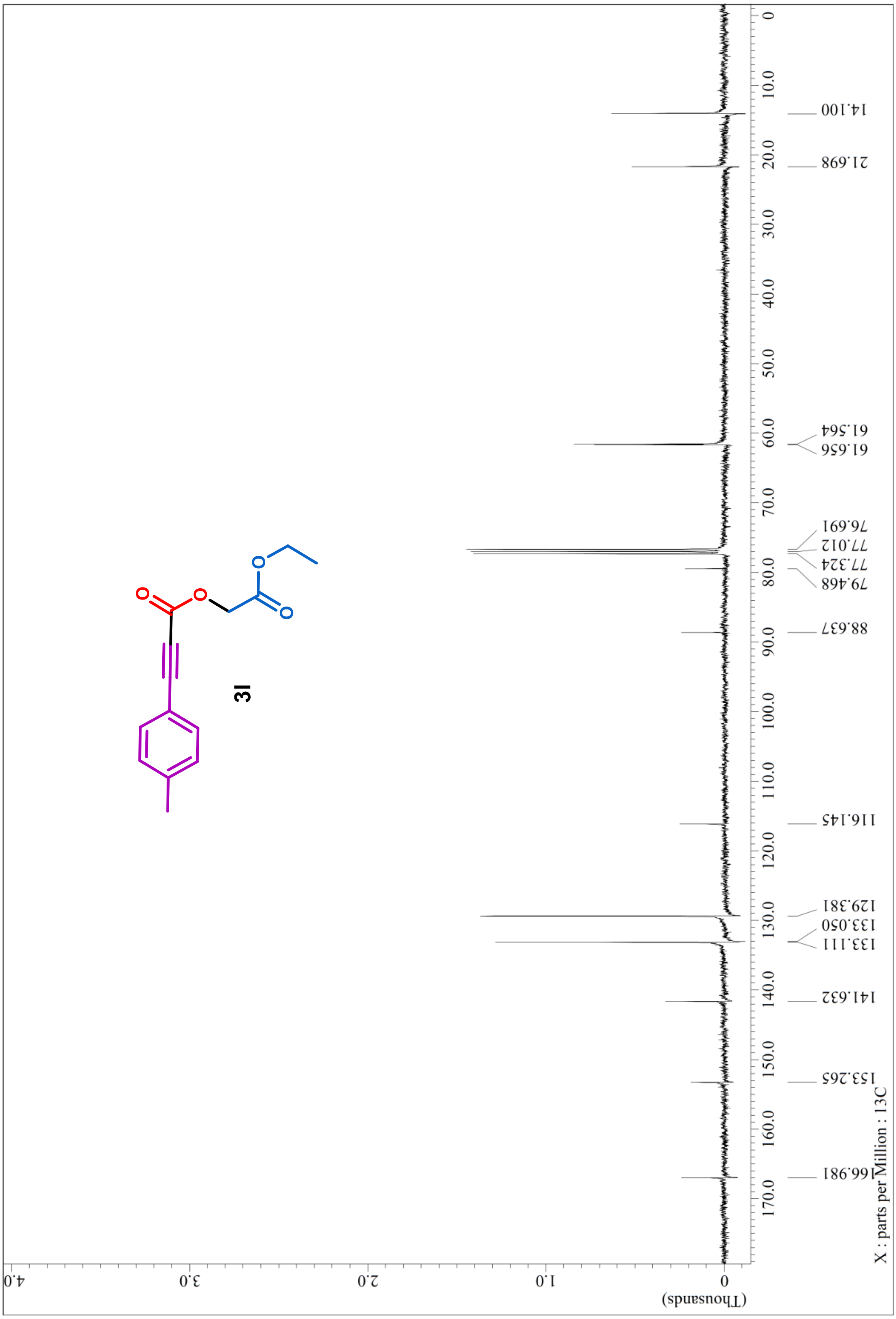

Figure S35. ^{13}C NMR spectrum of 2-Ethoxy-2-oxoethyl 3-(p-tolyl)propiolate (**3l**).

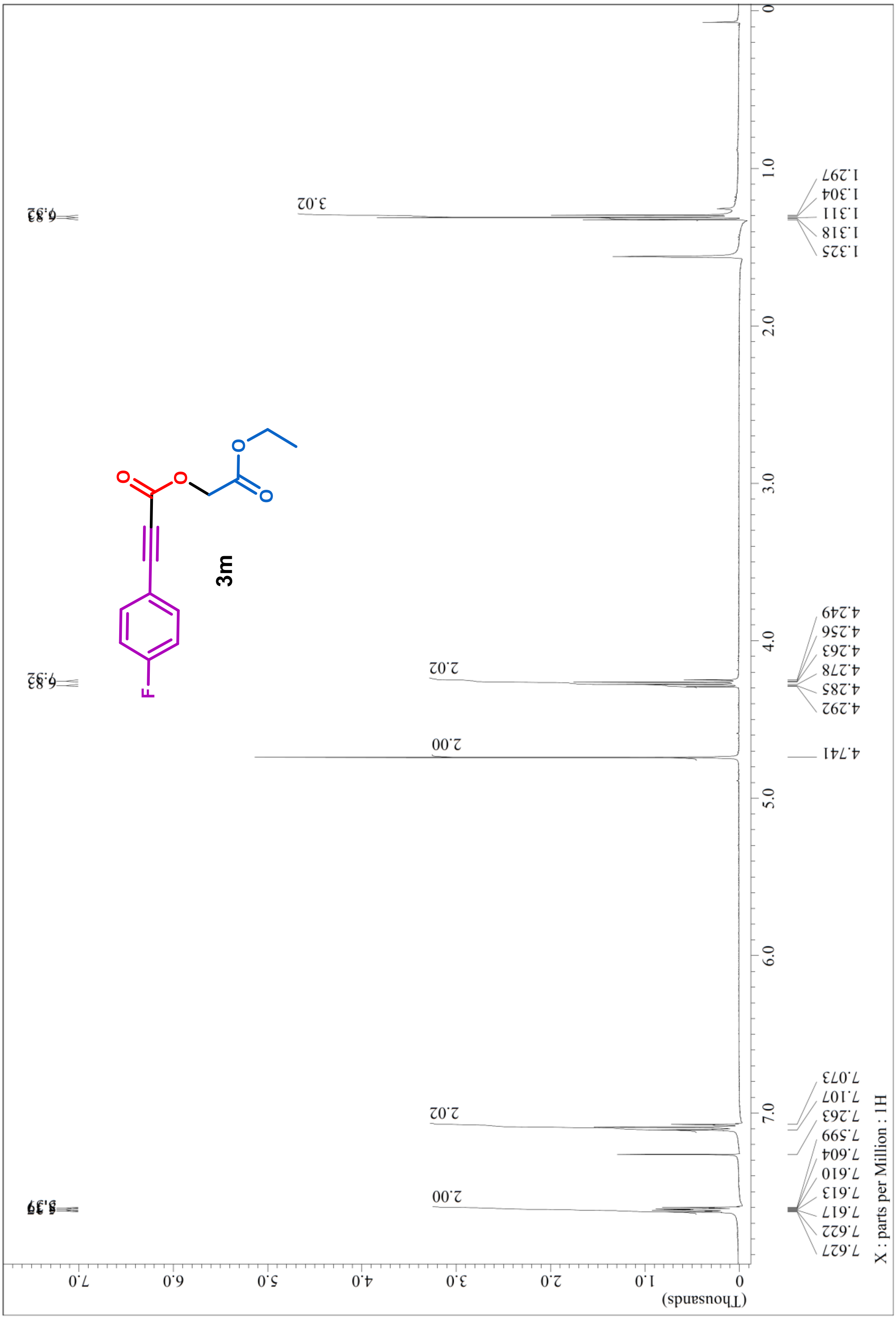

Figure S36. ^{1}H NMR spectrum of 2-Ethoxy-2-oxoethyl 3-(4-fluorophenyl)propiolate (**3m**).

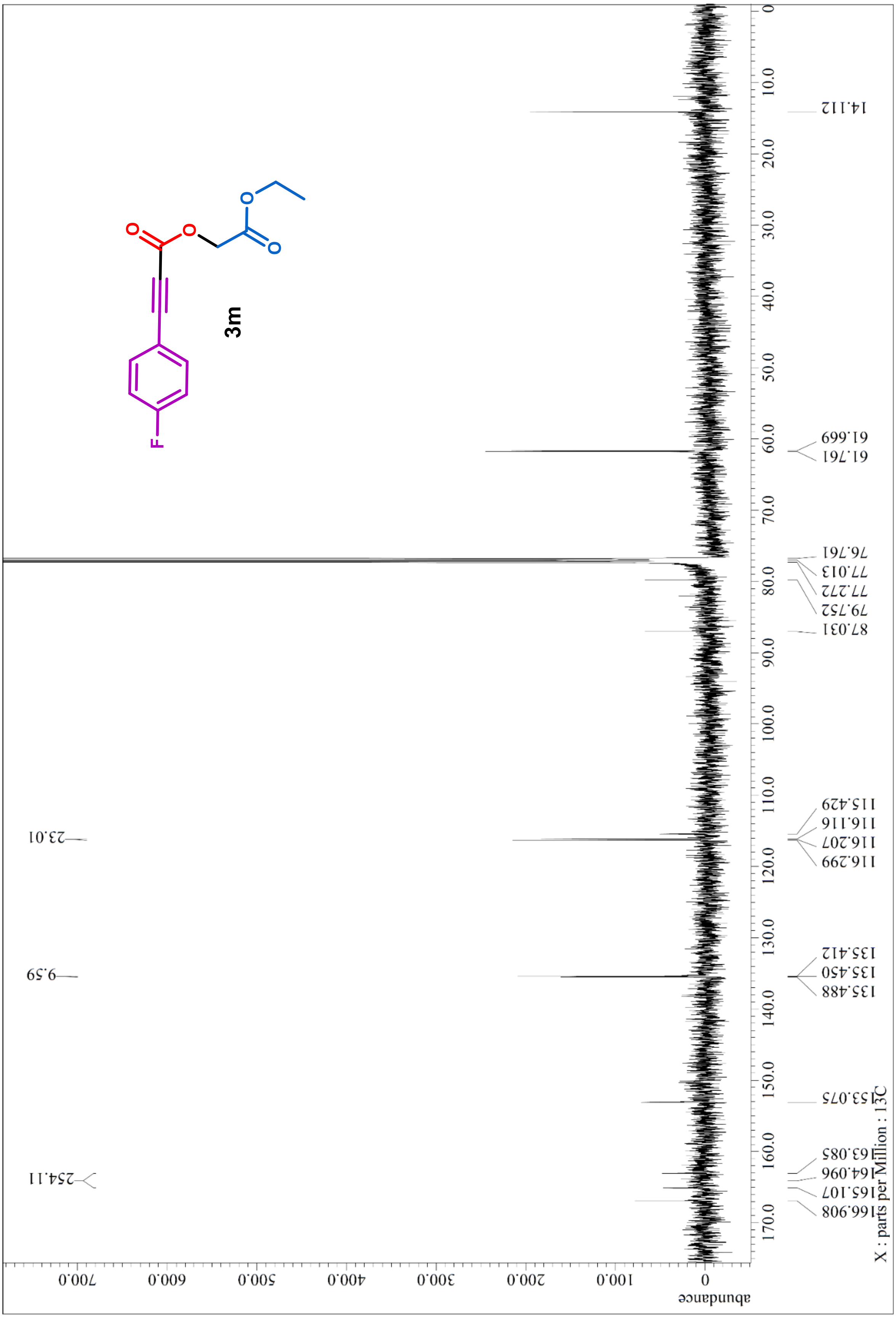

Figure S37. ^{13}C NMR spectrum of 2-Ethoxy-2-oxoethyl 3-(4-fluorophenyl)propiolate (**3m**).

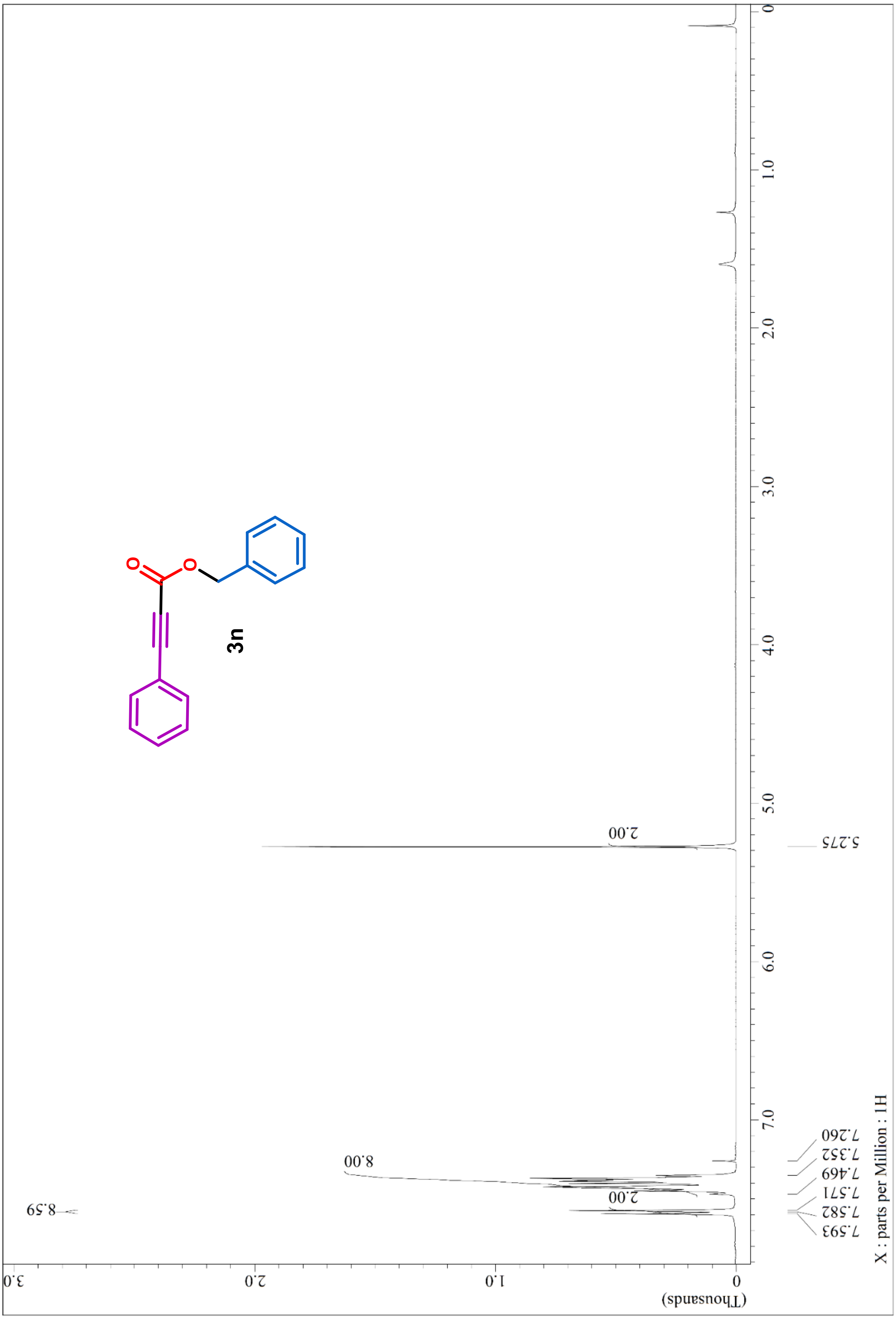

Figure S38. ^{1}H NMR spectrum of Benzyl 3-phenylpropiolate (**3n**).

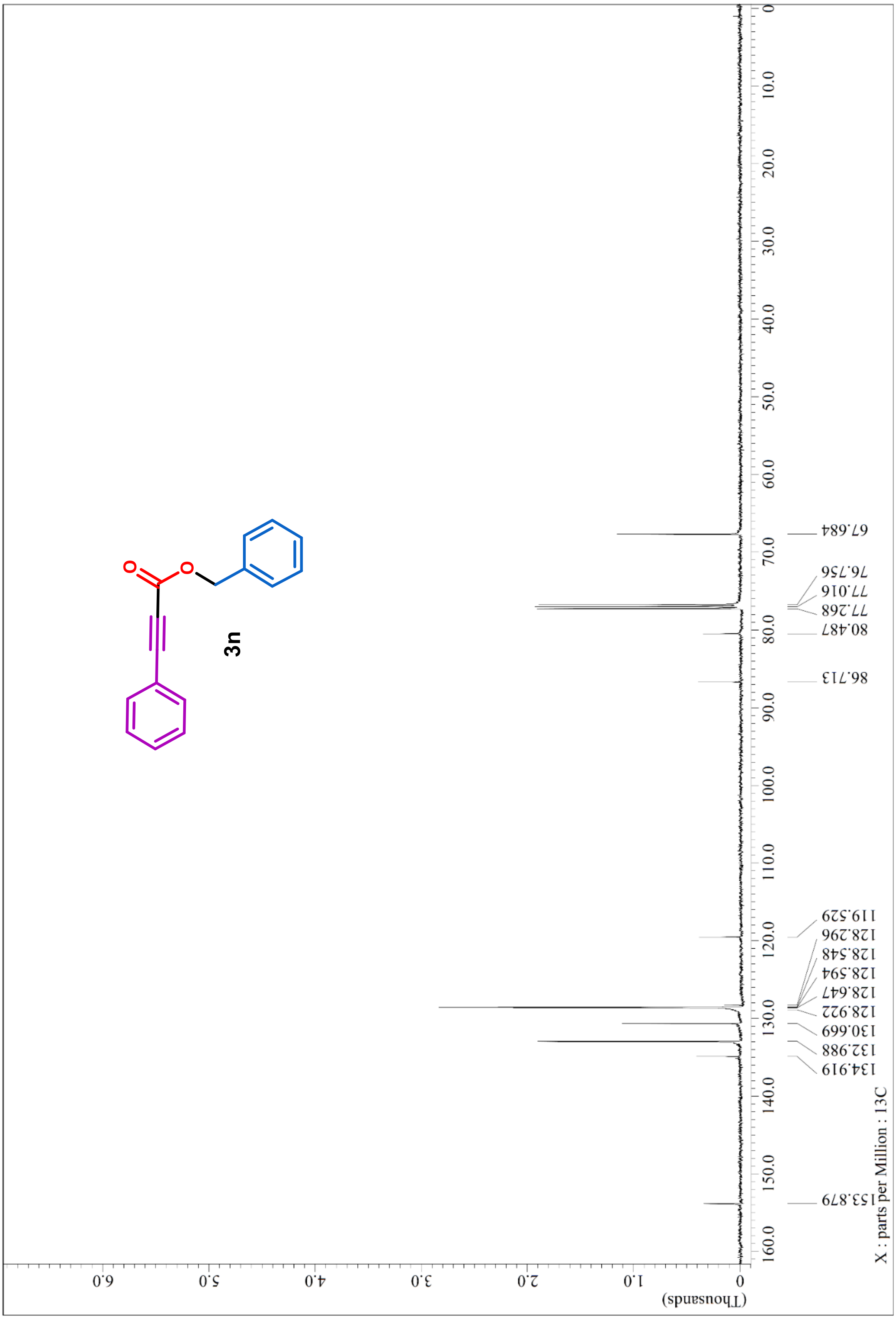

Figure S39. ^{13}C NMR spectrum of Benzyl 3-phenylpropiolate (**3n**).

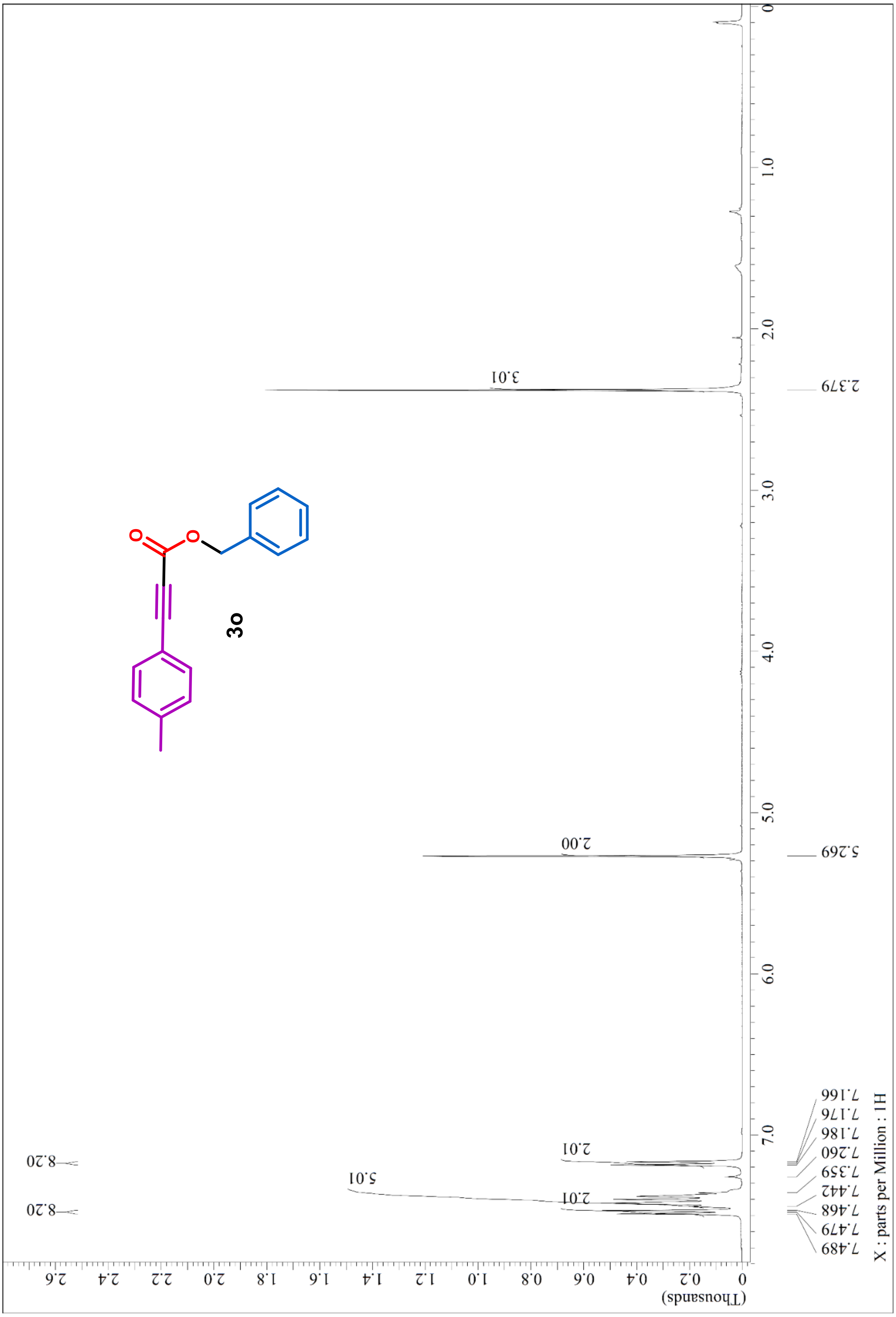

Figure S40. ^{1}H NMR spectrum of Benzyl 3-(p-tolyl)propiolate (**3o**).

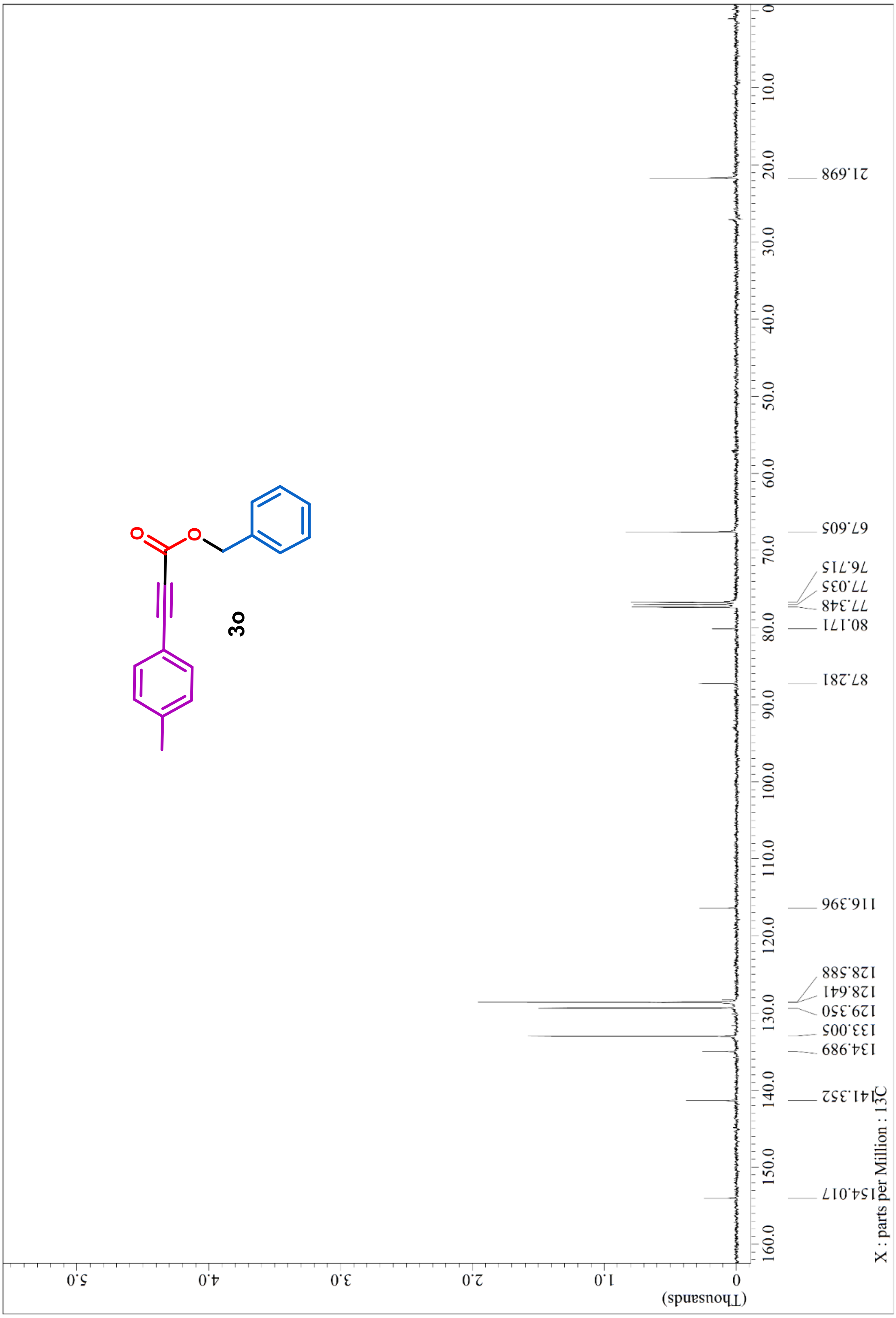

Figure S41. ^{13}C NMR spectrum of Benzyl 3-(p-tolyl)propiolate (**3o**).

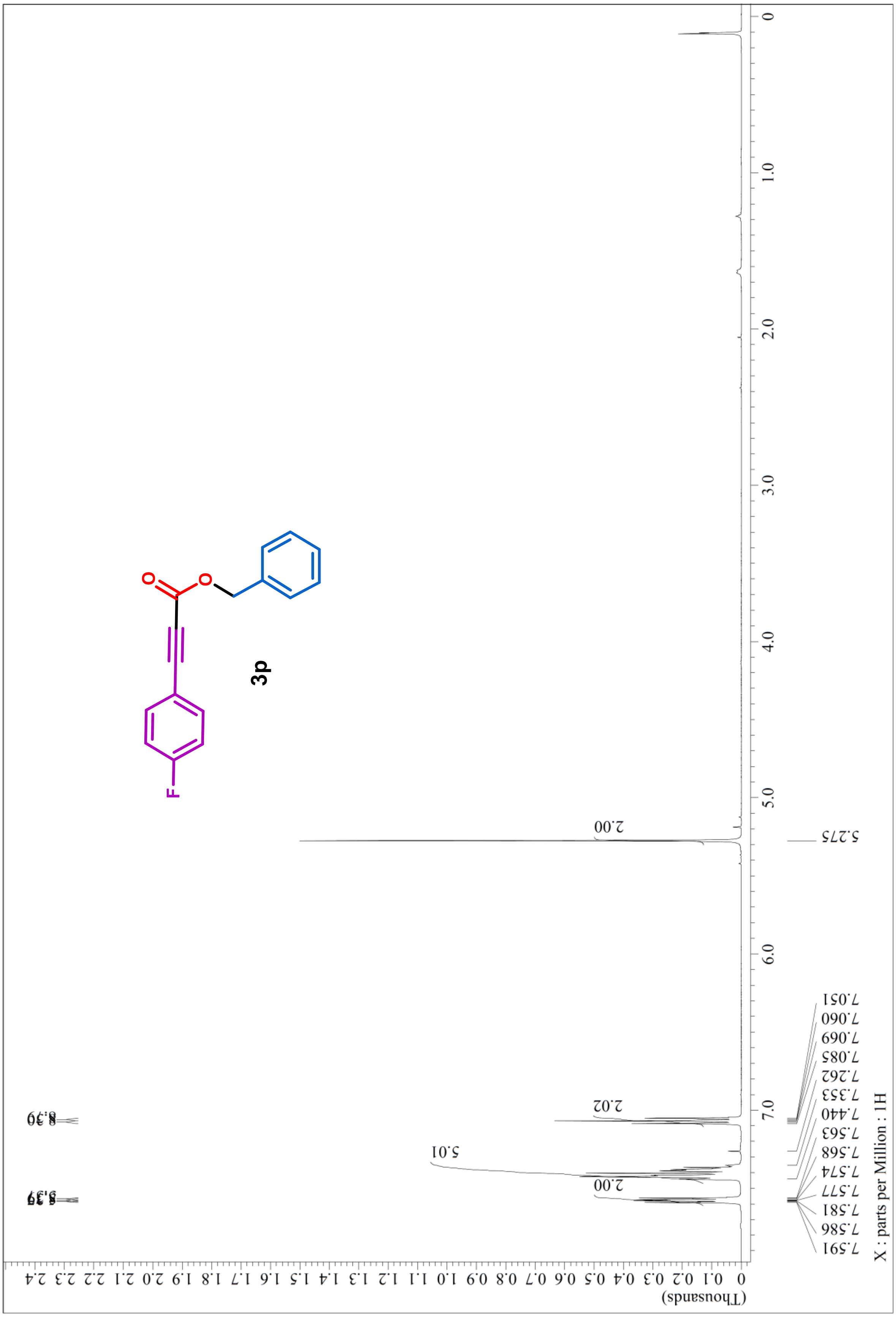

Figure S42. ^{1}H NMR spectrum of Benzyl 3-(4-fluorophenyl)propiolate (**3p**).

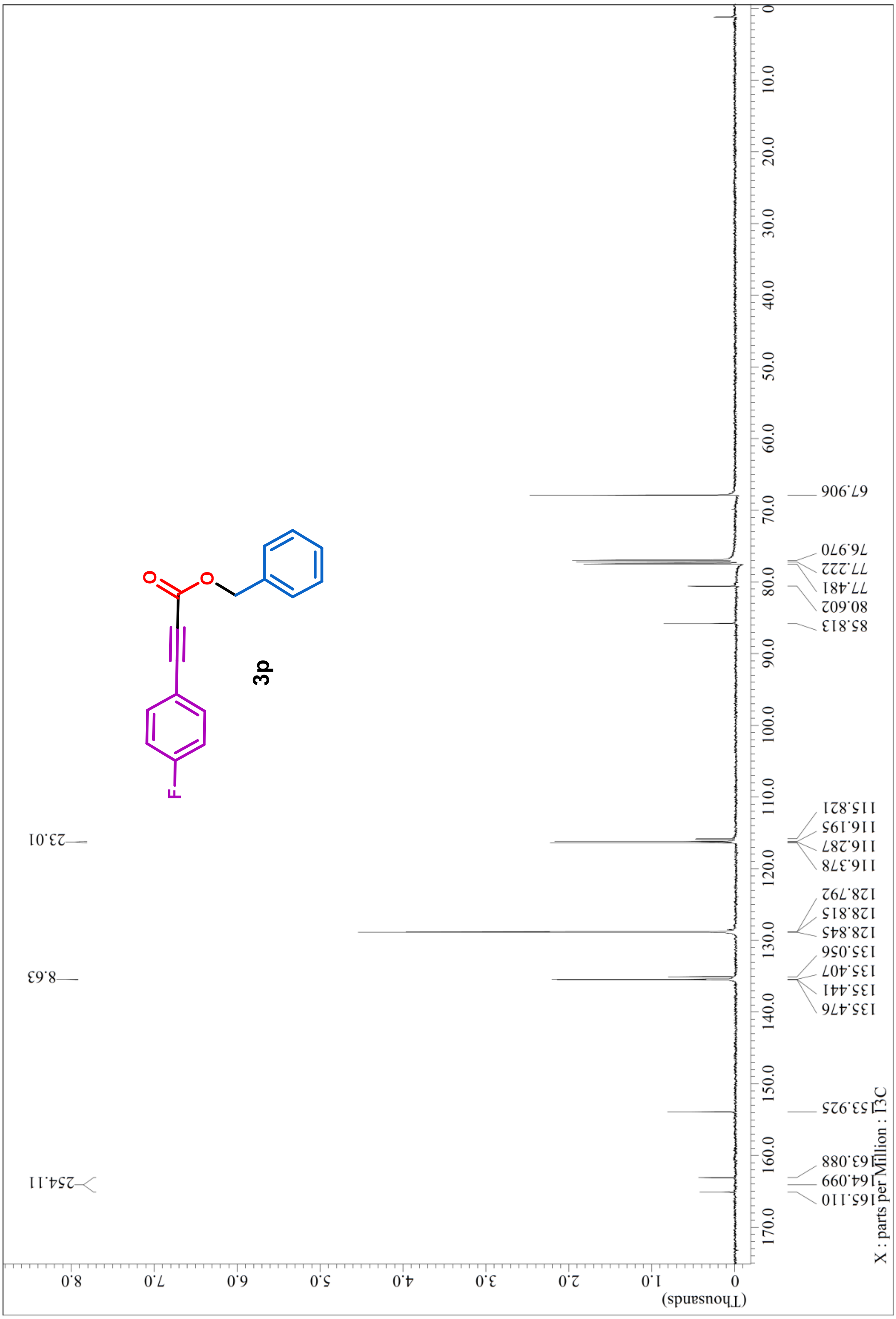

Figure S43. ^{13}C NMR spectrum of Benzyl 3-(4-fluorophenyl)propiolate (**3p**).

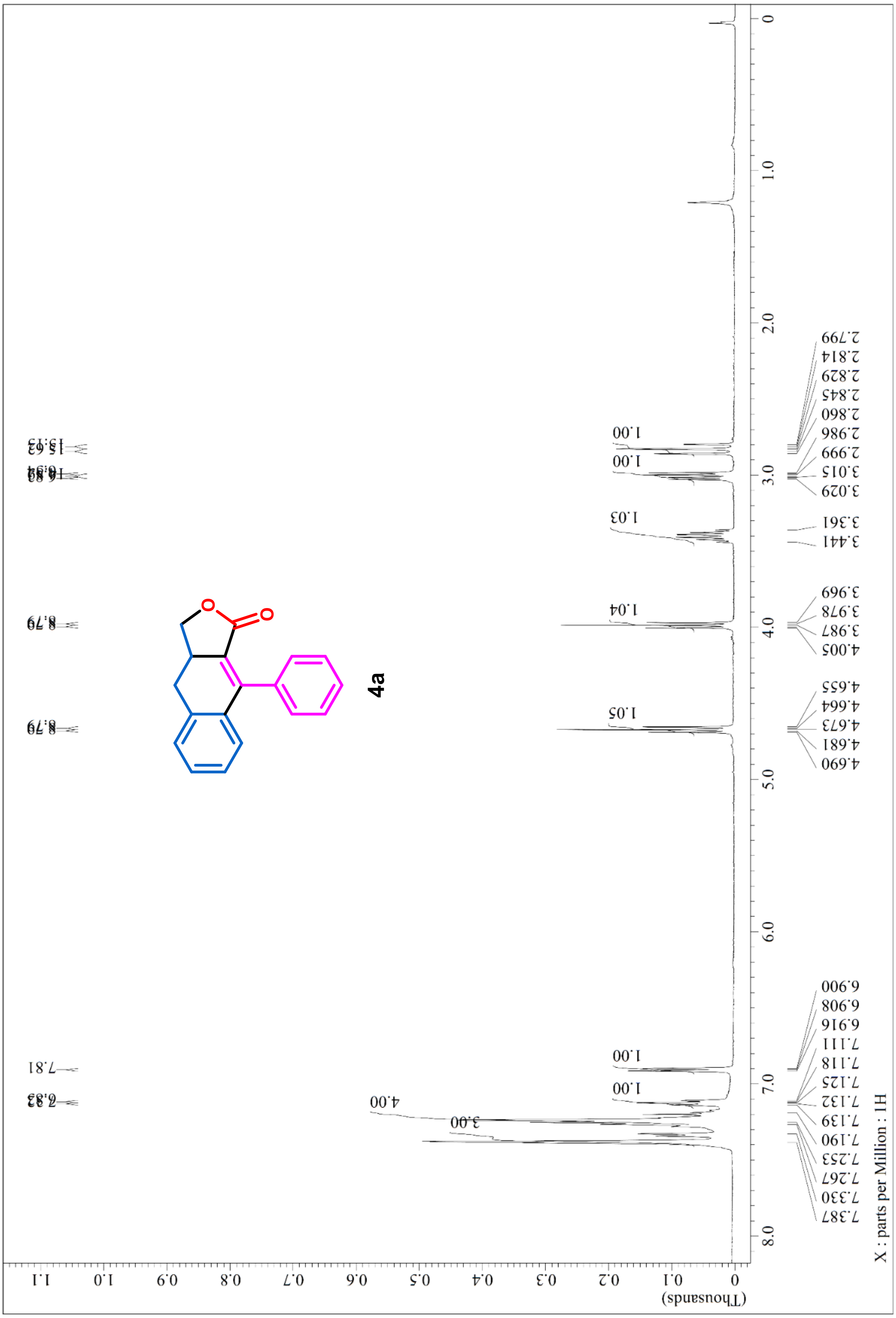

Figure S44. ^{1}H NMR spectrum of 9-Phenyl-3a,4-dihydronaphtho[2,3-c]furan-1(3*H*)-one (**4a**).

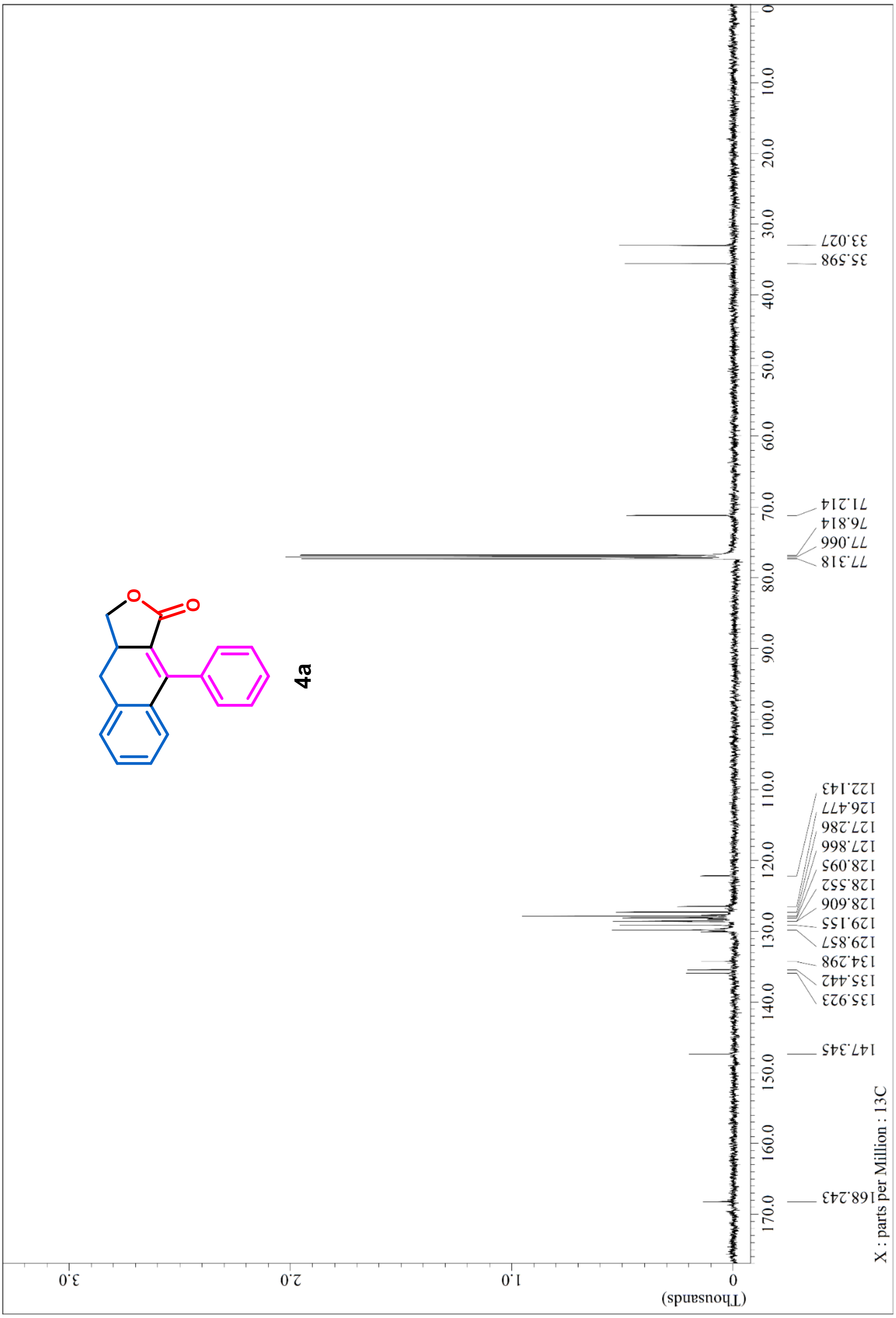

Figure S45. ^{13}C NMR spectrum of 9-Phenyl-3a,4-dihydronaphtho[2,3-c]furan-1(3*H*)-one (**4a**).

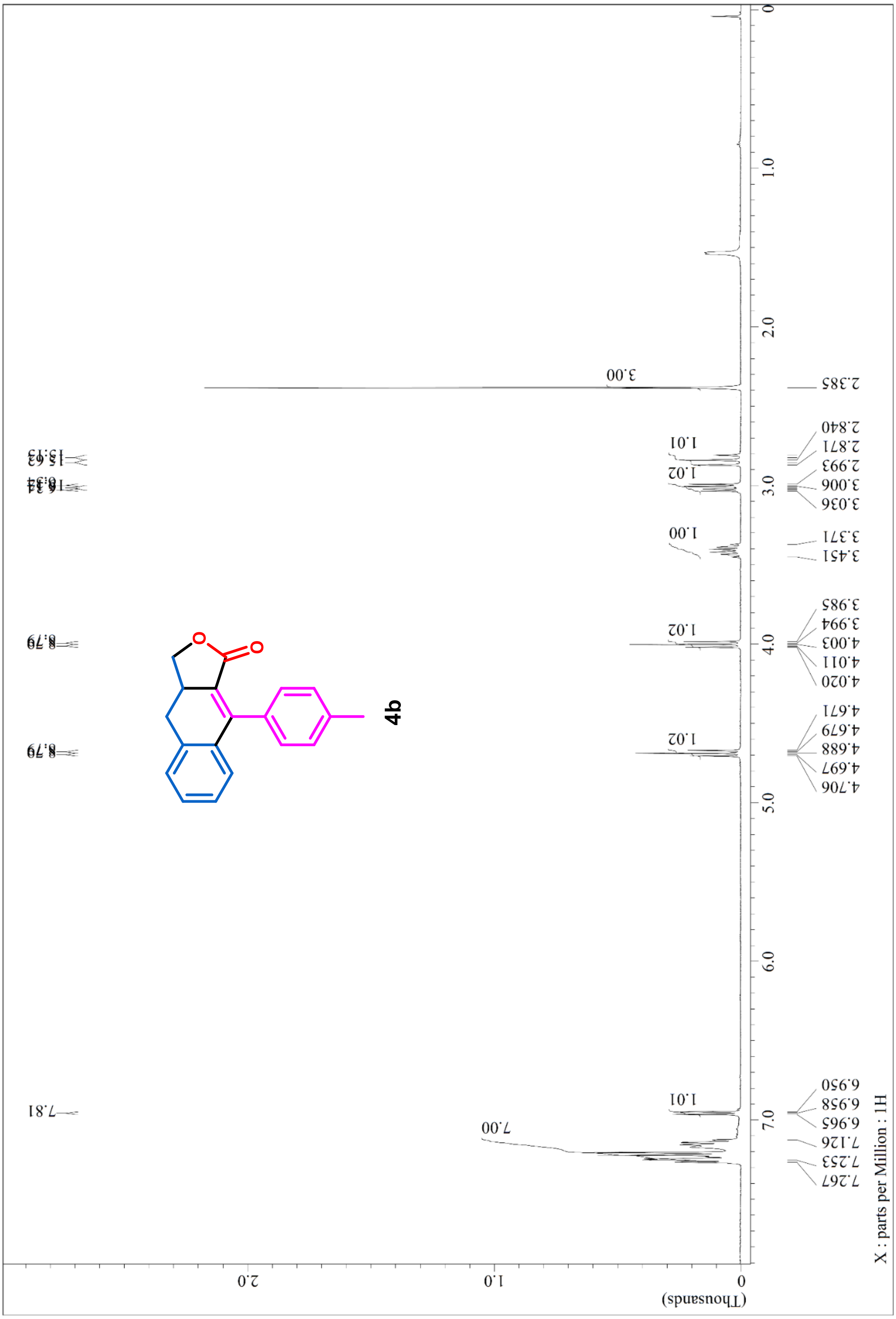

Figure S46. ^{1}H NMR spectrum of 9-(p-Tolyl)-3a,4-dihydronaphtho[2,3-c]furan-1(3*H*)-one (**4b**).

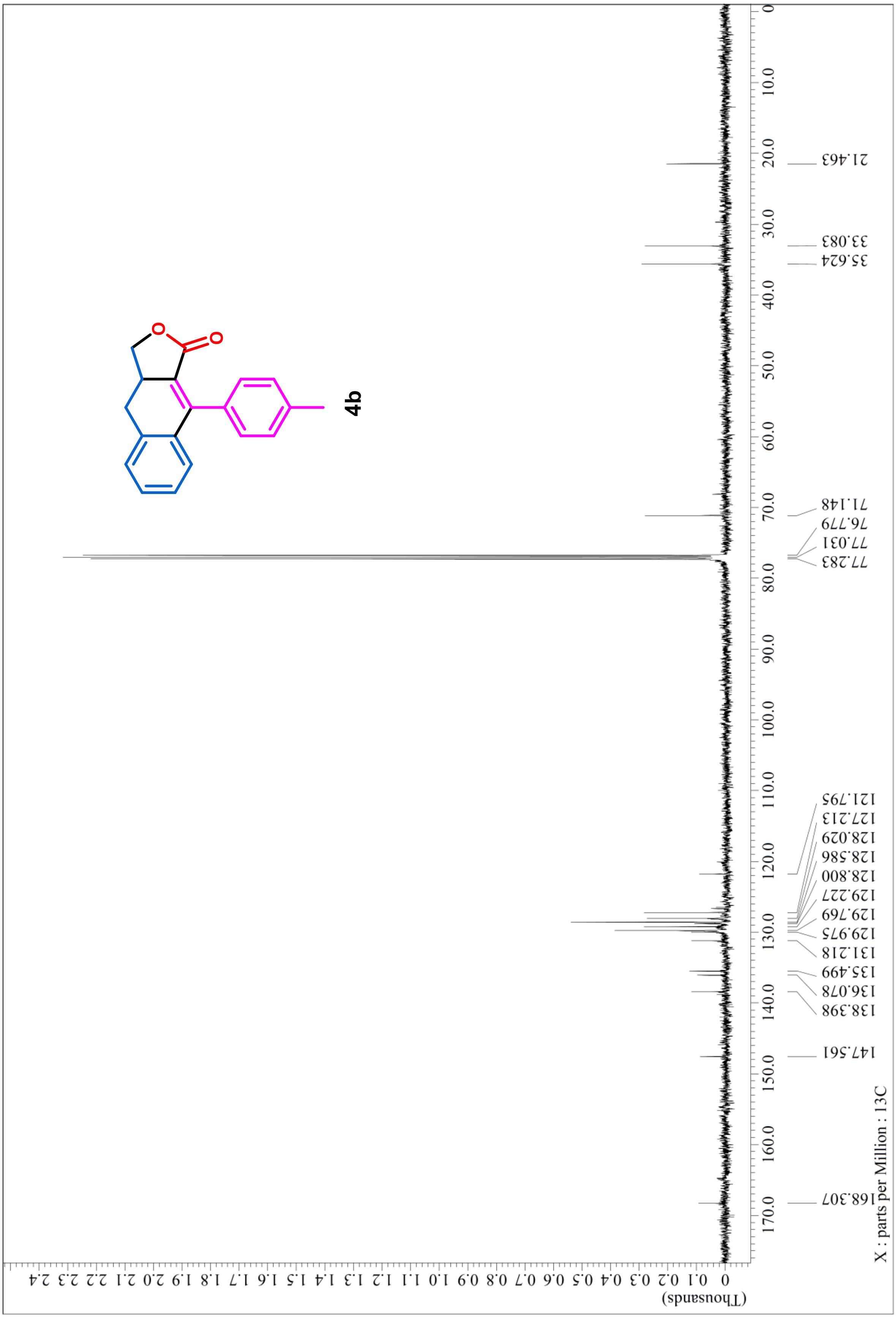

Figure S47. ^{13}C NMR spectrum of 9-(p-Tolyl)-3a,4-dihydronaphtho[2,3-c]furan-1(3*H*)-one (**4b**).

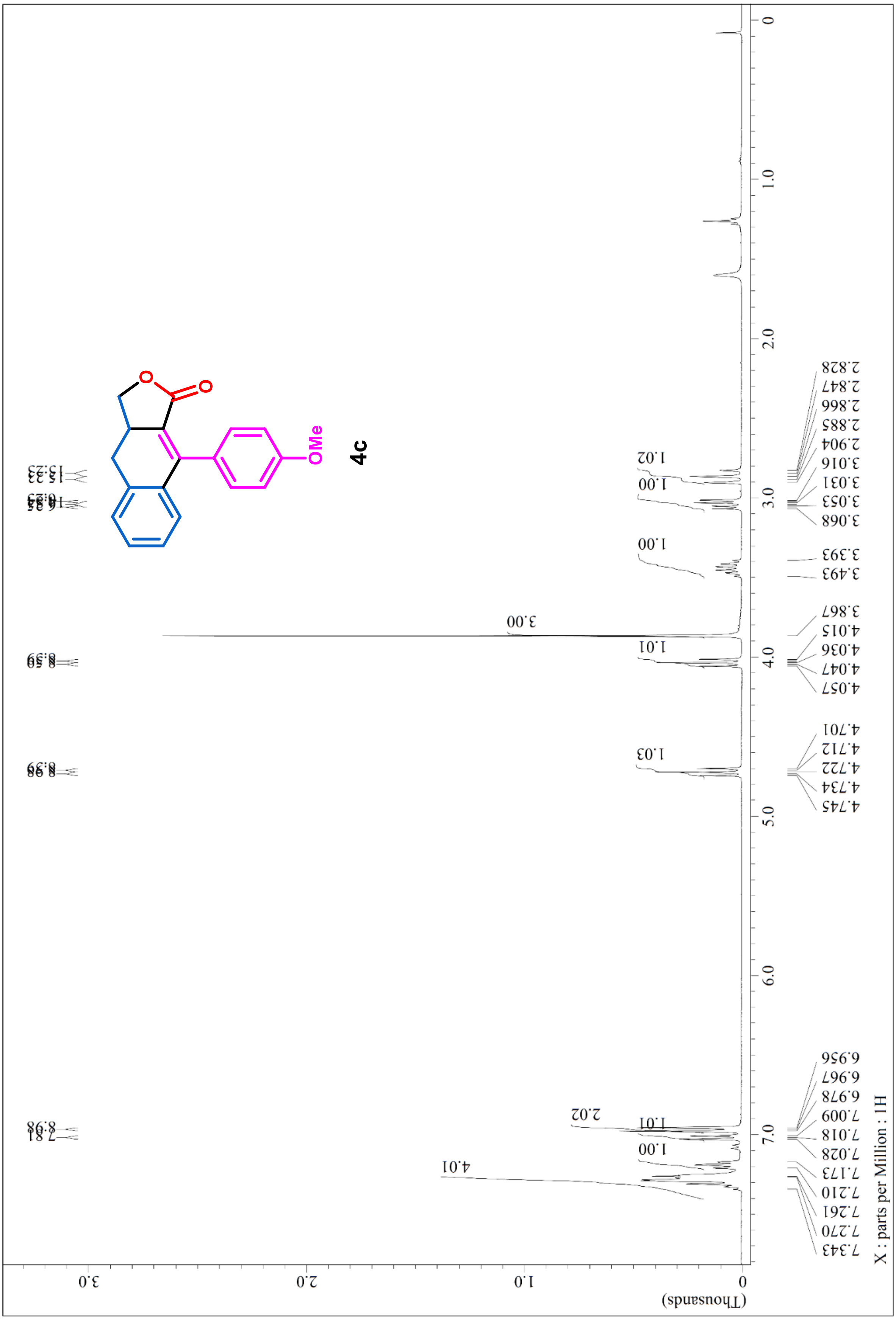

Figure S48. ^{1}H NMR spectrum of 9-(4-Methoxyphenyl)-3a,4-dihydronaphtho[2,3-c]furan-1(3*H*)-one (**4c**).

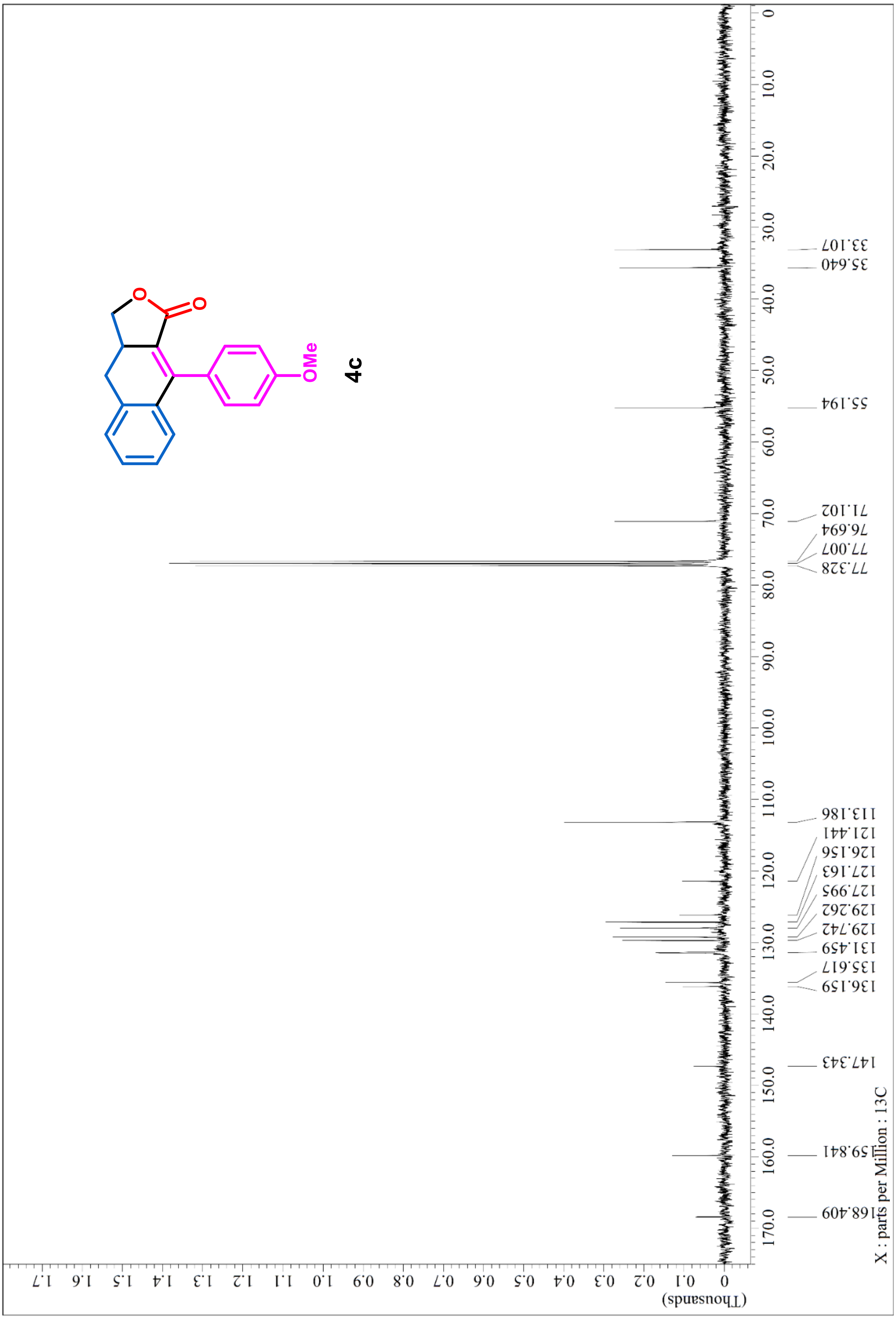

Figure S49. ^{13}C NMR spectrum of 9-(4-Methoxyphenyl)-3a,4-dihydronaphtho[2,3-c]furan-1(3*H*)-one (**4c**).

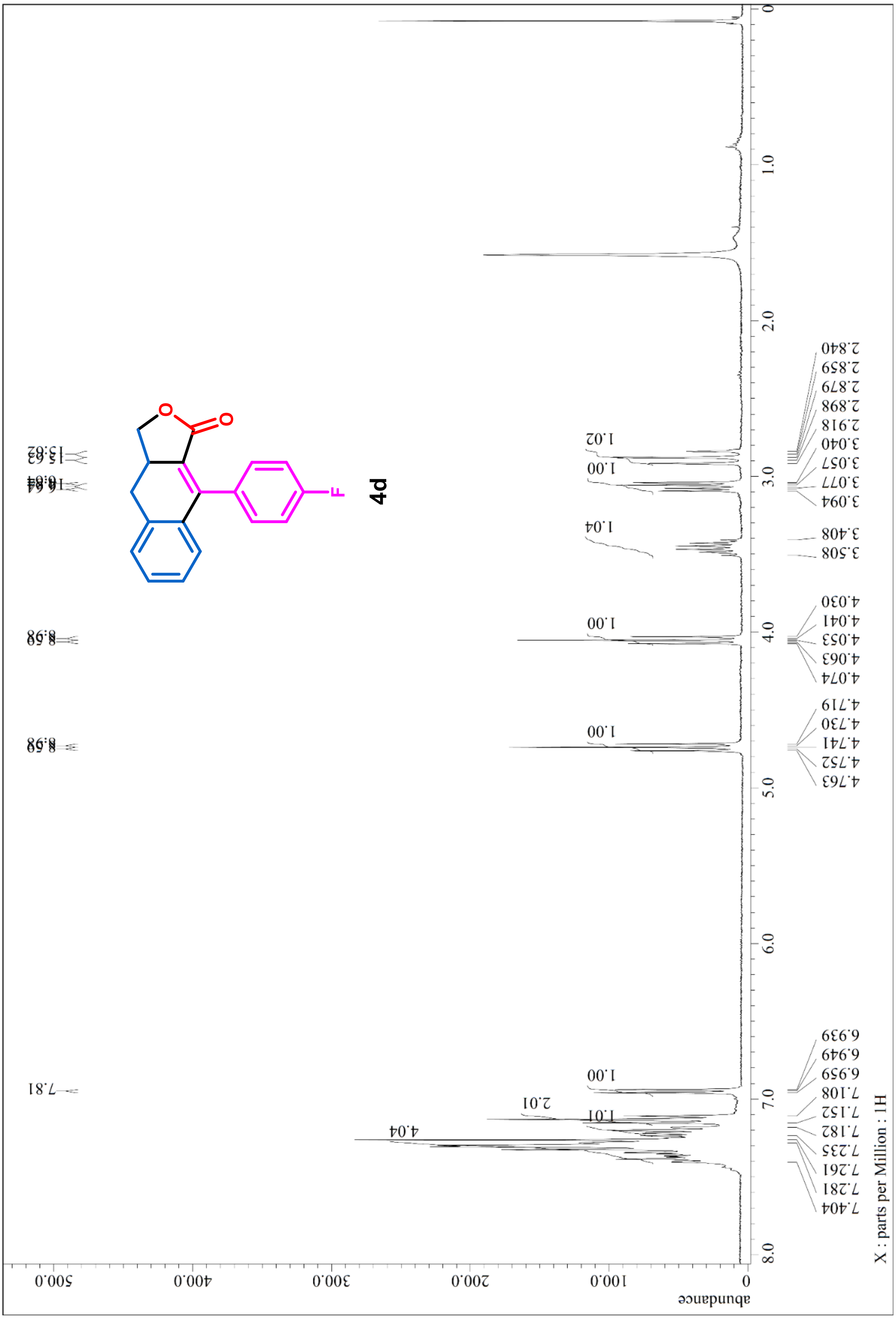

Figure S50. ^{1}H NMR spectrum of 9-(4-Fluorophenyl)-3a,4-dihydronaphtho[2,3-c]furan-1(3*H*)-one (**4d**).

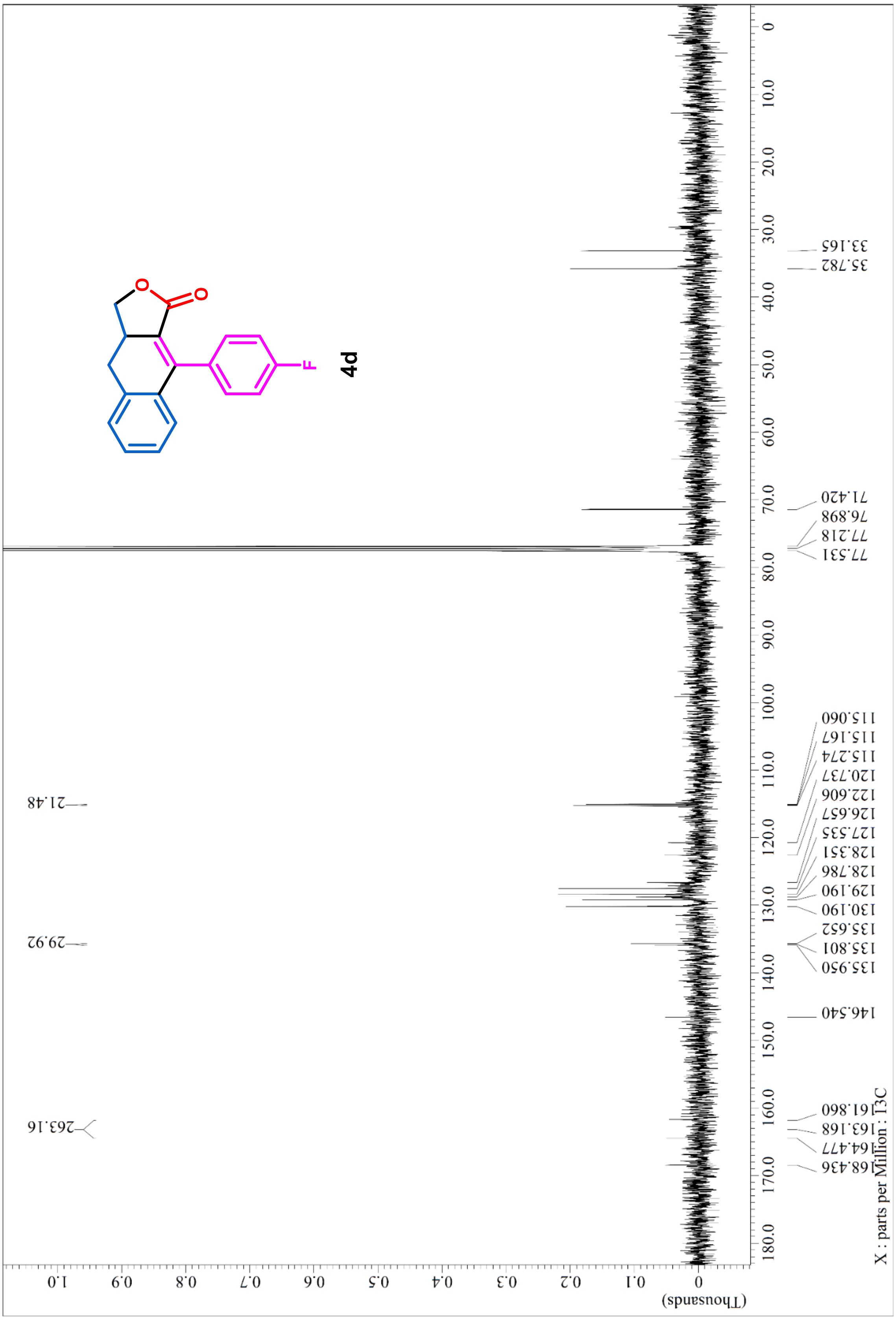

Figure S51. ^{13}C NMR spectrum of 9-(4-Fluorophenyl)-3a,4-dihydronaphtho[2,3-c]furan-1(3*H*)-one (**4d**).

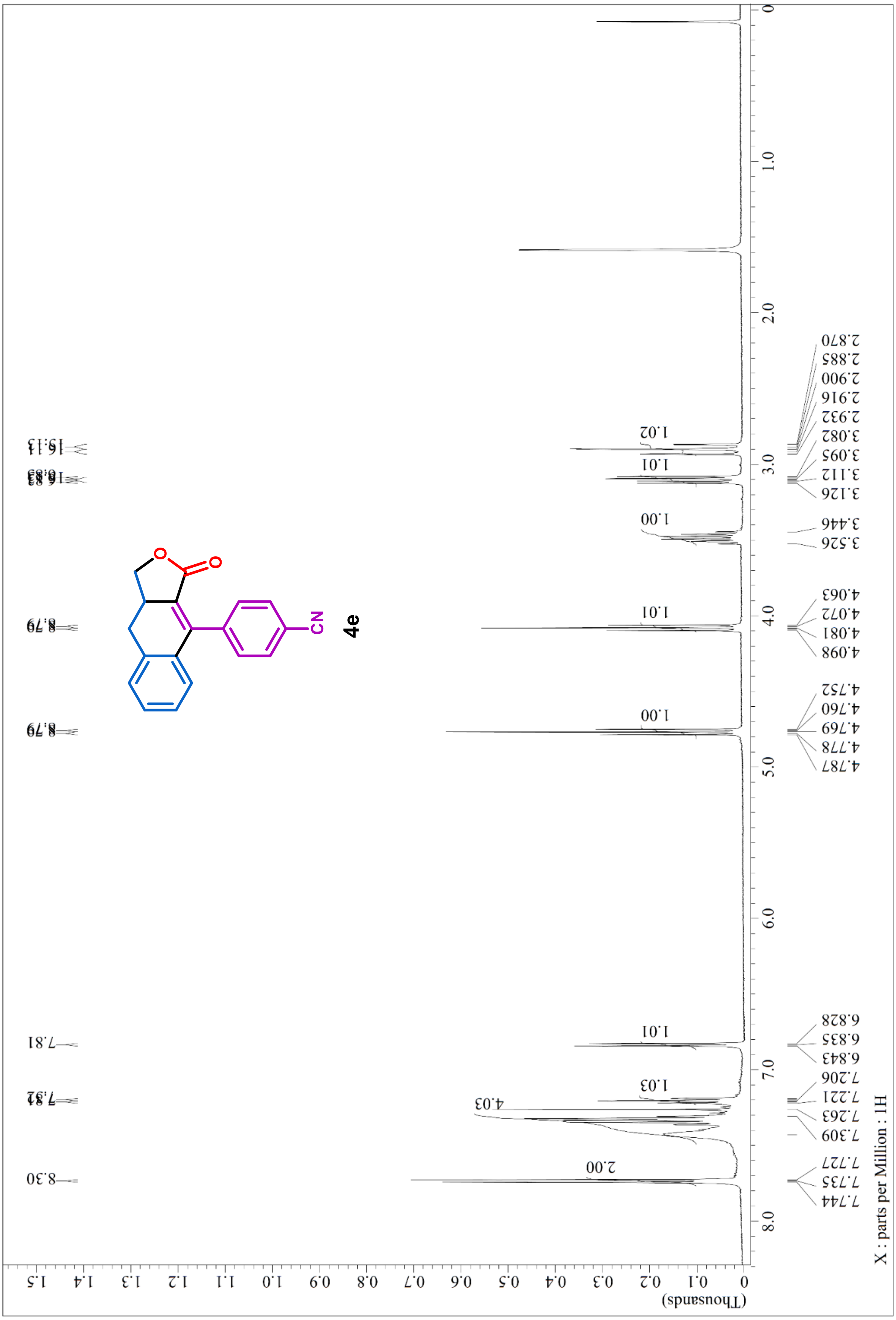

Figure S52. ^{1}H NMR spectrum of 4-(3-oxo-1,3,9,9a-tetrahydronaphtho[2,3-c]furan-4-yl)benzonitrile (**4e**).

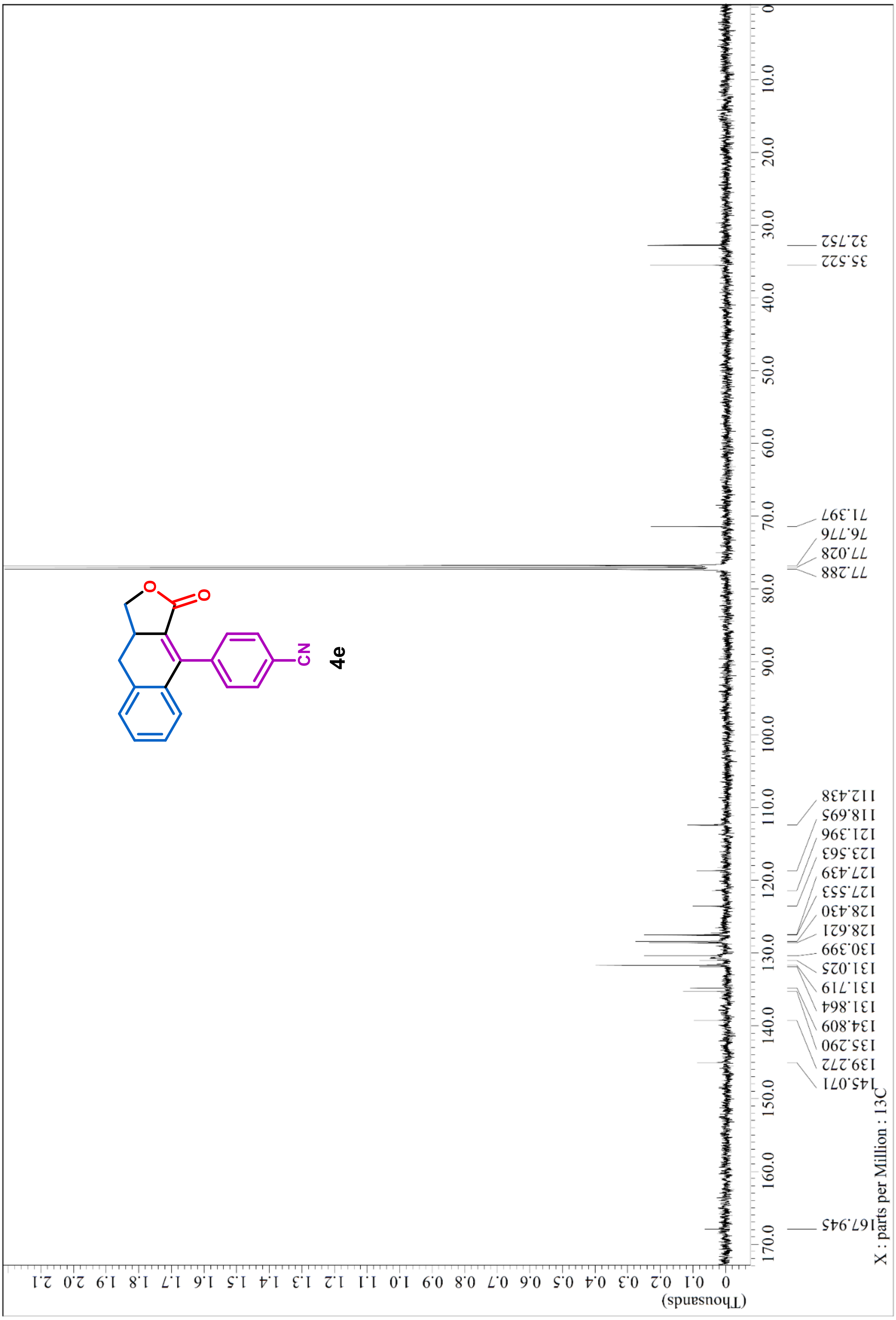

Figure S53. ^{13}C NMR spectrum of 4-(3-oxo-1,3,9,9a-tetrahydronaphtho[2,3-c]furan-4-yl)benzonitrile (**4e**).

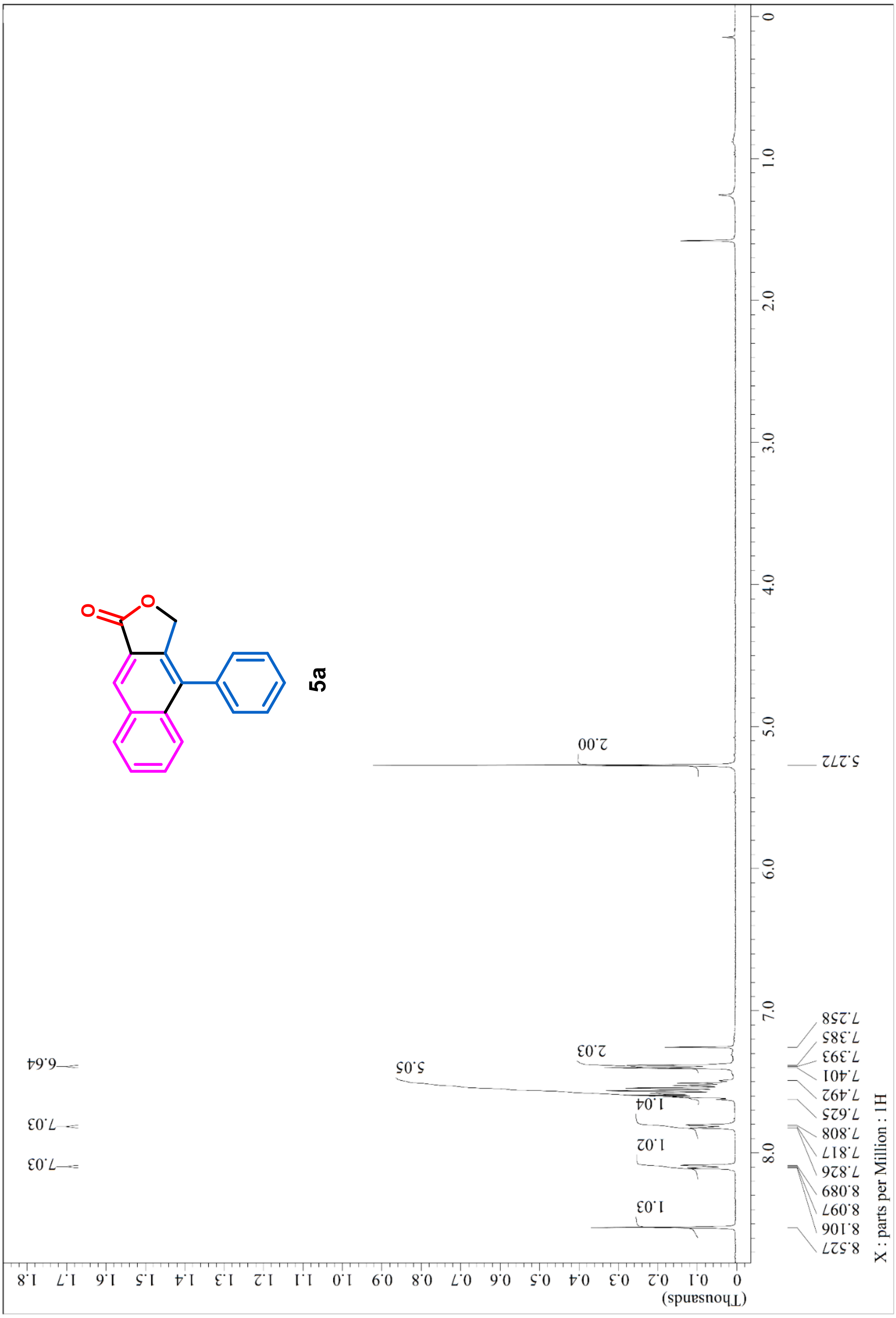

Figure S54. ^{1}H NMR spectrum of 4-Phenylnaphtho[2,3-c]furan-1(3*H*)-one (**5a**).

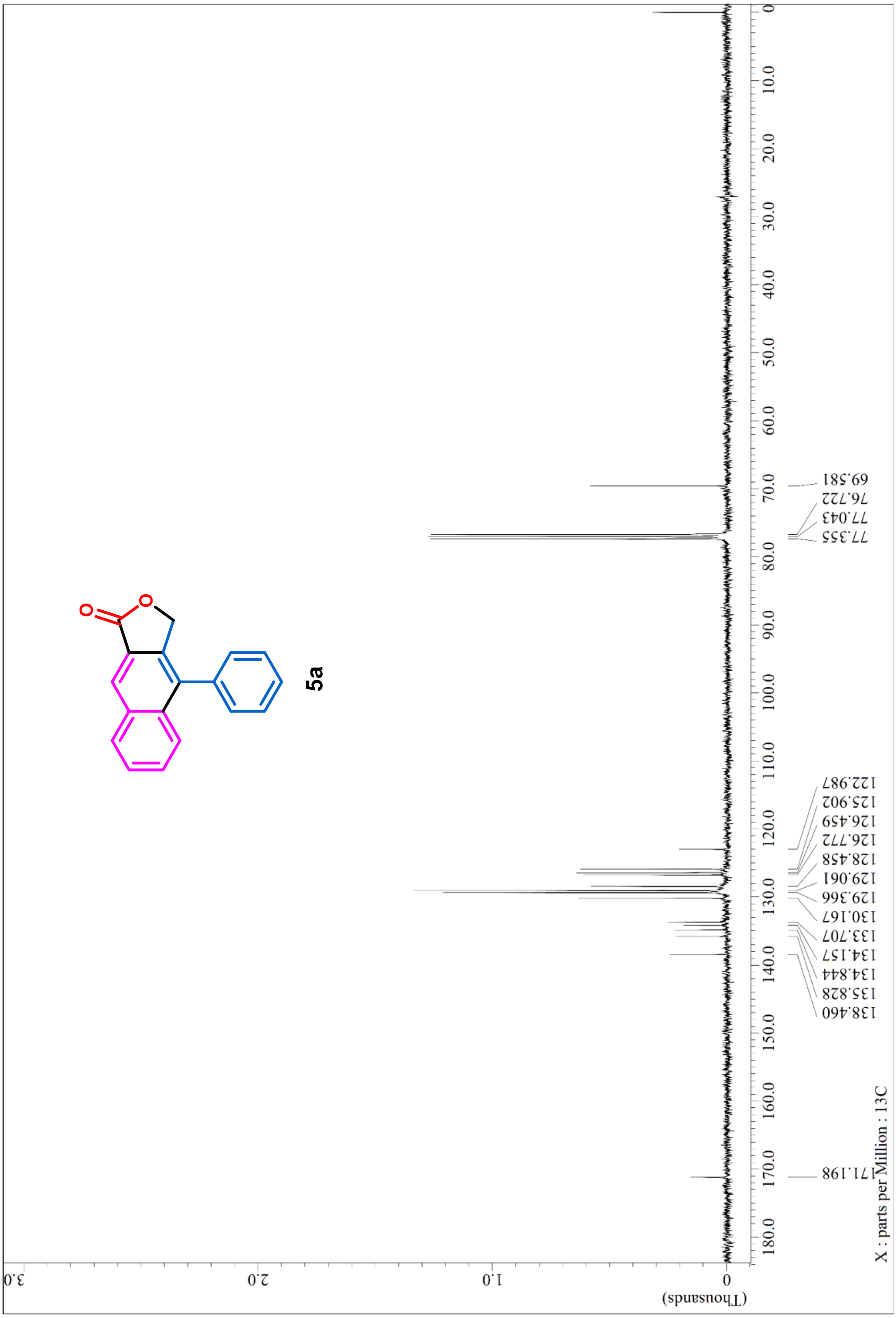

Figure S55. ^{13}C NMR spectrum of 4-Phenylnaphtho[2,3-c]furan-1(3*H*)-one (**5a**).

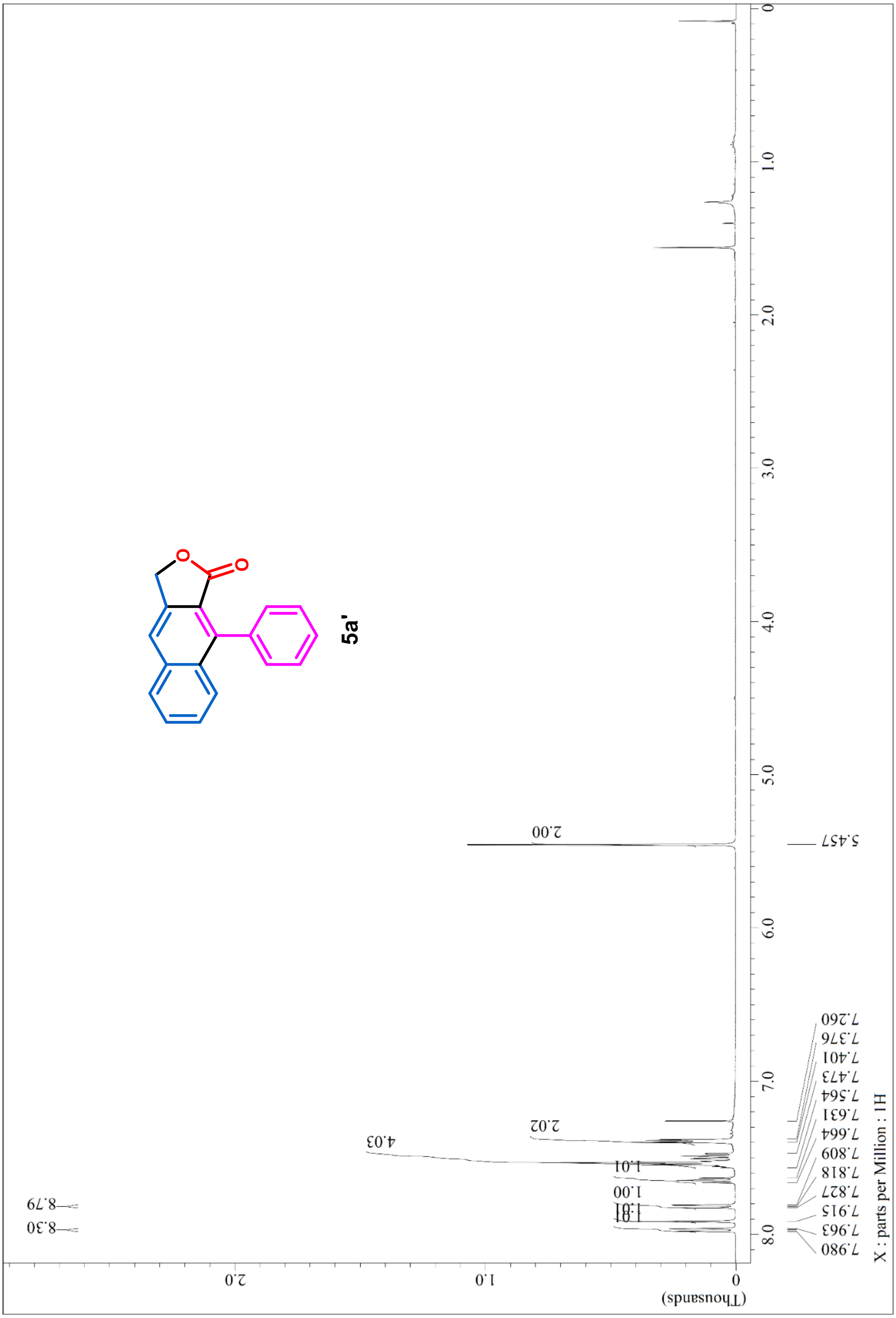

Figure S56. ^{1}H NMR spectrum of 9-Phenylnaphtho[2,3-c]furan-1(3*H*)-one (**5a'**).

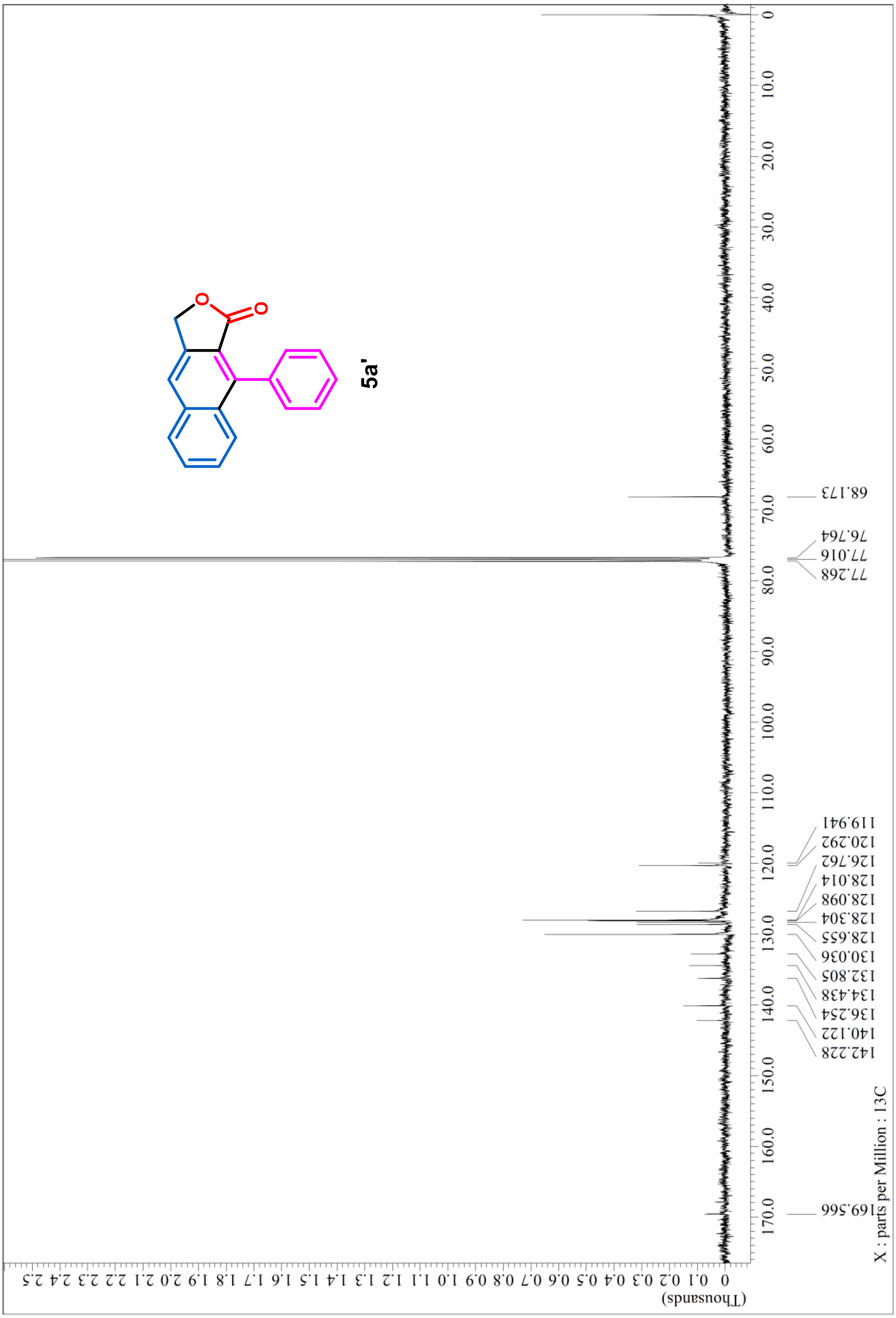

Figure S57. ^{13}C NMR spectrum of 9-Phenylnaphtho[2,3-c]furan-1(3*H*)-one (**5a'**).

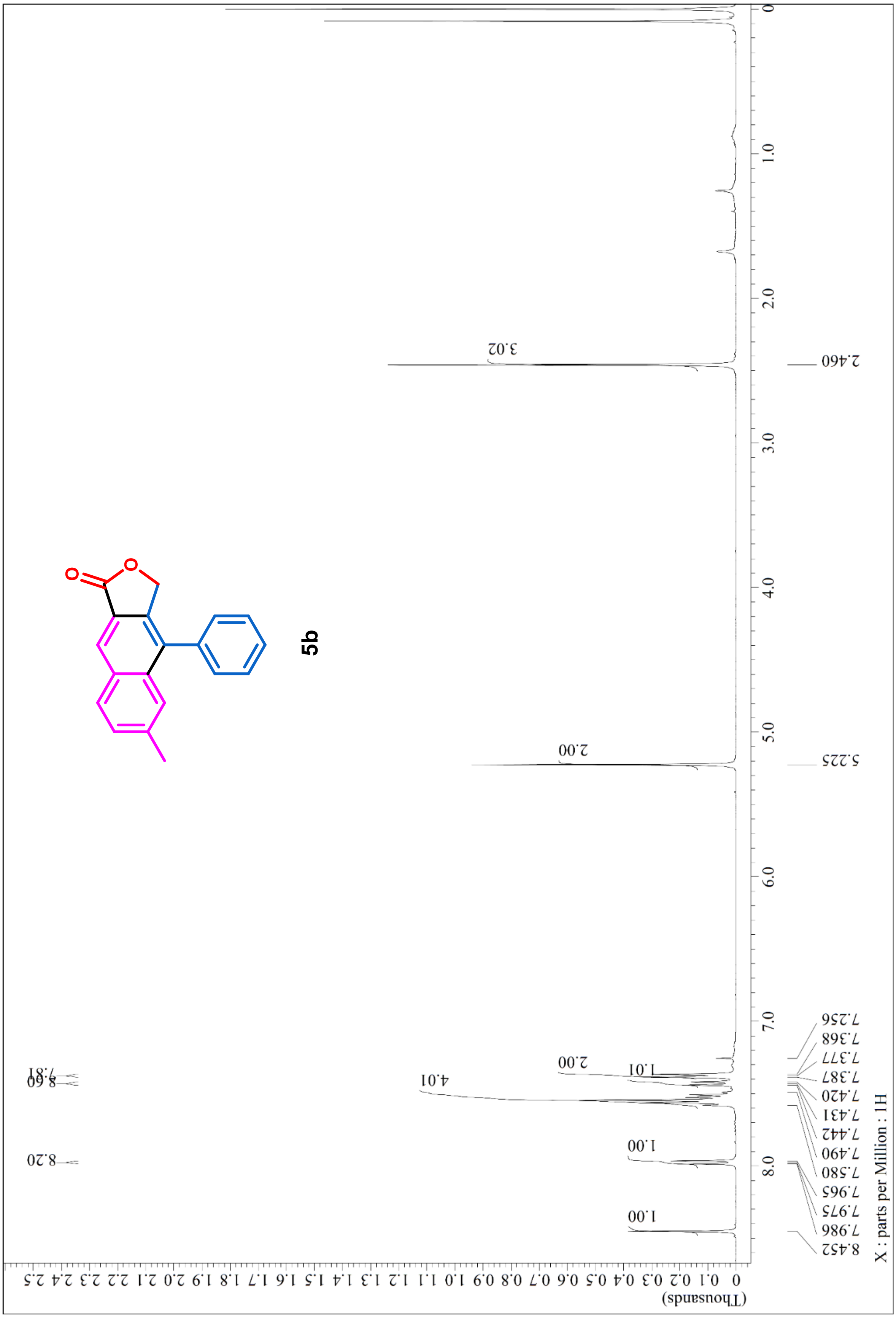

Figure S58. ^{1}H NMR spectrum of 6-Methyl-4-phenylnaphtho[2,3-c]furan-1(3*H*)-one (**5b**).

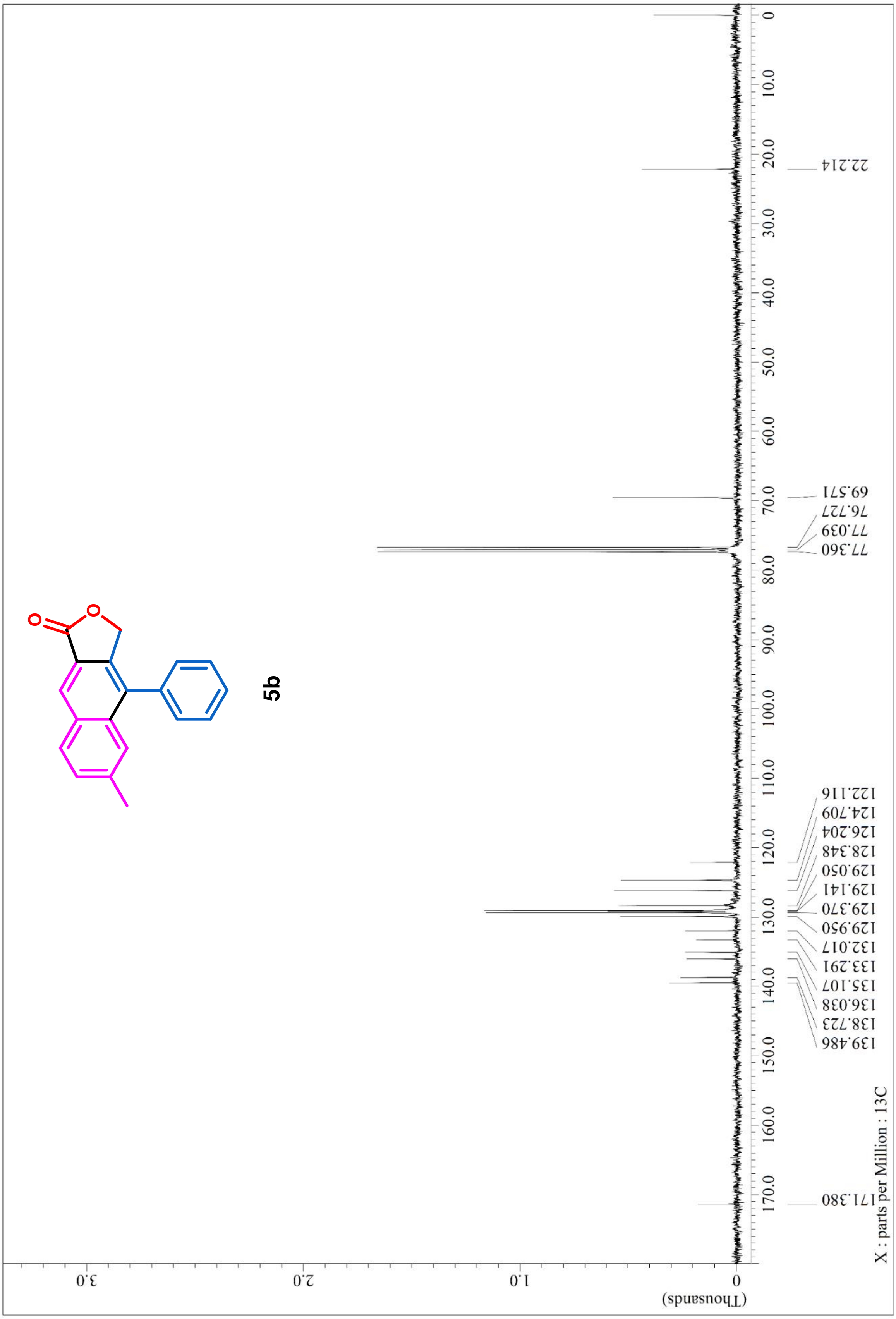

Figure S59. ^{13}C NMR spectrum of 6-Methyl-4-phenylnaphtho[2,3-c]furan-1(3*H*)-one (**5b**).

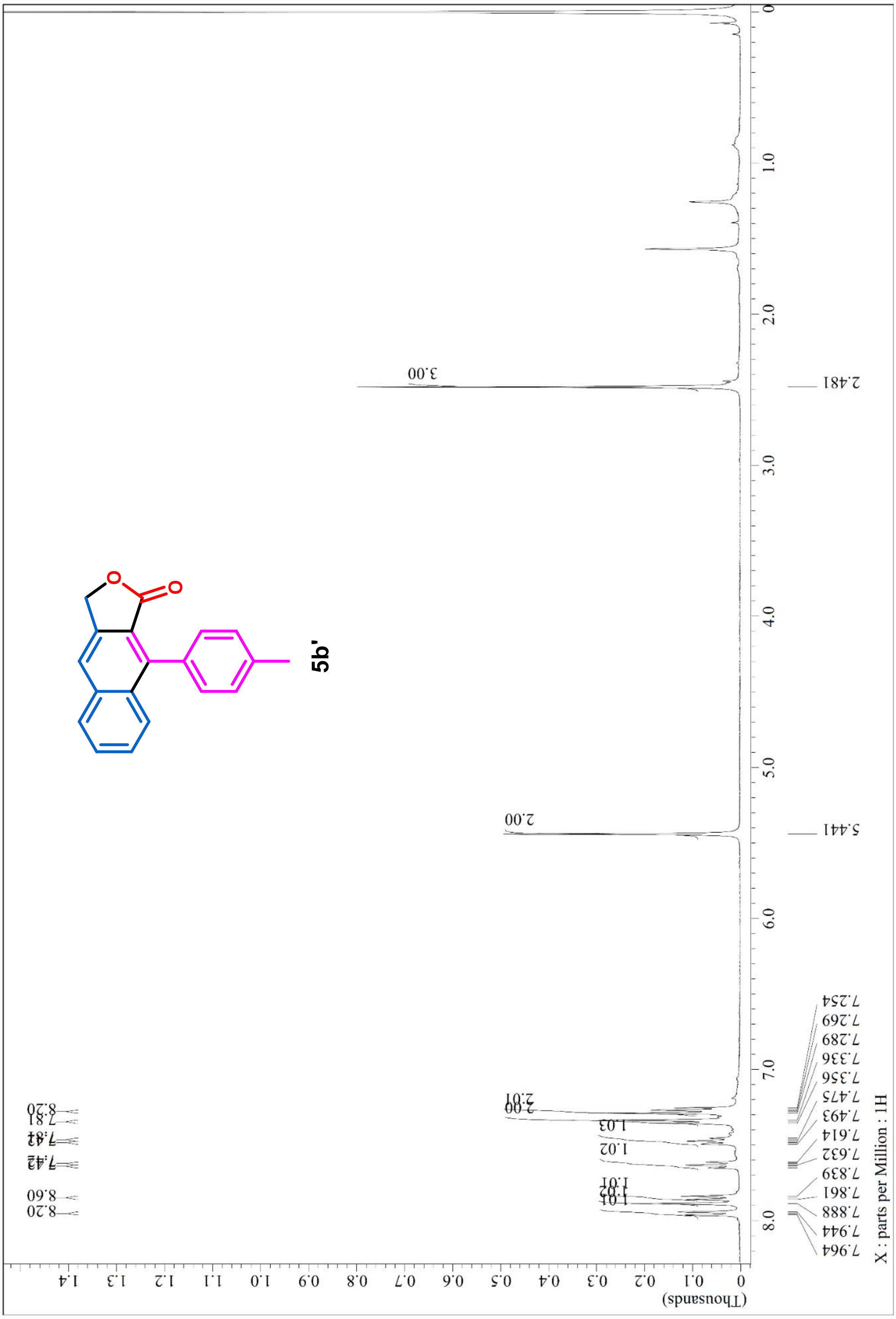

Figure S60. ^{1}H NMR spectrum of 9-(p-Tolyl)naphtho[2,3-c]furan-1(3*H*)-one (**5b'**).

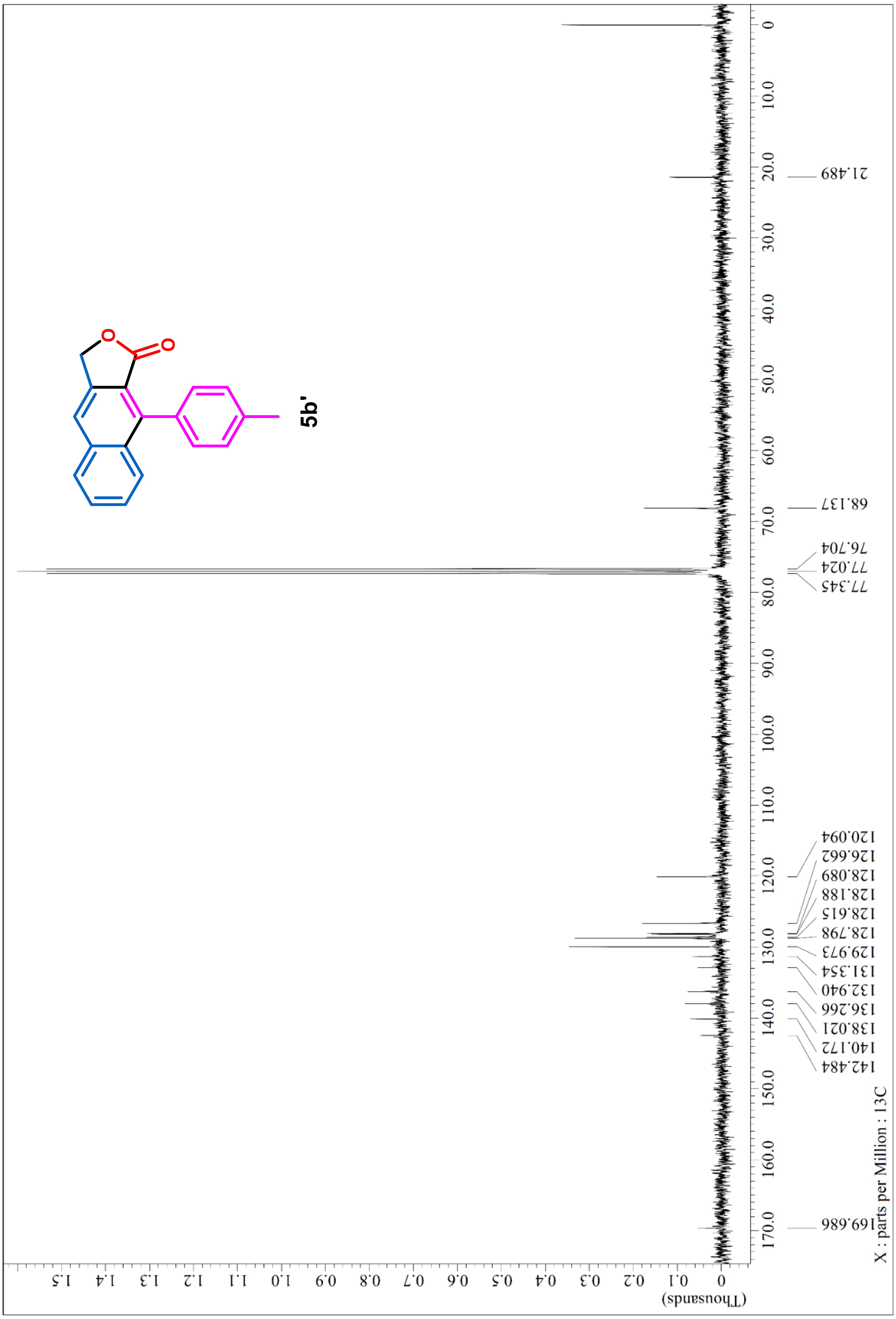

Figure S61. ^{13}C NMR spectrum of 6-Methyl-4-phenylnaphtho[2,3-c]furan-1(3*H*)-one (**5b'**).

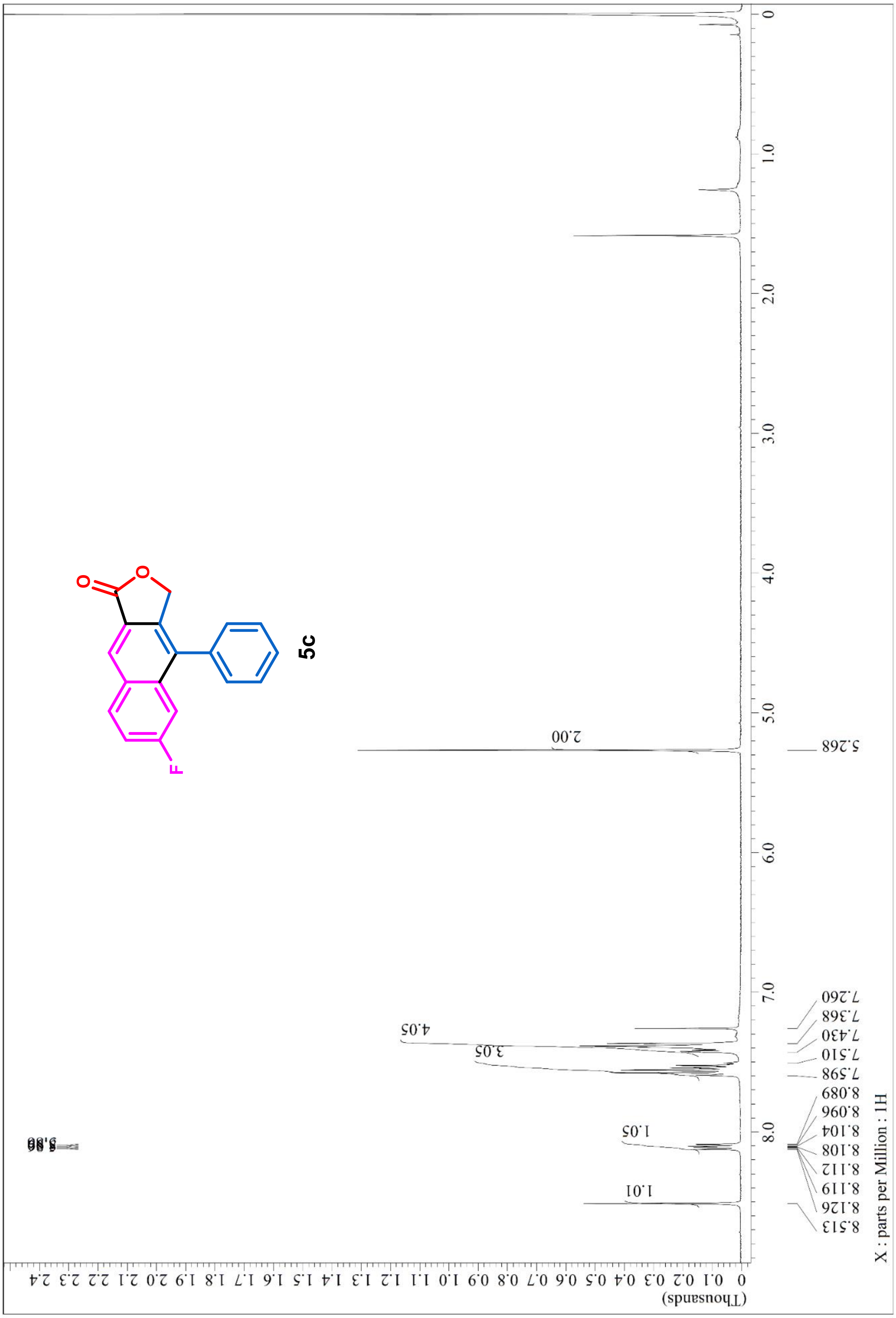

Figure S62. ^{1}H NMR spectrum of 6-Fluoro-4-phenylnaphtho[2,3-c]furan-1(3*H*)-one (**5c**).

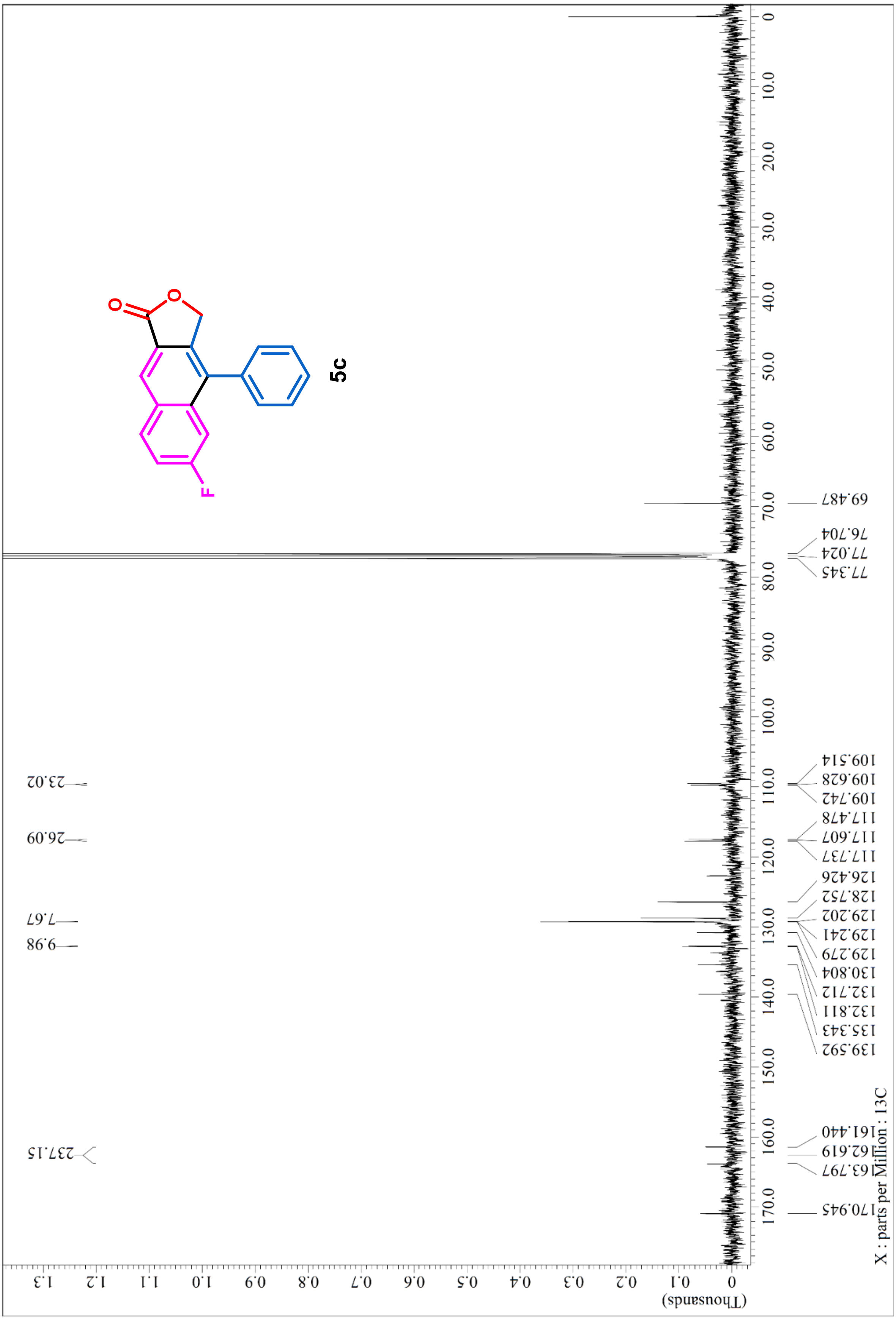

Figure S63. ^{13}C NMR spectrum of 6-Fluoro-4-phenylnaphtho[2,3-c]furan-1(3*H*)-one (**5c**).

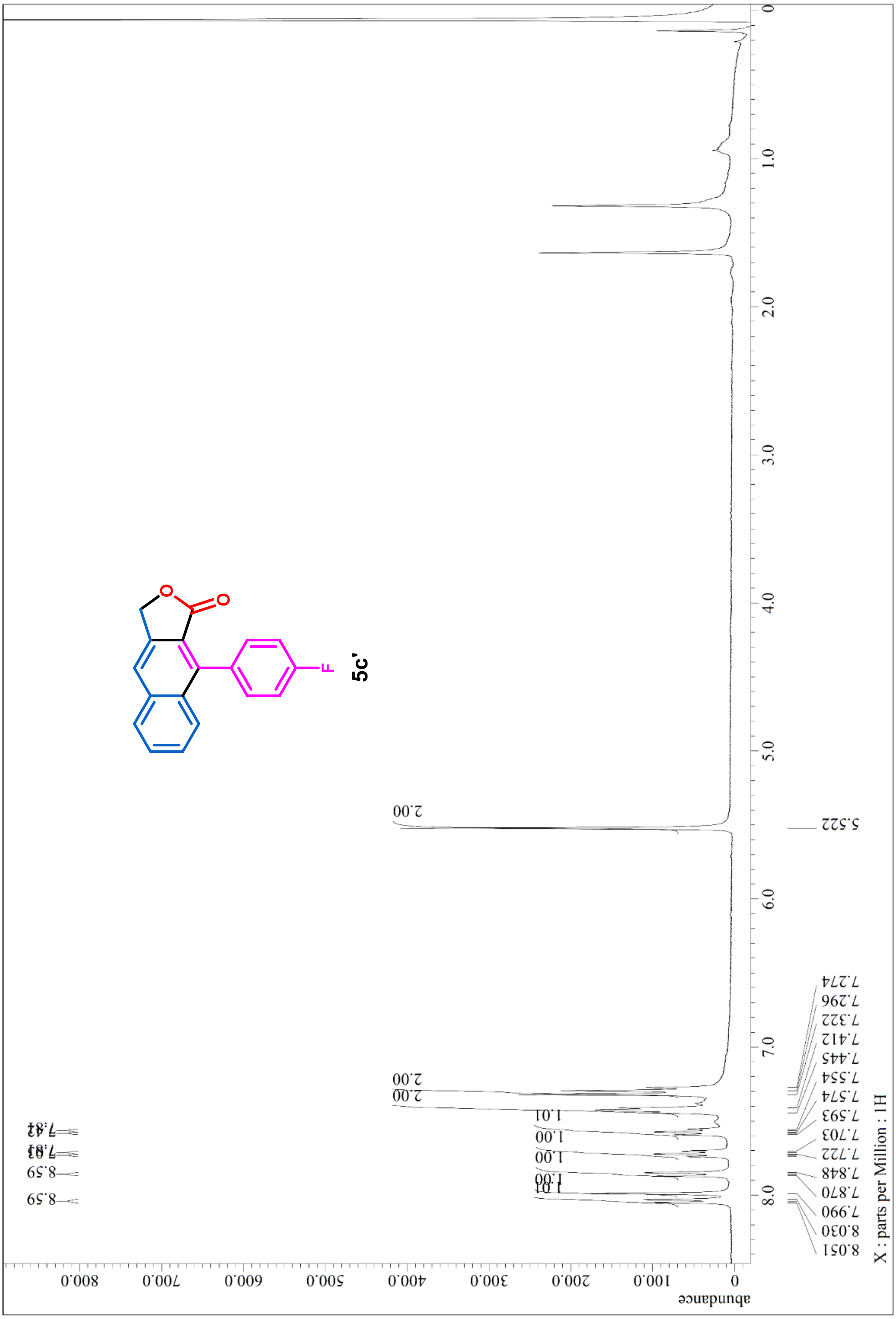

Figure S64. ^{1}H NMR spectrum of 9-(4-Fluorophenyl)naphtho[2,3-c]furan-1(3*H*)-one (**5c'**).

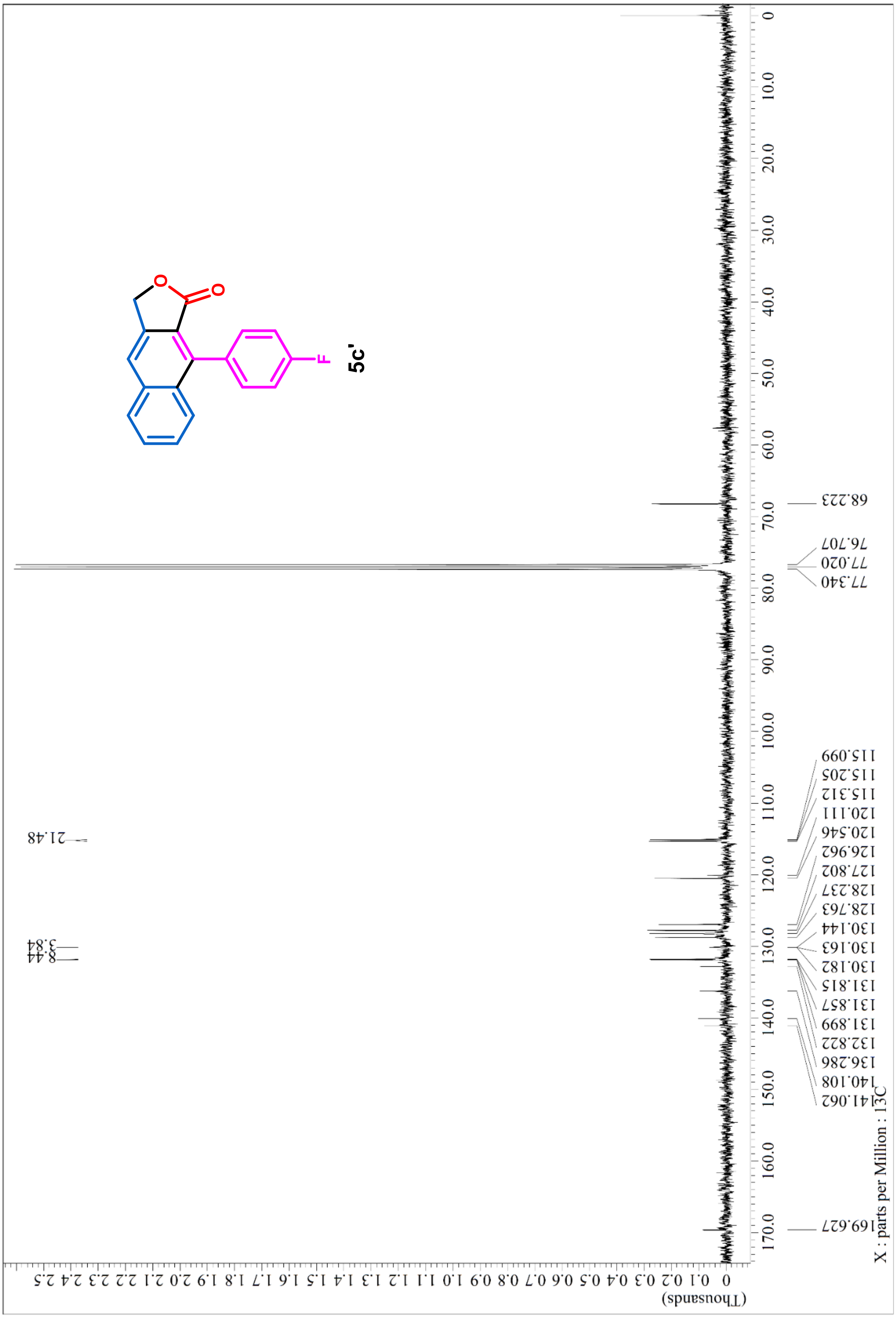

Figure S65. ^{13}C NMR spectrum of 9-(4-Fluorophenyl)naphtho[2,3-c]furan-1(3*H*)-one (**5c'**).

References

S1. X. Zhang; Y. Zheng; X. Feng; X. Han; Z. Bai; Z. Zhang, *RSC Adv.*, 2015, **5**, 86102-86112.

S2. J. Park; S. G. Kwon; S. W. Jun; B. H. Kim; T. Hyeon, *ChemPhysChem*, 2012, **13**, 2540-2543.

S3. Y. Yanagisawa; K. Takaoka; S. Yamabe; T. Ito, *J. Phy. Chem.*, 1995, **99**, 3704-3710.

S4. J. Hu; K. Zhu; L. Chen; C. Kübel; R. Richards, *J. Phy. Chem., C*, 2007, **111**, 12038-12044.

S5. G. A. Mutch; S. Shulda; A. J. McCue; M. J. Menart; C. V. Ciobanu; C. Ngo; J. A. Anderson; R. M. Richards; D. Vega-Maza, *J. Am. Chem. Soc.*, 2018, **140**, 4736-4742.

S6. A. Gennaro; A. A. Isse; E. Vianello, *Journal of Electroanalytical Chemistry and Interfacial Electrochemistry*, 1990, 289, 203-215.

S7. X. Zhang; D. Wang; M. Jing; J. Liu; Z. Zhao; G. Xu; W. Song; Y. Wei; Y. Sun, *ChemCatChem*, 2019, **11**, 2089-2098.

S8. X.-H. Liu; J.-G. Ma; Z. Niu; G.-M. Yang; P. Cheng, *Angew. Chem. Int. Ed.*, 2015, **54**, 988-991.

S9. N. N. Zhu; X. H. Liu; T. Li; J. G. Ma; P. Cheng; G. M. Yang, *Inorg. Chem.*, 2017, **56**, 3414-3420.

S10. J. Shi; L. Zhang; N. Sun; D. Hu; Q. Shen; F. Mao; Q. Gao; W. Wei, *ACS Appl. Mater. Inter*, 2019, **11**, 28858-28867.

S11. A. H. Chowdhury; S. Ghosh; S. M. Islam, *New. J. Chem.* , 2018, **42**, 14194-14202.

S12. W.-Z. Zhang; W.-J. Li; X. Zhang; H. Zhou; X.-B. Lu, *Org. Lett.*, 2010, **12**, 4748-4751.

S13. X. Zhang; W.-Z. Zhang; L.-L. Shi; C. Zhu; J.-L. Jiang; X.-B. Lu, *Tetrahedron*, 2012, **68**, 9085-9089.